Study on CO_2 capture using nanostructure carbon adsorbents

Thesis submitted in fulfillment of the requirement for the degree of

Doctor of Philosophy

By

JASMINDER SINGH
(Registration No.: 901609004)

Under the guidance of

Dr. Soumen Basu
Associate Professor
School of Chemistry and Biochemistry,
Thapar Institute of Engineering &
Technology (Deemed to be University), Patiala

Prof. Haripada Bhunia
Professor
Department of Chemical Engineering,
Thapar Institute of Engineering &
Technology (Deemed to be University), Patiala

School of Chemistry and Biochemistry
Thapar Institute of Engineering & Technology (Deemed to be University)
Patiala – 147004, Punjab (India)
www.thapar.edu

June 2019

Dedicated

To

My Parents

Mr. Surinder Singh & Mrs. Manjit Kaur

My Brother and Sisters

Mr. Jasmeet Singh, Mrs. Gagandeep Kaur, and Mrs. Amandeep Kaur

Certificate

This is to certify that the thesis entitled ***"Study on CO_2 capture using nanostructure carbon adsorbents"*** *being submitted by Mr. Jasminder Singh to School of Chemistry and Biochemistry, Thapar Institute of Engineering & Technology (Deemed to be University), Patiala for the award of degree of* ***Doctor of Philosophy****, is a record of bonafide research work carried out by him under our guidance and supervision and has fulfilled the requirements for the submission of this thesis, which to our knowledge has reached the requisite standard.*

The results embodied in the thesis have not been submitted in part or full to any other University or Institute for the award of any degree or diploma.

(Soumen Basu)
Associate Professor
School of Chemistry and Biochemistry,
Thapar Institute of Engineering &
Technology (Deemed to be University),
Patiala

(Haripada Bhunia)
Professor and Head
Department of Chemical Engineering,
Thapar Institute of Engineering &
Technology (Deemed to be University),
Patiala

Acknowledgments

"WAHEGURU JI KA KHALSA
WAHEGURU JI KI FATEH''

I devoutly thank WAHEGURU for granting me the strength to accomplish this project.

This work was carried out in the advanced nanomaterials laboratory and chemical engineering lab (Thapar Institute of Engineering and Technology) between 2016- 2019. I would like to thank most my supervisors ***Dr. Soumen Basu,*** *School of Chemistry and Biochemistry, Thapar Institute of Engineering & Technology (Deemed to be University) and* ***Prof. Haripada Bhunia****, Department of Chemical Engineering, Thapar Institute of Engineering & Technology (Deemed to be University), for providing me such a valuable research opportunity and for their countless guidance, knowledge and motivation during the course of my research. I learned a lot from them during the course of Ph. D work. Their daily practice of following up on recent scientific literature is something that I also tried to adopt and greatly benefitted. I really appreciate their unconditional support and encouragement towards doing high-calibre research. It's been a great honour to work under their guidance.*

I am extremely thankful to ***Prof. Prakash Gopalan****, Director, Thapar Institute of Engineering & Technology (Deemed to be University),* ***Prof. Rafat Siddique****, Dean of Research & Sponsored Projects, Thapar Institute of Engineering & Technology (Deemed to be University) and* ***Prof. Amjad Ali****, Head, School of Chemistry and Biochemistry, Thapar Institute of Engineering & Technology (Deemed to be University) for extending the opportunity to undertake this doctoral research.*

I would like to profoundly thank my doctoral committee members ***Prof. Kulvir Singh*** *of School of Physics and Materials Science,* ***Prof. Amjad Ali*** *and* ***Prof. Bonamali Pal****, School of Chemistry & Biochemistry, Thapar Institute of Engineering & Technology (Deemed to be University) for their immense help and guiding me towards the right direction. My heartful thanks the staff members of the School of Chemistry & Biochemistry and Department of Chemical Engineering, Thapar Institute of Engineering & Technology (Deemed to be University) for their valuable contribution, spiritual and moral support.*

I am also very thankful to ***Prof. Pramod K. Bajpai,*** *Former Distinguish Professor, Department of Chemical Engineering, Thapar Institute of Engineering and Technology for his guidance during my Ph.D. time period.*

I warmly thank all my friends and lab mates Dr. Manisha Sharma, Mrs. Akansha and Mrs. Balpreet Kaur for a great time and moral support. I will forever cherish the warmth shown by them, whose smiling faces always inspired me.

I would like to gratefully acknowledge the financial support from ***Department of Science & Technology (DST)****, Government of India throughout the course of this work.*

Besides this, I am thankful to the persons who knowingly and unknowingly helped me during the successful completion of this work.

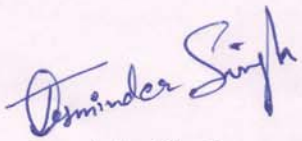

Jasminder Singh

TABLE OF CONTENTS

List of Figures

List of Tables

List of Symbols

atm	Standard atmosphere
b	Heat of adsorption, J mol^{-1}
B	Temkin constant related to the heat of adsorption, J mol^{-1}
C	Effluent CO_2 concentration, volume %
C_o	CO_2 inlet concentrations, volume %
C_p	Specific heat capacity of the adsorbent, J g^{-1} K^{-1}
k_1	Pseudo-first order rate constant, min^{-1}
k_2	Pseudo-second order rate constant, g $mmol^{-1}$ min^{-1}
k_n	Fractional order rate constant
K_L	Langmuir adsorption isotherm constant, atm^{-1}
K_F	Freundlich adsorption isotherm constant, mmol g^{-1} $atm^{-1/n}$
K_T	Temkin adsorption isotherm constant, atm^{-1}
kPa	kilopascal
M	Mass of the adsorbent, g
n	Fractional order model constant related to driving force
N	Total number of experimental points
P	CO_2 partial pressure in atm
psi	Pounds per square inch
$q_{t\ (exp)}$	Experimental CO_2 adsorption capacity, mmol g^{-1}
$q_{t\ (pred)}$	Predicted CO_2 adsorption capacity, mmol g^{-1}
q_e	Dynamic adsorption capacity at equilibrium, mmol g^{-1}
q_m	Maximum monolayer adsorption capacity, mmol g^{-1}
q_t	CO_2 adsorption capacity at time t, mmol g^{-1}
Q	Gas flow rate, ml min^{-1}
Q_{st}	Isosteric heat of adsorption, kJ mol^{-1}

Q_{th}	Thermal energy, J mol^{-1}
R	Universal gas constant, kJ mol^{-1} K^{-1}
R^2	Regression coefficient
S_{BET}	BET surface area, m^2 g^{-1}
t	Time, min
T	Temperature, K
V_{meso}	Mesopore volume, cm^3 g^{-1}
V_{micro}	Micropore volume, cm^3 g^{-1}
V_P	Total pore volume obtained at a relative pressure of 0.99, cm^3 g^{-1}

Greek Letters

$Å$	Angstrom
Θ	Theta
λ	Wavelength

List of Abbreviations

A%	Relative area contribution
B. E.	Binding energy
BET	Brunauer–Emmett–Teller
BJH	Barrett–Joyner–Halenda
C_{18}TAB	Octadecyltrimethylammonium bromide
FA	Furfuryl alcohol
GHG	Greenhouse gase
HF	Hydrofluoric acid
PEI	Polyethyleneimine
PEG	Polyethylene glycol
ppm	Parts per million
PSA	Pressure swing adsorption
PSD	Pore size distribution
SEM	Scanning electron microscopy
TMB	Trimethyl benzene
TEM	Transmission electron microscopy
TEPA	Tetraethylene penta amine
TEOS	Tetraethoxysilane
TG	Thermogravimetry
TPD	Temperature programmed desorption
TSA	Temperature swing adsorption
wt.%	weight%
XPS	X-ray photoelectron spectroscopy
XRD	X-ray diffraction

List of Publications

1.1. Related to Ph.D. work

i. **Jasminder Singh**, Haripada Bhunia, Soumen Basu, Synthesis of porous carbon monolith adsorbents for carbon dioxide capture: breakthrough adsorption study, *Journal of the Taiwan Institute of Chemical Engineers* 89 (2018) 140-150. (Impact Factor: 3.8)

ii. **Jasminder Singh**, Soumen Basu, Haripada Bhunia, Dynamic CO_2 adsorption on activated carbon adsorbents synthesized from polyacrylonitrile (PAN): kinetic and isotherm studies, *Microporous and Mesoporous Materials* 280 (2019) 357-366. (Impact Factor: 4.1)

1.2. In related area

i. **Jasminder Singh**, Soumen Basu, Haripada Bhunia, Synthesis of oxygen and sulphur enriched crack-free carbon monoliths for dynamic CO_2 capture, *Chemical Engineering Journal*, 374 (2019) 1-9. (Impact Factor: 8.3)

ii. **Jasminder Singh**, Haripada Bhunia, Soumen Basu, CO_2 adsorption on oxygen enriched porous carbon monoliths: kinetics, isotherm and thermodynamic studies, *Journal of Industrial and Engineering Chemistry* 60 (2018) 321–332. (Impact Factor: 4.9)

iii. **Jasminder Singh**, Soumen Basu, Haripada Bhunia, CO_2 capture by modified porous carbon adsorbents: Effect of various activating agents, *Journal of the Taiwan Institute of Chemical Engineers*, 102 (2019) 438-447. (Impact Factor: 3.8)

iv. **Jasminder Singh**, Haripada Bhunia, Soumen Basu, Adsorption of CO_2 on KOH activated carbon adsorbents: Effect of different mass ratios, *Journal of Environmental Management*, 250 (2019) 109457. (Impact Factor: 4.8)

v. Balpreet Kaur, **Jasminder Singh,** Raj Kumar Gupta, Haripada Bhunia, Porous carbons derived from polyethylene terephthalate (PET) waste for CO_2 capture studies, *Journal of Environmental Management*, 242 (2019) 68-80. (Impact Factor: 4.8)

Conferences/Workshops

- International Workshop on Carbon Capture & Sequestration at GNDU, Amritsar, Punjab on November 12-16, 2016.
- National Symposium on Applications of Radioisotopes and Radiation Technology in Industry, Healthcare and Agriculture at TIET, Patiala, Punjab on November 28-29, 2016.
- 70^{th} Annual Session of Indian Institute of Chemical Engineers, CHEMCON – 2017 at Dept. of Chemical Engineering, Haldia Institute of Technology, Kolkata, India on December 27 – 30, 2017.

Abstract

The increasing trend of CO_2 concentration in the atmosphere is the main cause for the enhancement in global warming which is known as the biggest environmental problem. The combustion of fossil fuels by humans raises the concentration of CO_2 in the atmosphere day by day. Increase in the fossil fuels burning leads to enhance the CO_2 emissions in the atmosphere which increases the greenhouse effect. Among the various mitigation pathways, Carbon capture and storage (CCS) is the most significant technology to reduce the CO_2 concentration in the environment by capturing it from the large point sources. The CCS has three techniques i.e. post-combustion, pre-combustion and oxy-combustion capture, among which post-combustion capture is known to be effective in the reduction of greenhouse gas (GHG) emissions. It includes several methods like absorption, cryogenics, adsorption, membrane, and other techniques. Among them, adsorption via solid materials is one of the effective techniques in CO_2 capture practical applications due to its cost-effectiveness, high CO_2 uptake, and low energy necessities.

Porous carbons are known to be most efficient adsorbents because of their high surface area and large pore volume. These adsorbents can be developed from various low cost sources using different methods like carbonization of low-cost precursors, sol-gel method, nanocasting technique, chemical activation method, etc. Nanocasting and chemical activation methods are known to be effective methods for the development of high surface area carbon adsorbents. In the nanocasting technique, generation of porous structure and tuning of their surface area can be easily done in the preparation of carbon adsorbents. This method consists of three major steps: synthesis of the template, precursor impregnation and then template removal. On the other side, chemical activation method consists of the impregnation of carbon precursor with the chemical activating agents followed by the carbonization process (inert atmosphere) and then acid washing. This results in the formation of micropores in the structure via dehydration process and incorporates various heteroatoms like oxygen, sulfur, boron, nitrogen in the carbon framework. Such heteroatoms help to increase the Lewis basic character of the adsorbent via addition of the various basic functionalities on the adsorbent surface and beneficial to capture CO_2.

In the present work, two different types of nanostructured carbon adsorbents have been developed i.e. nanocasted carbon monoliths and polyacrylonitrile (PAN) activated carbons. Carbon monoliths were prepared by using nanocasting technique and activated PAN adsorbents were synthesized by using chemical activation process. The CO_2 adsorption experiments were performed using the fixed bed adsorption system under various conditions (5-12.5 % CO_2 and 30-100 °C temperature). Regeneration, kinetics, adsorption isotherm and thermodynamic studies have been also performed in details. Finally, energy duty for desorption of adsorbed CO_2 was also estimated.

Porous carbon monoliths were obtained through nanocasting technique from silica monoliths (hard template) and furfuryl alcohol (precursor). These carbon adsorbents were evaluated as sorbents for CO_2 capture by using fixed-bed adsorption set up under dynamic conditions. Carbonization at different temperatures (550 to 950°C) was carried out and resulted in the generation of different carbon adsorbents containing oxygen functional groups. The textural characterization results reveal the effect of nanocasting technique, which is confirmed from the generation of mesopores (0.41 $cm^3\ g^{-1}$), micropores (0.85 $cm^3\ g^{-1}$) and high surface area (1225.1 $m^2\ g^{-1}$) of adsorbent carbonized at 950 °C. It shows highest CO_2 uptake of 1.0 mmol g^{-1} at 30 °C and 12.5 % CO_2 concentration. The increase in the adsorption capacity with increasing CO_2 concentration and decrease with the increasing adsorption temperature confirms the physisorption process. Five adsorption-desorption cycles show established materials with excellent regeneration stability as an adsorbent. Furthermore, three kinetic models along with three isotherms were used in the present study to analyze the adsorption data and found that fractional order kinetic model and Temkin isotherm fitted best. Thermodynamic studies suggest the exothermic, spontaneous as well as the feasibile nature of the adsorption process.

PAN-based activated carbon adsorbents have been synthesized by using the simple and cost-effective route of carbonization followed by chemical activation process. The effect of different activating agents like $NaNH_2$, NaOH, K_2CO_3, and KOH on the textural properties of PAN and its adsorption potential for CO_2 under dynamic conditions was investigated. The KOH activated carbon adsorbent exhibited the surface area of 1890 $m^2\ g^{-1}$ whereas, $NaNH_2$, NaOH, and K_2CO_3 activated carbons showed the surface area of 833 $m^2\ g^{-1}$, 1020 $m^2\ g^{-1}$ and 1250 $m^2\ g^{-1}$ respectively. The porosity of the adsorbents was affirmed by SEM and HRTEM analysis. Whereas, XPS analysis have revealed the various types of basic functional groups which contain oxygen and nitrogen elements on the carbon surface. The adsorbent, PAN-KOH shows the best CO_2 uptake of 1.2 mmol g^{-1} which is about four times the adsorption

capacity of the carbonized PAN (0.32 mmol g^{-1}) with the flowing 12.5 % CO_2 concentration. Moreover, the adsorbents showed a stable adsorption capacity over multiple sorption cycles. The best information of the adsorption at all adsorption temperatures was given by fractional order kinetic model whereas, the best fit of Freundlich isotherm model with the adsorption data and high Q_{st} values confirms the adsorbents' surface heterogeneity. Thus, the present study provides a two-step synthesis process to produce nitrogen and oxygen-containing activated carbons from low-cost and commercially available PAN for its use in the CO_2 capture practical applications.

Chapter 1 – Introduction

1.1 Effects of CO_2 emission

In the Earth's atmosphere, greenhouse gases like CH_4, CO_2, O_3 and N_2O are considered to be responsible for the rapid climate change [1]. Among these, CO_2 contributes greatly to the global warming because its emission is the main contributor to the atmosphere. The emissions of CO_2 into the environment from both natural and human sources contribute greatly to the global warming [2, 3] which leads to rise the average global surface temperature and ocean acidification [4]. The CO_2 emissions in the environment are almost entirely caused by the fuels combustion which are used to generate energy [5]. Also, the unusual usage of carbon-emitting fuels is a serious threat to the environment [6].

Today (June 2019), the global average CO_2 concentration is 411.97 ppm [7] and expected to reach the level of 570 ppm by the year 2100 [8]. It has been calculated that ca. 35 billion metric tons of CO_2 is released in the atmosphere by the humans every year, majorly from energy sources [9]. This increase in the CO_2 concentration will create problems such as sudden climate change, increase in the acidity of oceans and serious health issues for the living-beings [10, 11]. In 2008, India, European Union, USA, and China contributed global CO_2 emissions 6 %, 13 %, 19 %, and 23 % respectively and it is expected that India's contribution will increase to 10 % CO_2 emissions till 2035 [12]. The global surface temperature has increased by 0.85 (±2) °C from the year 1880 to 2012 [13] and predicted to rise by 2-6 °C in the future (21^{st} century) [14, 15]. The global sea level has increased by 0.19 m in the time period of 1901-2010. The pH drop by 0.1 leads to increase the ocean acidity and hence effects the marine life [16-18]. In 2010, CO_2 emissions from fossil fuels reached 32±2.7 gigatonnes CO_2 per year and further increased by ~3 % in 2011 and by ~1-2 % in 2012 [19]. It also affects the functioning of the ecosystem along with tree physiology and growth. Moreover, the increasing concentration of CO_2 distorted the global carbon balance in the ecosystem and stimulate photosynthesis [20]. There was the drastically increase in the global greenhouse gas (GHG) emissions during the year 1980 to 2019 [5].

1.2 Mitigation pathways

Various techniques like geo-engineering technologies, reducing in energy demand by using energy conversion devices, renewable energy sources, utilization of low carbon fuels and carbon capture and storage (CCS) technology are implemented to decrease the emissions of CO_2. Currently, CCS is the main technology to reduce GHG emissions as well as CO_2 concentration in the environment [21]. Most importantly, CCS has the potential to decrease the CO_2 emissions by ~85-90 % from fixed point sources [22].

1.3 CO_2 capture and sequestration

CCS concept was introduced in 1977 when it was proposed that CO_2 can be captured from the power plants and then stored geologically [23]. International Energy Agency (IEA) claimed that CCS has the ability to decrease 17 % CO_2 emission globally by the year 2050 [24]. Basically, CCS involves the CO_2 capture along with its storage to decrease the atmospheric CO_2 amount. In this process, CO_2 is captured from the power plants or industrial sources and then separated from the other gases. Then it will be compressed and transported to the storage site as shown in Fig. 1.1. The compressed CO_2 will be then underground stored i.e. sedimentary basins, saline aquifers, and coal reservoirs or stored in the ocean. This way the emitted CO_2 can be stored in the secured places for hundreds of years. The research in this CCS technology is fast growing and broad techniques have been investigated and developed. Although, some invented techniques require improvement in terms of efficiency and cost-effectiveness.

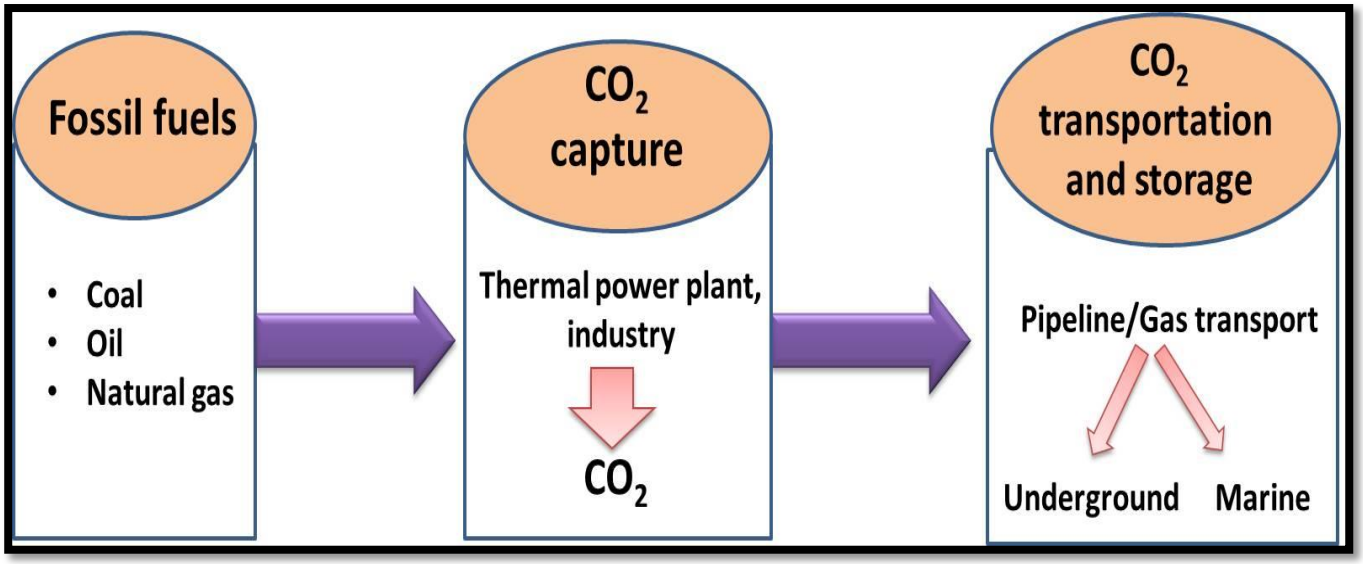

Fig. 1.1 CO_2 capture and storage concept (reproduced from reference [25])

1.3.1 CO_2 capture technologies

The CCS technology consists of three main techniques as shown in Fig. 1.2.

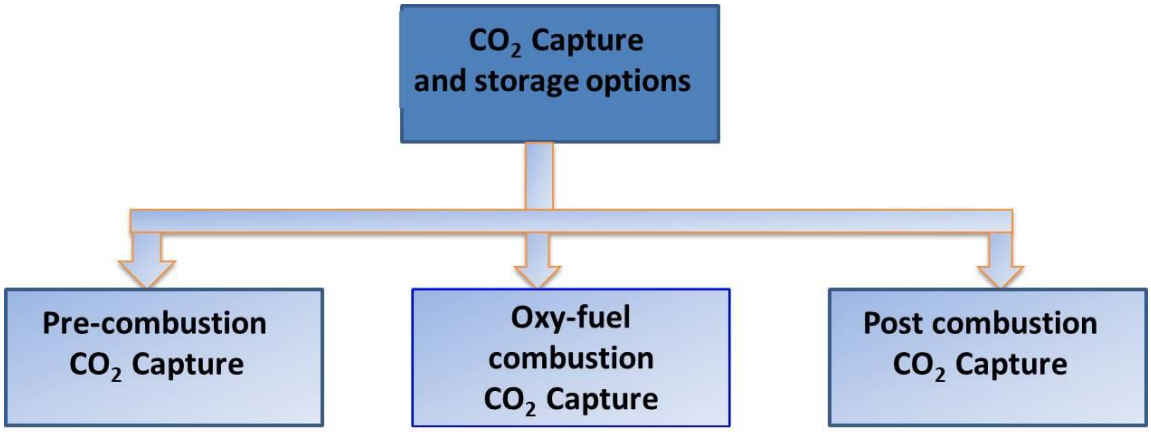

Fig. 1.2 Techniques in the CO_2 capture and storage

1.3.1.1 Pre-combustion capture

In the pre-combustion capture, CO_2 capture occurred prior to the fossil fuel combustion as shown in Fig. 1.3. In this process, the water gas shift reaction occurred after the fossil fuel conversion into the syn gas. The CO_2 has been captured and then separated while H_2 is used as fuel for other applications. This process has several advantages like carbon-free fuel is produced and major product i.e. syn gas can be used in the synthesis of various chemicals. But this technology generally used in the fertilizer industry and for hydrogen generation [26, 27]. Also, this process is known to be expensive as compared to the other techniques.

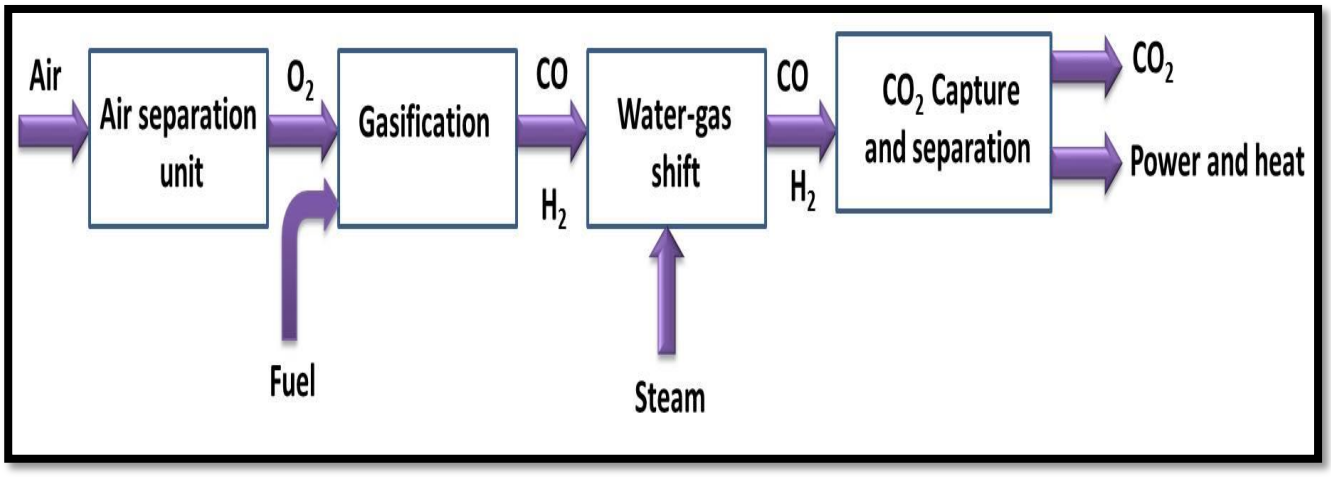

Fig. 1.3 Schematic diagram for a pre-combustion process

1.3.1.2 Oxy-fuel combustion capture

The CO_2 has been captured during the combustion of a fuel with O_2 (> 95 % purity). The schematic diagram for the oxy-fuel combustion process can be seen in Fig. 1.4. High purity CO_2 stream can be produced by using this process in the oxy-fuel combustion process. But, this process consumes a high amount of O_2 from the air separation unit which increases its entire cost. Also, oxygen affects the boiler which causes a lot of risks. Moreover, the flue gas required to recycle again to balance the boiler temperature due to the higher combustion rate of oxygen as compared to that with the air [28].

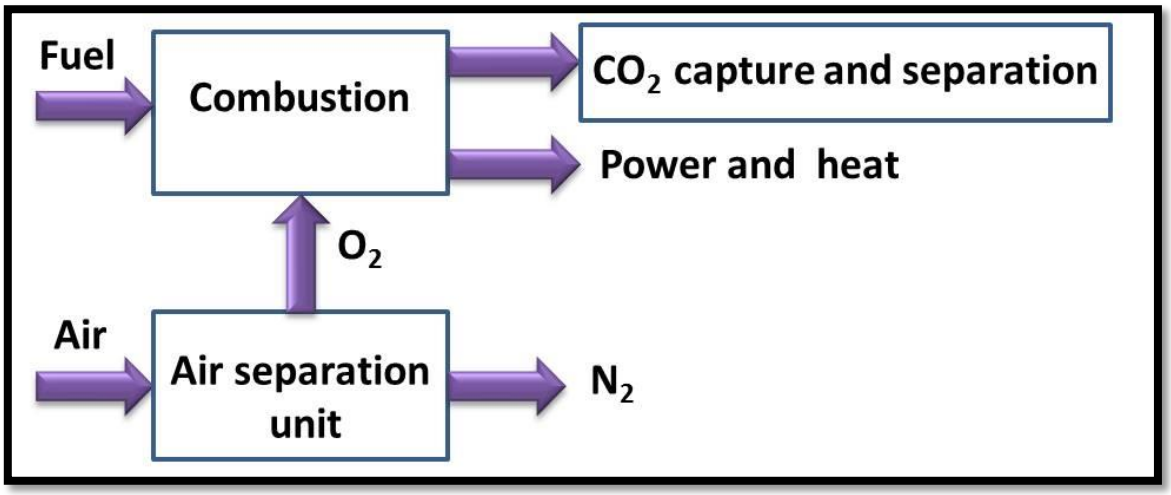

Fig. 1.4 Schematic diagram for the oxy-fuel combustion process

1.3.1.3 Post-combustion capture

A post-combustion technique has been widely implemented in the various chemical processing industries. Here, CO_2 has been captured after the combustion process as shown in Fig. 1.5. This technique is known to be effective for reducing the CO_2 emissions, as it can easily be applied in the power plants without any radical changes [29]. The dry or wet adsorbents have been used in the CO_2 capture process. The exhaust stream is treated prior to the combustion to reduce the concentration of secondary species like sulfur oxide (SO_x), nitrogen oxide (NO_x) and water vapor [30]. This makes it more effective, as the chances for the presence of secondary species is less as compared to the other techniques. The location of the capture plant is nearer to the stack and desulfurization unit, where atmospheric pressure is maintained and CO_2 concentration is in between 10-15 % [31]. The various processes for post-combustion are shown in Fig. 1.6. This process has various advantages as follows:

i. This technique is simpler to implement in the existing plants without any variation in the configuration technology.

ii. Its maintenance doesn't hinder the overall process and it can be easily controlled or regulated. Also, it is flexible and more suitable than the other CO_2 capture techniques.

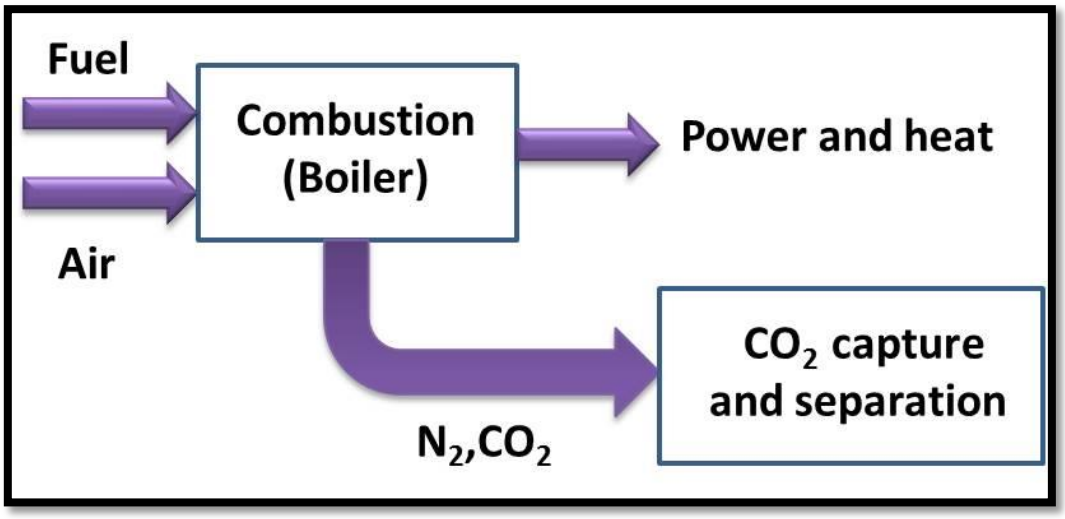

Fig. 1.5 Schematic diagram for a post-combustion process

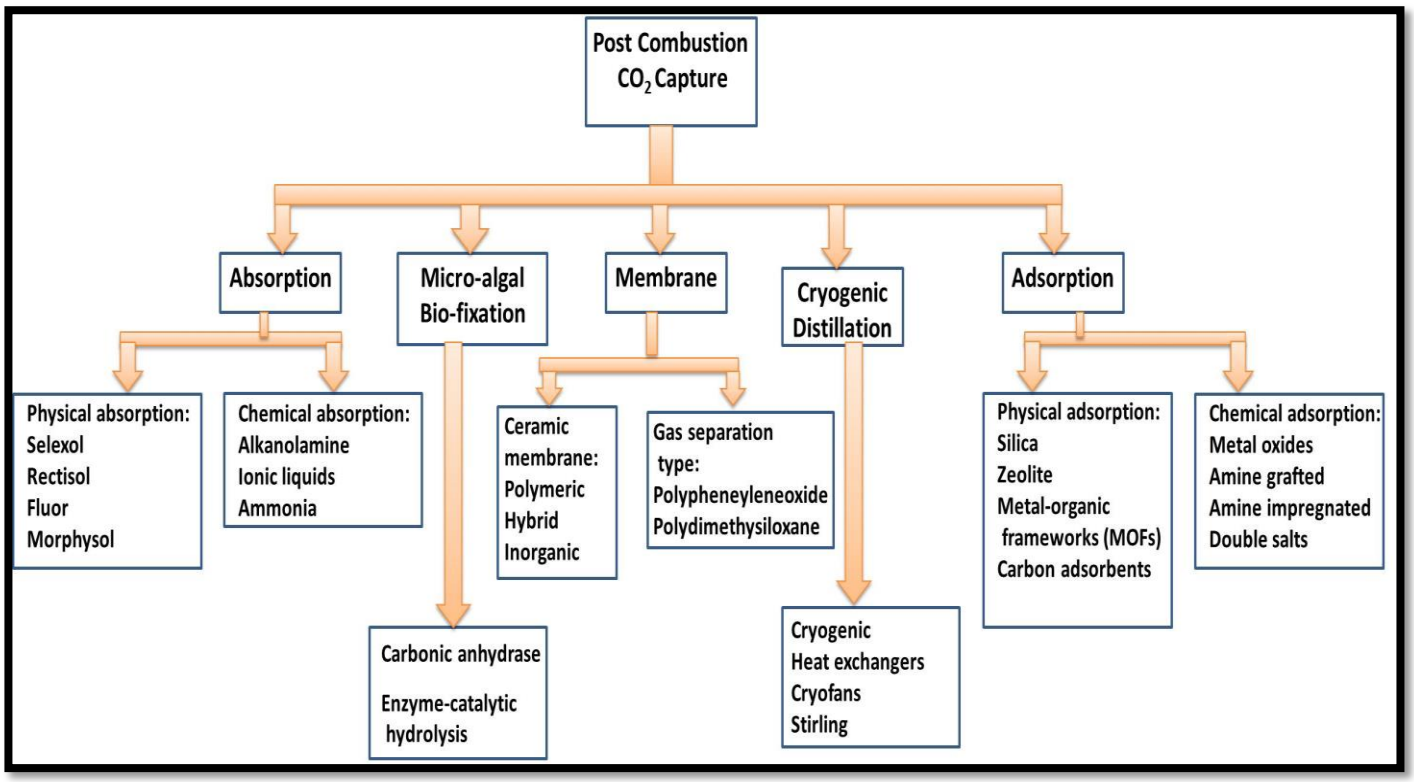

Fig. 1.6 Various processes for post-combustion CO_2 capture

1.3.1.3.1 Absorption

The CO_2 capture via absorption is of two types: physical and chemical absorption. CO_2 is absorbed at a lower temperature in the physical absorption and desorbed at a higher temperature. There are various commercial processes such as selexol, rectisol, fluor and morphysorb. In the chemical absorption, the absorbent is thermally regenerated in absorber and stripper. The flue gas moves in the absorber from the bottom side and gets absorbed by the absorbent. The CO_2 absorbed solvent is passed through the stripper for the regeneration process [32]. For the cyclic use, the absorbent goes back to the absorber after the regeneration process. The captured CO_2 in the stripper is transported and then stored. Most widely, alkanolamines absorbents are used for CO_2 capture applications. The disadvantages of this technology are; (i) low CO_2 capture capacity, (ii) high energy requirement for regeneration, (iii) high corrosion rate of the equipment, and (iv) effect on the absorbent quality due to the infiltration process for the separation of by-products like NO_X, $SO_{X,}$ etc.

1.3.1.3.2 Membrane separation

The membrane separation process is one of the efficient solutions for CO_2 capture. In greenhouse gas separation applications, polymer or ceramic membranes are mainly applied [33] (Fig. 1.7). The disadvantage of this technique is that it is implemented at low CO_2 concentration and pressure. Moreover, it is used to separate O_2 from CO_2 from natural gas [34, 35].

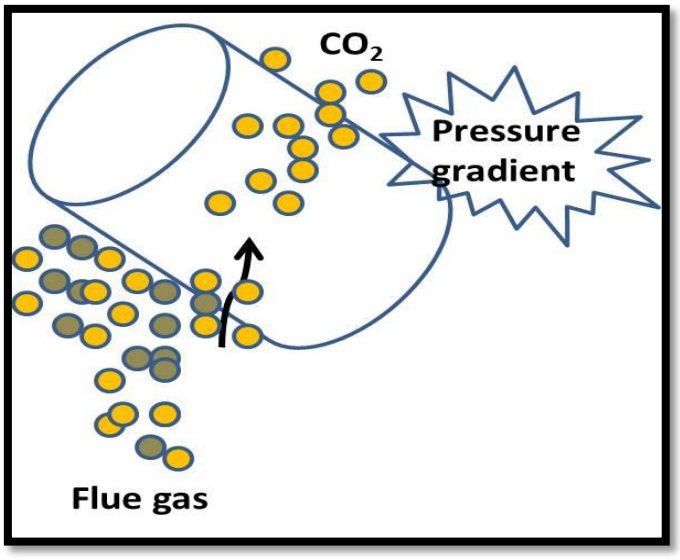

Fig. 1.7 Schematic diagram for the membrane carbon capture process

1.3.1.3.3 Cryogenic distillation

Cryogenic separation technique involves the pressure difference between the flue gas and liquid state temperature. The CO_2 gas gets cooled, condensed and removed from flue gases. Its disadvantages are that it requires huge energy and implemented at higher CO_2 concentrations [34, 36].

1.3.1.3.4 Microalgal bio-fixation

Microalgal bio-fixation CO_2 capture process involves the utilization of photosynthetic organisms (microalgae) for the capture of CO_2. Aquatic microalgae have larger carbon fixation rates which make it effective in this process. The used micro-algal culturing is cost-effective and the obtained products have great value for the revenue generation [37].

1.3.1.3.5 Adsorption

As compared to the above-mentioned techniques in the post-combustion CO_2 capture, adsorption is more energy efficient process as well as of low operation cost. The adsorption process using different adsorbents is a better option because of (i) low energy demand (ii) minimal environmental impact and (iii) low costs [38, 39]. An ideal adsorbent should have the right characteristics such as well-developed pore-structure, basic character, high CO_2 uptake capacity, selectivity, easy regenerability and stability [40].

1.4 Thesis motivation and objectives

It has been observed that the researchers put many efforts for the enhancement in CO_2 adsorption performance of the conventional materials through amine impregnation or via high thermal treatment using different chemical agents. But it leads to create some problems like less stability, pore blockage of the relevant adsorbents etc. Therefore, porous carbon adsorbents are found to be more effective, have low-cost, fast kinetics, wide availability, tunable porosity, and excellent stability over a broad range of operating conditions [41, 42]. Many researchers have developed carbon adsorbents via direct carbonization process or using various activation processes like physical and chemical activation, which requires a high amount of energy and also time-consuming. Also, the prepared carbons are in powder form, has some disadvantages like low heat/mass transfer, high-pressure drop and mechanical

attrition [43]. Moreover, the CO_2 adsorption of these adsorbents was evaluated under static conditions which are not useful for the practical application point of view [44]. Very less attention has been given by the researchers on the nanocasting technique for the preparation of monoliths for CO_2 capture which is very important to control the textural properties of the adsorbents. Therefore, the objectives of this work are to develop the carbon adsorbents in the form of monoliths using nanocasting technique and study the influence of various activating agents on low-cost carbon material like PAN. The dynamic CO_2 capture performance was evaluated using a fixed bed adsorption set up at various CO_2 concentrations from 5 to 12.5 %. The goal of this study is to establish simple way to synthesize the porous carbons for the continuous removal of CO_2 from a point source. The specific objectives are:

- Synthesis of carbon adsorbents with specific pore structures and surface areas using nanocasting and without nanocasting method from various carbon precursors and silica as a template.
- Modification of synthesized carbon adsorbents by chemical activation.
- Performance evaluation of the carbon adsorbents using fixed bed adsorption set-up and study the effects of various parameters like temperature, pressure, CO_2 concentration, etc. on the CO_2 removal performance.
- To fit the equilibrium and kinetic models for the experimental data.

1.5 Thesis overview

This thesis consists of **six chapters**. Porous carbon monoliths were synthesized using nanocasting method and activated polyacrylonitrile adsorbents were developed via carbonization followed by chemical activation process using various activating agents. The carbons were thoroughly characterized by different techniques to examine the textural as well as surface properties. The CO_2 adsorption analysis of the carbons was investigated using the fixed bed CO_2 adsorption system under various conditions (5-12.5 % CO_2 and 30-100 °C). In addition, regenerability, adsorption kinetic, isotherm, CO_2/N_2 selectivity including thermodynamic studies have also been explored in details. The required energy for CO_2 desorption was also calculated. The schematic presentation of the overall thesis work is represented in Fig. 1.8.

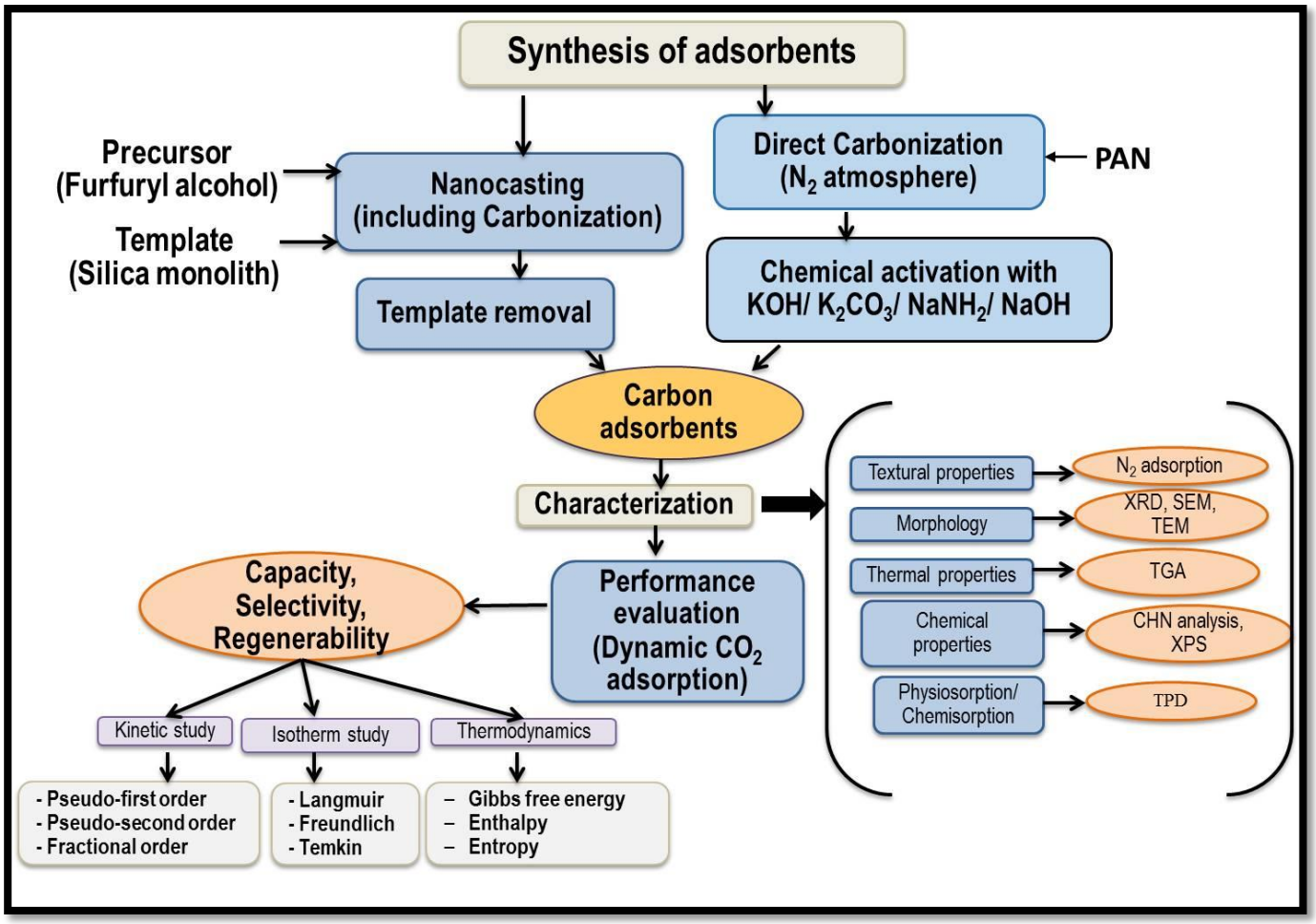

Fig. 1.8 Schematic presentation of the overall thesis work

Chapter 1 is the introduction which deals with the current environmental problems caused by the emission of harmful gases like CO_2. It explains the effect of increasing CO_2 emissions globally and mitigation pathways for reducing its concentration. It involves the brief depiction of CO_2 capture including the research gap and the specific objectives of this work.

Chapter 2 deals with the literature review on the adsorption technology with the detailed study on different adsorbents like silica, zeolite and porous carbon for CO_2 capture. The carbon-based adsorbents have been explored in details as the present work focuses on it.

Chapter 3 covers the materials used for the preparation of the adsorbents and the experimental methods used for the characterization. The experimental set up which has been used for conducting the adsorption-desorption experiments are also presented in detail. The adsorption kinetic and isotherm theories have also been discussed in this chapter including thermodynamic parameters.

Chapter 4 discusses the synthesis of carbon monoliths via nanocasting method using furfuryl alcohol (carbon precursor) and monolithic silica (template). CO_2 capture performance of the carbons has been evaluated and the results are related to their physico-chemical properties. The CO_2 capture performance for the monoliths was evaluated under various parameters like CO_2 feed concentration and adsorption temperature. This chapter also includes the complete kinetic, isotherm and thermodynamic study for the adsorbents. Furthermore, the experiments for CO_2 selectivity and regeneration study were also conducted. Finally, energy duty required for CO_2 desorption was investigated.

Chapter 5 covers the development and characterization of activated polyacrylonitrile carbon adsorbents via direct carbonization followed by the chemical activation using various activating agents. CO_2 adsorption-desorption studies on these carbons were carried out under dynamic conditions and the optimized sample was investigated comprehensively. This study also explains the adsorption isotherm and kinetics for the adsorbents at different temperatures. Furthermore, the experiments for CO_2 selectivity and regeneration study were conducted. The energy duty needed for CO_2 desorption was also calculated.

Chapter 6 presents the conclusions and the recommendations for future work.

At last, the references cited in this work have been listed.

Chapter 2 – Literature Review

2.1 Adsorption technology

In the adsorption process, the adsorbent surface holds the adsorbate molecules i.e. CO_2 and creates its film on the adsorbent. It may be physisorption or chemisorption. In the physisorption process, the adsorbate held on the adsorbent surface via weak Van der Waals forces. After the adsorbent gets saturated with CO_2, desorption process is carried out by increasing the temperature of its surface. Initially, adsorption begins as a monolayer then multilayer adsorption takes place. In the chemisorption process, the interaction of adsorbate and adsorbent takes place via chemical bonds. It is a monolayer as well as irreversible process and releases the heat greater than the heat of condensation. By increasing the temperature, the chemisorption first increases and then decreases.

In the adsorption technology, CO_2 adsorption can be done by using various approaches; like pressure swing adsorption (PSA) and temperature swing adsorption (TSA). PSA process is known to be simple, cyclic and low energy requiring process. It is basically a high-pressure phenomenon, the adsorbate gases are held on the adsorbent surface. The pressure has been varied between the CO_2 adsorption and desorption. Initially, the gas mixture passed to the column under high pressure until the adsorbent gets saturated with CO_2. Afterward, the stability and reusability of the adsorbent are investigated by changing the pressure. In this way, the adsorption cycle can be performed in the fixed bed after the completion of the regeneration process. However, the disadvantage is that, it includes a low recovery rate [45]. In the TSA process, the temperature of the column is changed for CO_2 adsorption and desorption. The flue gas is firstly passed through the column and the desired temperature is maintained. After the adsorbent gets saturated with CO_2, the temperature of the bed is increased to nearly 200 °C to execute the desorption process. Later, the bed is cooled down to the desired temperature and the other adsorption cycle can be continued. TSA process requires more time as compared to PSA but it gives the higher purity of CO_2 (> 95 %) and ca. 80 % of recovery which makes it more effective than the other processes [46, 47].

2.2 Types of adsorbents

The adsorption technology can be made successful by selecting the appropriate adsorbent. The number of porous solid adsorbents based on zeolites, silica, porous carbons, and carbon nanotubes has been used by various researchers [48, 49]. These adsorbents generally show good CO_2 adsorption capacity, high selectivity, and regenerability. The properties of the adsorbents are discussed in the subsequent section. The main focus will be given on the carbon-based adsorbents, as they are employed in the present work.

2.2.1 Zeolite based adsorbents

Zeolite consists of microporous features with the crystalline structure with good thermal stability and used in a wide variety of industrial applications [50]. It has the uniform pore size of 0.5-1.2 nm with the interconnecting channels network [51-53]. Most importantly, the CO_2 adsorption efficiencies are dependent on its basicity, charge density, pore size distribution and chemical composition of cations [54]. The zeolites are further modified by different amines like ethylenediamine, monoethanolamine, etc. Also, the alkali and alkaline-earth cations in the zeolite are exchanged for the enhancement in the CO_2 uptake. However, the CO_2 adsorption capacity can be enhanced via these approaches but still have disadvantages like low CO_2/N_2 selectivity along with low CO_2 uptake capacity [55]. In the presence of moisture, its CO_2 capture capacity declines and requires higher temperature (> 300 °C) for the regeneration process. Zeolites based adsorbents can be divided into three main types i.e. synthetic zeolites, zeolites with metal-exchanged skeletons and zeolitic imadazolate frameworks (ZIFs).

2.2.1.1 Synthetic zeolites

The synthetic zeolites like NaX, NaKA, zeolite Rho, are commonly used for CO_2 capture applications using vacuum swing adsorption (VSA) and pressure swing adsorption (PSA) system [56]. Akhtar *et al.* [57] synthesized porous zeolite NaKA monoliths with pulsed current processing and further modified with K^+. They found very high CO_2-over-N_2 selectivity for the as prepared monoliths and obtained the highest CO_2 adsorption capacity of 4 mmol g^{-1} at 25 °C. Krishna investigated the CO_2 capture for NaX zeolite from the mixture of CO and CH_4 using a pressure swing adsorption system at ~26 °C, and found the CO_2/CH_4 and CO_2/CO selectivity greater than 25.40. The strong CO_2 affinity of the adsorbents resists the desorption process and hydrophilic features of the adsorbent lead to effective water

adsorption than CO_2 [58]. To improve this limitation, Miyamoto *et al.* [59] used CHA type zeolite for CO_2 adsorption in the PSA system. They obtained the CO_2 adsorption capacity of 3.1 mmol g^{-1} (40 °C, 1.6 MPa total pressure) and low nitrogen selectivity (< 0.1 mmol g^{-1}) which is much higher than the zeolite 13X. Interestingly, the adsorbents showed hydrophobic characteristics. As a result of this, co-existing water has no influence on the CO_2 uptake capacity. Cavenati *et al.* [60] prepared the zeolite 13X and CO_2 capture performance was evaluated using a pressure swing adsorption system and found the uptake capacity of 6.5 mmol g^{-1} at 10 bar and 25 °C.

2.2.1.2 Zeolites with metal-exchanged skeletons

The electropositive and large cations have been introduced into the zeolite structure for enhanced CO_2 adsorption. Yang *et al.* [61] synthesized zeolites via hydrothermal process and further modified it by ion exchange method using Li^+, Na^+, and Ca^{2+} ions. The CO_2 sieving is dependent on the orifice diameter of the adsorbents and Na-zeolites exhibited the highest CO_2 selectivity in comparison to Li-zeolites and K-zeolites.

Medina *et al.* [62] synthesized silicate-1 membrane zeolite via hydrothermal process and modified it using lithium solution. The modified zeolite membrane showed the CO_2/N_2 separation factor up to 6 at 25 psi and 400 °C which was much greater than the unmodified zeolite (1.46 psi). The surface diffusion mechanism affected positively on the excellent performance of the zeolites. The zeolite Rho was used for the CO_2/CH_4 separation in the PSA set up. They obtained the selectivity of ~10 at higher pressure (400-600 kPa) and ~75 at lower pressure of 100 kPa at 30 °C [63]. It was found that the enhanced CO_2 uptake capacity leads to the extremely high selectivity of the adsorbent.

2.2.1.3 Zeolitic imidazolate frameworks (ZIFs)

ZIFs are the metal organic frameworks consist of tetrahedral coordinated metal ions like Zn, Co linked with imidazolate. Due to the several advantages of porous nature, thermal and chemical stability, these are used for CO_2 adsorption applications [64].

Keskin *et al.* [65] investigated the CO_2/CH_4 and H_2/CO_2 separation performance for ZIF membranes using molecular separation method. They found that the membrane of ZIF-11 showed the high CO_2/CH_4 separation performance whereas the membrane of ZIF-65 is the good adsorbent for H_2/CO_2 separation.

ZIF-95 membrane has been prepared using the solvothermal process and found the 25.7 mixture separation factor for H_2/CO_2. In the presence of steam, the H_2/CO_2 selectivity was found to be constant for 24 h, showing the excellent hydrothermal stability of ZIF-95 molecular sieve membrane [66] .

2.2.2 Silica-based adsorbents

Silica materials exhibit the high surface area and tunable porosity which make them suitable for the enhanced CO_2 capture [67]. However, the pure form of silica is not capable to offer the more adsorption sites to adsorb CO_2. The hydroxyl groups on the surface facilitate the grafting of various amine groups which enhance its affinity towards CO_2 molecules.

Ji *et al.* [68] analyzed the increasing trend in CO_2 capture capacity from 3.2 to 4.5 mmol g^{-1} by increasing the temperature from 30 to 75 °C for pentaethylenehexamine loaded hierarchical porous silica. The highest value of CO_2/N was 0.35 at 75 °C. Afterwards, they found the decrease in the adsorption capacity (3.5 mmol g^{-1}) by increasing the temperature to 90 °C. Mesoporous silica SBA-15 was impregnated by varying the amount of polyethyleneimine (PEI) and analyzed the effect of adsorption temperature [69]. The maximal CO_2 uptake of 2.04 mmol g^{-1} was acquired for SBA-15-PEI (50) at 1 bar and 75 °C. The adsorption-desorption cycles were conducted in successive cycles and found the excellent regenerability because of its chemisorption character. The amine coating increases the N-content of the adsorbents but decreases the microporous volume of carbons which decreased the CO_2 adsorption capacity at room temperature.

Hierarchical porous silica-based monoliths have been prepared and then impregnated with polyethylenimine (PEI) and tetraethylenepentaamine (TEPA). Amine-impregnated monolith silica exhibited higher CO_2 capture capacity than other amine-based silica adsorbents and showed a durable as well as reversible sorption performance. In particular, the PEI/monolith exhibited CO_2 uptake of 4.77 mmol g^{-1} at 75 °C under pure CO_2 flow and also, showed excellent performance in moisture-containing CO_2 condition [70].

Alkhabbaz *et al.* [71] synthesized amino silica adsorbents using poly(allylamine) (PAA) and guanidinylated poly(allylamine) (GPAA) for dynamic CO_2 capture. They found the highest CO_2 adsorption capacity for PAA impregnated and GPAA adsorbents of 1.53 mmol g^{-1} and 1.38 mmol g^{-1} (under 10 % CO_2 at 25 °C) respectively.

The SBA-15 silica was impregnated with polyethyleneimine (PEI) and exhibited the static CO_2 uptake of 2.04 mmol g^{-1} at 75 °C and 1 bar, for the sample with the PEI

impregnation of 70 wt% [72]. Liu *et al.* [73] loaded mesoporous silica with tetraethylenepentamine (TEPA). They found the increase in the CO_2 uptake from 1.5 mmol g^{-1} to 2.9 mmol g^{-1} by varying the loading of TEPA from 10 wt% to 50 wt% at 60 °C under 10% CO_2 concentration. They found a decrease in the CO_2 uptake by 5 % after 40 multiple cycles of adsorption-desorption.

The nano-silica adsorbent has been prepared using amine immobilization on the silica surface and found the maximal CO_2 uptake of 3.8 mmol g^{-1} (at 40°C and 100 kPa CO_2) for the adsorbent grafted with a higher molecular weight of PEI [74]. Le *et al.* [75] synthesized tetraethylenepentamine (TEA) functionalized silica microspheres using dodecylamine as a template and tetraethoxysilane as a precursor followed by functionalization with TEA. They found the maximal uptake of 4.27 mmol g^{-1} for the 34 wt% TEA loaded sample at 75 °C and found the good regenerability over multiple cycles.

Xu *et al.* [76] modified MCM-41-type molecular sieves with PEI for CO_2 capture studies. They found the maximum CO_2 uptake of 3.02 mmol g^{-1} (at 75 °C under pure CO_2 flow, rate- 100 ml min^{-1}) at 1 atm pressure, ca. 24 times greater than the untreated MCM-41. Hicks *et al.* [77] prepared aminosilica-based SBA-15 adsorbents and found the uptake of 3.09 mmol g^{-1} at 25 °C (at 10% CO_2/Ar saturated with water flow rate- 20 mL/min). The sample showed a negligible loss in the adsorption capacity after recycling it.

The wet impregnation method has been used for the synthesis of silica monoliths with the loading of PEI. The CO_2 capture performance was evaluated using thermogravimetric analysis. The maximum CO_2 adsorption capacity of 2.4 mmol g^{-1} at 75 °C (100 kPa CO_2 partial pressure) obtained for the adsorbent with the loading of 60 wt% of PEI. Furthermore, excellent regenerabiltiy for the adsorbents was obtained for 8 cyclic runs of adsorption and desorption [78]

Kjdary *et al.* [79] synthesized mercaptopropyl-modified silica and then incorporated Cu, Fe, g, and Au nanoparticles. The CO_2 performance evaluation was done on a thermogravimetric basis. The Cu based silica adsorbents exhibited the maximal CO_2 capture capacity of 0.52 mmol g^{-1} at 50 °C and 1.0 atm pressure. Moreover they found the heat of adsorption of 35 kJ/mol.

The MCM-41 silica has been modified with amine and exhibited the CO_2 uptake of 0.70 mmol g^{-1}, greater than the untreated MCM-41 (0.12 mmol g^{-1}) at a lower pressure (0.1 bar). At higher pressure (2.1 bar), amine-modified silica showed the CO_2 uptake capacity of 1.15 mmol g^{-1} and MCM-41 exhibited the uptake of 1.0 mmol g^{-1} [80].

2.2.3 Carbon based adsorbents

Porous carbons preferred more as compared to the silica and zeolite materials for CO_2 capture studies because of its well-developed porous structure (can be prepared with a large fraction of micropores). Also, it exhibits wide availability, low cost, adjustable porosity and requires low energy for regeneration [41, 42]. Different types of carbon-based adsorbents like commercial activated carbons, carbon adsorbents from renewable resources as well as synthetic polymers and carbon nanotubes (CNT) have been used for CO_2 capture. The detailed study on different carbon adsorbents is discussed below.

2.2.3.1 Commercial activated carbons

Due to the low cost and high textural properties of commercial carbon materials like charcoal, activated carbons, they have been utilized in CO_2 adsorption studies. Most of the researchers used these carbons for high-pressure swing CO_2 adsorption.

Plaza *et al.* [81] used Norit R2030CO2 for dynamic CO_2 capture. They found the CO_2 capture capacity of 0.77 mmol g^{-1} at 30 °C and 130 kPa. Na *et al.* [82] found the CO_2 uptake capacities of 3.2 and 1.6 mmol g^{-1} at 15 °C and 55 °C (at 1 bar under pure CO_2 flow) respectively, for the commercial activated carbon. Pressure swing adsorption system was used for the CO_2 adsorption performance of the carbons.

MAXSORB commercial activated carbon has been used for the CO_2 capture studies and exhibited the static CO_2 uptake of 25.7 mmol g^{-1} at 30 bar and 25 °C [83].

Raganati *et al.* [84] used activated carbon DARCO FGD (Norit) for CO_2 capture performance in sound assisted fluidized bed. They found the CO_2 capture capacity of 0.38 mmol g^{-1} with the breakthrough time of 10 s at room temperature under 15 % CO_2.

2.2.3.2 Carbon adsorbents from renewable resources

Porous carbons have been prepared from carbon containing renewable precursors such as peat, wood, coconut husk, cellulose, etc. These precursors produce the porous carbons either by treatments like carbonization or activation processes. Such carbons are enriched in porosity, which makes them suitable for effective CO_2 adsorption. In the carbonization process, the selected precursor was carbonized in the inert atmosphere to produce the porous carbonaceous char [85]. On the other side, activated carbons from

renewable carbon precursors are prepared by using two major methods: physical and chemical activation. The carbonaceous precursor is carbonized in the flow of CO_2, steam, air or sometimes the mixture of various gaseous activating agents [86, 87]. It has been reported that this method is time-consuming, cost-intensive and requires more energy for the production of microporous carbons [86-88]. The selected carbon precursor is carbonized with the various activators like KOH, K_2CO_3, NaOH, $NaNH_2$, $ZnCl_2$, etc. in the chemical activation method. This process generates the highly porous structure via pyrolytic decomposition of the precursor's structure. However, the activation temperature, time and heating rate play an essential role in achieving ACs with specific characteristics [89].

Wang *et al.* [90] prepared porous carbons from waste celtuce leaves via air-drying, pyrolysis (600 °C) in an argon atmosphere and then activated with KOH. They found the CO_2 uptake capacity of 6.04 mmol g^{-1} at 0 °C under ambient pressure. In another study, carbon adsorbents from fungi-based carbons via KOH activation was synthesized for CO_2 uptake studies and found the highest CO_2 adsorption capacity of 5.5 mmol g^{-1} and CO_2/N_2 selectivity of 27.3 at 0 °C and 1 bar [91]. Shen *et al.* [92] prepared hierarchical microporous carbons using yeast as a carbon precursor and found the CO_2 capture capacity of 4.77 mmol g^{-1} at 25 °C. However, the samples were regenerated through the evacuation at 150 °C for 2 h under 103 mbar. The bean dreg was used for the development of activated carbon via KOH activation for CO_2 capture by Xing *et al* [93]. The adsorbents exhibited the CO_2 uptake of 4.24 mmol g^{-1} at 25 °C (1 atm pressure). This was attributed to the fact that the basic nitrogen functionalities in the adsorbent attracted CO_2 molecules effectively and enhanced the CO_2 uptake capacity. Sevilla *et al.* [94] developed N-doped carbons via KOH activation of polypyrrole and activated temperature was varied from 600 to 800 °C. They obtained the CO_2 capacity of 6.2 mmol g^{-1} at 0 °C under 1 atm and found the CO_2/N_2 selectivity of 5.3. They found the good regenerability for 6 multiple adsorption-desorption cycles.

Gonzalez *et al.* [95] developed activated carbons from the olive stones and almond shells via physical activation with CO_2. They found the CO_2 capture capacity of 0.61 mmol g^{-1} and 0.58 mmol g^{-1} for olive stone and almond shell carbons respectively, at 14 % CO_2 concentration, 50 °C and 120 kPa. Furthermore, CO_2/N_2 selectivity was found to be 18 for olive based and 20 for almond based adsorbent respectively.

The carbonized polysaccharides were chemically activated with KOH in different mass ratios of 1-4 [96]. The optimized carbon sample with the KOH mass ratio of 2, exhibited the surface area of 1260 m^2 g^{-1} and found the highest CO_2 capture capacity of 6.1 mmol g^{-1} at 0 °C under 100 % CO_2 flow.

Singh *et al.* [97] developed activated carbons from prolific waste biomass activated with $ZnCl_2$ using pressure swing adsorption system. They found the maximal surface area and CO_2 adsorption capacity of 1863 m^2 g^{-1} and 18.2 mmol g^{-1}, respectively at 0 °C under 30 bar pressure.

Porous carbons have been developed from camphor leaves via hydrothermal carbonization followed by KOH activation [98]. The PSA system was used for CO_2 uptake studies and the pressure was varied from 1 to 4 bar. They found the highest surface area of 1633.71 m^2 g^{-1} and CO_2 uptake capacity of 6.63 mmol g^{-1} at 25 °C and 0.4 MPa for the sample treated at activation temperature of 240 °C.

Gil *et al.* [99] synthesized the carbons from phenol–formaldehyde resins, biomass residue, and olive stones. The CO_2 capture performance was evaluated thermogravimetrically and found the maximal CO_2 uptake of 2.11 mmol g^{-1} at 35 °C under pure CO_2 flow, rate-100 ml min^{-1}under atmospheric pressure.

The carbon adsorbents from rice husk have been prepared via KOH activation at various activation temperatures from 640 to 780 °C [100]. They found the maximum CO_2 adsorption capacity of 6.24 mmol g^{-1} (1 bar) at 0 °C for the sample activated at 780 °C.

2.2.3.3 Carbon adsorbents from synthetic polymers

In comparison to the conventional activated carbons, the porous carbons prepared from synthetic polymers exhibited many advantages like tunable porosity, easy to attain the precise morphology and better chemical composition control. These carbons can be synthesized via various techniques like nanocasting, direct carbonization and chemical activation [101, 102]. This section consists of two major parts: template-free synthesis i.e. carbonization/activation and nanocasting technique i.e. including template.

2.2.3.3.1 Template free synthesis

Liu *et al.* [103] synthesized carbon adsorbents from furfural resin by using the carbonization temperature of 600 °C for 4 h under N_2 flow. They obtained the maximum CO_2 uptake capacity of 1.6 mmol g^{-1} at 25 °C. Przepiorski *et al.* [104] treated CWZ-35 carbon with high-temperature ammonia and CO_2 capture performance was evaluated thermogravimetrically. They found the highest uptake of 1.72 mmol g^{-1} (30 °C at 1025 hPa under pure CO_2 concentration with the flow rate of 25 ml min^{-1}) for the sample treated at 400 °C.

The carbon adsorbents have been developed by the loading of PEI on mesoporous carbons [105]. The carbons with 65 wt% loading of PEI showed the maximum adsorption capacity of 4.82 mmol g^{-1}, under 15 % CO_2/N_2 flow at 75 °C. The adsorbents showed the easy regenerability at 100 °C and stability over multiple cycles.

Chen *et al.* [106] developed carbons from terephthalaldehyde and melamine-based polymer synthesized under modified solvothermal reaction conditions. They obtained the maximal adsorption capacity of 3.20 mmol g^{-1} under pure CO_2 flow at 25 °C, 1 atm and CO_2/N_2 selectivity of 32. The adsorbents exhibited the good regenerability over ten consecutive adsorption-desorption cycles.

The textural parameters like surface area along with the meso-/micro/-pore volume are significant parameters for the enhancement of the gas adsorption on carbons. Therefore, the carbonaceous material is further modified with various activating agents (eg. KOH, NaOH, etc.) to generate the microporous structure in it [107].

The carbon adsorbents developed by phenolic resins and Pluronic F127 (as a soft template) subjected to KOH activation. The CO_2 adsorption performance was evaluated at 0 and 25 °C and found that adsorbent with KOH activation prepared at 500 °C exhibited CO_2 uptake of 7 mmol g^{-1} at 0 °C and 760 mmHg pressure [108].

Wickramaratne *et al.* [109] developed carbon spheres via carbonization followed by KOH chemical activation process. The sample activated with KOH mass ratio of 4 exhibited the surface area of 2400 m^2 g^{-1} with the maximum CO_2 adsorption capacity of 4.6 mmol g^{-1} at 23 °C and 1 bar.

Nitrogen enriched carbons have been synthesized using soybean via $ZnCl_2$ activation followed by physically activation (CO_2). The adsorbents exhibited CO_2 adsorption capacity of 0.51 mmol g^{-1}, greater than the commercial carbon (0.36 mmol g^{-1}) at 75 °C under 15.4 % CO_2 concentration. The existence of nitrogen functionalities in the adsorbent matrix showed the basic character of the adsorbent [110].

Zhu et al. [111] used petroleum coke as a precursor and chemically activated with KOH for CO_2 adsorption studies. They found the CO_2 adsorption capacity of 3.43 mmol g^{-1} along with the CO_2/N_2 selectivity of 9.4 at 0.1 MPa for the carbon adsorbent prepared at activated temperature of 700 °C.

The sulfur-doped activated carbons have been developed for CO_2 adsorption studies by some researchers. Saha *et al.* [112] prepared S-doped carbons using sodium thiosulfate and found the CO_2 uptake capacity of 2.06 mmol g^{-1} at 25 °C under pure CO_2 concentration. S-doped carbon materials have been synthesized using reduced-graphene-oxide/poly-thiophene

as activating agent and acquired the CO_2 capture capacity of 4.5 mmol g^{-1} at 25°C and 1 atm [113].

The novel mesoporous carbons have been prepared using $NaNH_2$ activation and further loaded with pentaethylenehexamine. The CO_2 adsorption performance was evaluated thermogravimetrically and found the uptake capacity of 2.34 mmol g^{-1} of the 53.7wt% loaded PEHA adsorbent at 30 °C under pure CO_2 concentration [114].

Kim *et al.* [115] developed N-doped carbon adsorbents from PAN via KOH activation and acquired the CO_2 uptake of 1.02 mmol g^{-1} at 25 °C under 0.15 bar. Bai *et al.* [116] prepared KOH treated PAN fibers which shows the CO_2 uptake of 0.76 mmol g^{-1} under 1 bar at 25 °C. Also, PAN activated carbon fibers are prepared by using KOH as activator by Shen *et al.* [117] and found the CO_2 capture capacity of 1.3 mmol g^{-1} at 25 °C.

The spent coffee grounds were carbonized and KOH activated with different mass ratios (1-4) to prepare the activated carbons. The maximum adsorption capacity was obtained 3.0 mmol g^{-1} at 25 °C for the sample with the KOH mass ratio of 3 using thermobalance apparatus in atmospheric pressure [118]. On the other side, Gonzalez *et al.* [119] obtained the adsorption capacity of 5 mmol g^{-1} at 0 °C and 120 kPa for the same sample using volumetric apparatus.

Marco-Lozar *et al.* [120] synthesized activated carbon via NaOH (N) and KOH (K) activation of anthracite (A), sub-bituminous coals (Sb), and lignite (L). The NaSB31, KL31, and KA21 activated carbons exhibited the CO_2 uptake capacities of 27, 22 and 17.5 mmol g^{-1} respectively, at 25 °C and 4000 kPa.

2.2.3.3.2 Nanocasting technique

Nanocasting technique utilizes the removable inorganic template to generate the macro-/meso-/micro-porous carbons. It is mainly three-step process consisting of (i) impregnation of the precursor into the micrometer or nanometer size pores of the template; (ii) carbonization of the impregnated template under controlled atmosphere and (iii) lastly removal of the template framework [121]. The schematic diagram for the nanocasting technique is shown in Fig. 2.1.

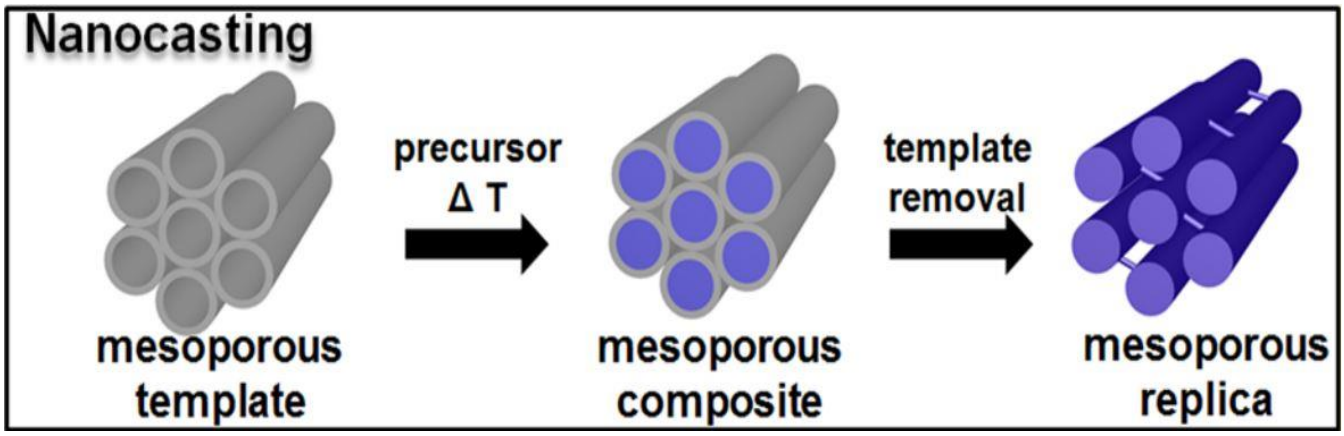

Fig. 2.1 Schematic diagram for the nanocasting technique (reproduced from reference [122])

Silica template based nanostructured carbon adsorbents were synthesized from resorcinol–formaldehyde precursor prepared under different carbonization temperatures. The sample synthesized at 700 °C showed the maximum CO_2 capture capacity of 0.761 mmol g^{-1} at 30 °C under 12.5 % CO_2 [123].

Tiwari *et al.* [8] developed mesoporous carbon adsorbent using zeolite and epoxy resin. The CO_2 capture performance was evaluated at different temperatures (30 to 100 °C) by using fixed bed adsorption experimental setup and found the maximum uptake of 0.65 mmol g^{-1} under 12.5 % CO_2 flow at 30 °C. In another study, oxygen enriched carbon adsorbents developed via nanocasting technique and modified thermogravimetric analyzer was used for the CO_2 capture studies. They found the CO_2 uptake capacity of 0.91 mmol g^{-1} at 30 °C [124].

S-doped carbon adsorbents have been synthesized by using nanocasting technique (zeolite and 2- thiophenemethanol were used as template and sulfur source). The static CO_2 uptake capacity was found to be 2.4 mmol g^{-1} at 25 °C [125].

Sevilla *et al.* [126] prepared mesoporous carbons by nanocasting technique and chemical activation by KOH. Furfural alcohol was taken as the main precursor and mesostructured silica as a template. The obtained optimized sample showed the CO_2 uptake of 3.2 mmol g^{-1} at 25 °C under pure CO_2 concentration. Also, they concluded that the existence of micropores < 1 nm increases the CO_2 capture capacity instead of surface area.

2.2.3.4 Carbon monolith adsorbents

Porous carbons are excellent adsorbents and exhibit broad morphologies both on the macroscopic and microscopic level [127]. In the macroscopic level, a monolithic adsorbent exhibit the wide flexibility of operation in contrast to its powder counterparts whereas, microscopic monolith exhibits significant advantages such as fast heat and mass transfer, easy to deal, and high contacting efficiency [128-130]. It has been reported that the micropores, as well as macropores, are highly beneficial for CO_2 uptake. Microporosity is believed to be most important to trap the CO_2 molecules whereas macropores provided the low resistant pathways for CO_2 diffusion [131]. The various carbon monoliths are compared to a one cent coin in Fig. 2.2.

Fig. 2.2 Photograph of the carbon monoliths compared to a one cent coin (reproduced from reference [132])

Hosseini *et al.* [133] synthesized carbon coated monoliths from furfuryl alcohol as a carbon precursor and found the CO_2 adsorption capacity of 0.52 mmol g^{-1} at 30 °C using 15 % CO_2 concentration. Furthermore, monoliths modified with NH_3 and KOH acquired CO_2 adsorption capacity of 0.58 mmol g^{-1} and 0.66 mmol g^{-1} respectively under same conditions.

MOFs based carbon monolith was synthesized by Qian *et al.* [134] and found the maximum dynamic CO_2 capture capacity of 0.76 mmol g^{-1} at 25 °C under 16% CO_2

concentration. Ding *et al.* [135] synthesized porous carbon monolith via carbonization of IRMOF-3 and found the CO_2 capture capacity of 1.64 mmol g^{-1} at 0 °C and 0.15 bar.

Nandi *et al.* [136] developed N-doped carbon monoliths via carbonization and physical activation (in the presence of CO_2) of PAN monoliths. They found the CO_2 uptake of 5.14 mmol g^{-1} at ambient temperature and pressure.

Carbon monolith has been synthesized from phenolic resin mixed with carbon nanotubes and carbonized under an inert atmosphere. Further, the resulted carbons are physically activated under CO_2 atmosphere. They obtained the CO_2 capture capacity of 1.18 mmol g^{-1} at 25 °C and 114 mmHg under 15% CO_2 concentration [137]. Geng *et al.* [138] developed microporous carbon monoliths derived from biomass using NH_3 assisted activation process and found the CO_2 uptake of 2.81 mmol g^{-1} at 25 °C and 1 bar under pure CO_2 concentration.

Thiruvenkatachari *et al.* [139] analyzed the dynamic CO_2 uptake performance of the monolithic carbon fibre composites. They obtained the CO_2 capture capacity of 3.1 mmol g^{-1} under 13 % CO_2 concentration at 25 °C (101.3 kPa).

Dassanayake *et al.* [140] developed activated carbon from aerocellulose monoliths via carbonization under CO_2 and obtained the adsorption capacity of 5.8 mmol g^{-1} at 0 °C and 1 atm while, at 25 °C, the uptake was 3.7 mmol g^{-1} under pure CO_2 concentration.

2.2.3.5 Carbon nanotubes

Carbon nanotubes exhibit good thermal conductivity, excellent chemical and physical properties. Also, it is easier for the modification of their surface via addition of chemical function groups [32]. Due to these advantages, carbon nanotubes are widely used in CCS.

Sawant *et al*. [141] developed horn-shaped carbon nanotubes via low-temperature solvothermal method using tetrachloroethylene as a precursor. They acquired the surface area of 728.6 m^2 g^{-1} and static CO_2 adsorption capacity of 2.01 mmol g^{-1} at 30 °C and 850 mmHg pressure.

From the literature, it has been found that the current research interests are mainly focused on techniques like direct carbonization or physical/chemical activation for the development of carbons. Not much significant work has been done on the nanocasting technique for the preparation of carbons. Theoretically, CO_2 capture performance evaluation under static conditions (0 or 30 °C), exhibited the superior CO_2 adsorption capacity but in terms of practical application point of view, the CO_2 capture performance should be

investigated under the dynamic conditions. Therefore, there is a need to develop the adsorbents via effective and advanced synthesis processes like nanocasting technique, carbonization followed by chemical activation using effective activating agents. Moreover, performance evaluation of these adsorbents should be done under flue gas conditions i.e high temperature and low CO_2 partial pressure.

Chapter 3 – Experimental Methods, Kinetics and Isotherm Models

3.1 Materials

TEOS was purchased from Alfa Aesar. PEG (MW 400–35,000 g mol^{-1}) and C_{18}TAB was purchased from Sigma Aldrich. TMB, FA, 98 %, oxalic acid, HF, 40 %, sodium amide (95 %), sodium hydroxide (99 %), potassium carbonate (99 %) and potassium hydroxide (99 %) were obtained from Loba Chemie Pvt. Ltd, India. All reagents were used without any further purification. PAN (nitrogen 25.85 %, carbon 13 % and volatile matter 86 %) was obtained from Indian Acrylics Ltd. India and was treated to synthesize the activated carbons.

Various gases (carbon dioxide 99.99 %, helium 99.995 % and nitrogen 99.99 %) used in this work were taken from M/s Sigma Gases and Services, India.

3.2 Characterization methods

3.2.1 Surface area and pore size distribution

The BET surface area and pore size were analyzed through BET surface area analyzer of Bel, Japan, Inc (Microtec BELSORP MINI-II). Before the analysis, the samples were outgassed at 200 °C for 6 h to remove physically adsorbed gases and moisture. The pore volume was calculated at a relative pressure range (P/P_0 = 0.1-0.99) with the amount of nitrogen adsorbed and the pore size distribution (PSD) curves were collected from BJH (Barrett-Joyner-Halenda) method. The micropore size distribution analysis was done by MP plot and NLDFT method.

3.2.2 X-ray diffraction analysis (XRD)

X-ray diffraction analysis of the adsorbents was performed by PANALYTICAL X'Pert PRO diffractometer . Before the analysis, the sample was manually grinded using mortar and pestle. The Cu $K_{\alpha 1}$ radiation (λ= 1.5406 Å) was used and operated at 45 kV. The wide angle 2θ range was varied from 10-80°.

3.2.3 Scanning electron microscopy (SEM)

The SEM images of the samples were collected by JEOL-JSM – 6510 SEM. The accelerating voltage was taken 20.0 kV. Before the analysis, the sample particles was firstly placed on the double sided sticky carbon tape on the plate and then coated with the gold.

3.2.4 Transmission electron microscopy (TEM)

For the TEM analysis, the samples were firstly dispersed on the carbon film coating TEM grids. An extremely small amount of material is suspended in ethanol, after that the carbon-coated grids were immersed into the suspension and allowed to dry. Then, the TEM micrographs were taken at 200 kV using JEOL JEM-2100 microscope.

3.2.5 Thermogravimetric analysis (TGA)

For the thermal degradation investigation of the adsorbents, the thermal analyzer (TA Instruments, Q500, US) was used. Initially, the carbon material (~15 mg) was taken in a pan and then elevated the temperature to ca. 900 °C with the heating rate of 15 degree per minute.

3.2.6 Elemental composition analysis

Thermo Scientific Flash (2000) system was used for the elemental composition (C, H, N) of the adsorbents.

3.2.7 Fourier transform infrared (FTIR) spectroscopy

For the Fourier transform infrared spectroscopy (FTIR) analysis, the powder carbon sample mixed with KBr to form the pellet. Then, it was scanned by Perkin Elmer Spectrum 100 FTIR spectrophotometer in the selected spectral range (4000–600 cm^{-1}).

3.2.8 X-ray photoelectron spectroscopy (XPS)

Surface characterization of the monoliths was done by X-ray photoelectron microscopy (XPS, Omicron ESCA+) with monochromated aluminum source (Al ka radiation at 15 V, hv = 1486.7 eV). The $2X10^{-9}$ torr pressure was maintained in the chamber. XPS peak 4.1 software was used for the data processing of the samples.

3.2.9 Temperature programmed desorption (TPD)

Micromeritics Autochem II 2920 chemisorption was used for the TPD analysis which was equipped with the TCD (Thermal conductivity detector). The pre-treatment was done at 200 °C using helium gas then it allowed to cool at 30 °C for adsorption and CO_2 gas was passed for 30 min. The desorption was performed by passing He and raising the temperature to 250 °C.

3.3 Performance evaluation of adsorbents

The CO_2 performance evaluation was done using fixed bed CO_2 adsorption system (height: 30 cm and inner diameter: 0.93 cm) as shown in Fig. 3.1. The bed temperature was examined by a thermocouple (K-type) fixed with the column. About 2 g of the sample was taken in the adsorption column with a height of the packing ca. 22 cm and elevating the temperature to 200 ºC under a pure N_2 atmosphere for the time period of 2 h. Then it was cooled to the desired temperature (30-100 ºC) and the desired gas mixture (N_2 and CO_2) at 80 cm^3 min^{-1} (elevated at 20 ºC and pressure of 1 atm) was passed through it. The CO_2 volumetric concentration was varied from 5 to 12.5 %. The CO_2 concentration at the bed exit was monitored as a function of time until the outlet CO_2 concentration approached the inlet CO_2 concentration i.e., until the saturation is achieved. Agilent 7890A gas chromatograph (connected with a computer) gives the CO_2 concentration after the complete adsorption process. After the sample gets saturated, the temperature was elevated to 200 °C and pure N_2 was passed through the column to initiate the desorption process. These multiple cycles were performed five times for the regeneration study. The CO_2 uptake capacity (mmol g^{-1}) was evaluated by the eqn. 3.1 [142].

$$q_t = \frac{1}{m}\int_0^t Q\left(C_O - C\right)dt \tag{3.1}$$

where C_o and C are the inlet and effluent concentrations of CO_2 (percent in volume), Q is the gas flow rate in ml min^{-1}, m is the mass of the adsorbent in gram.

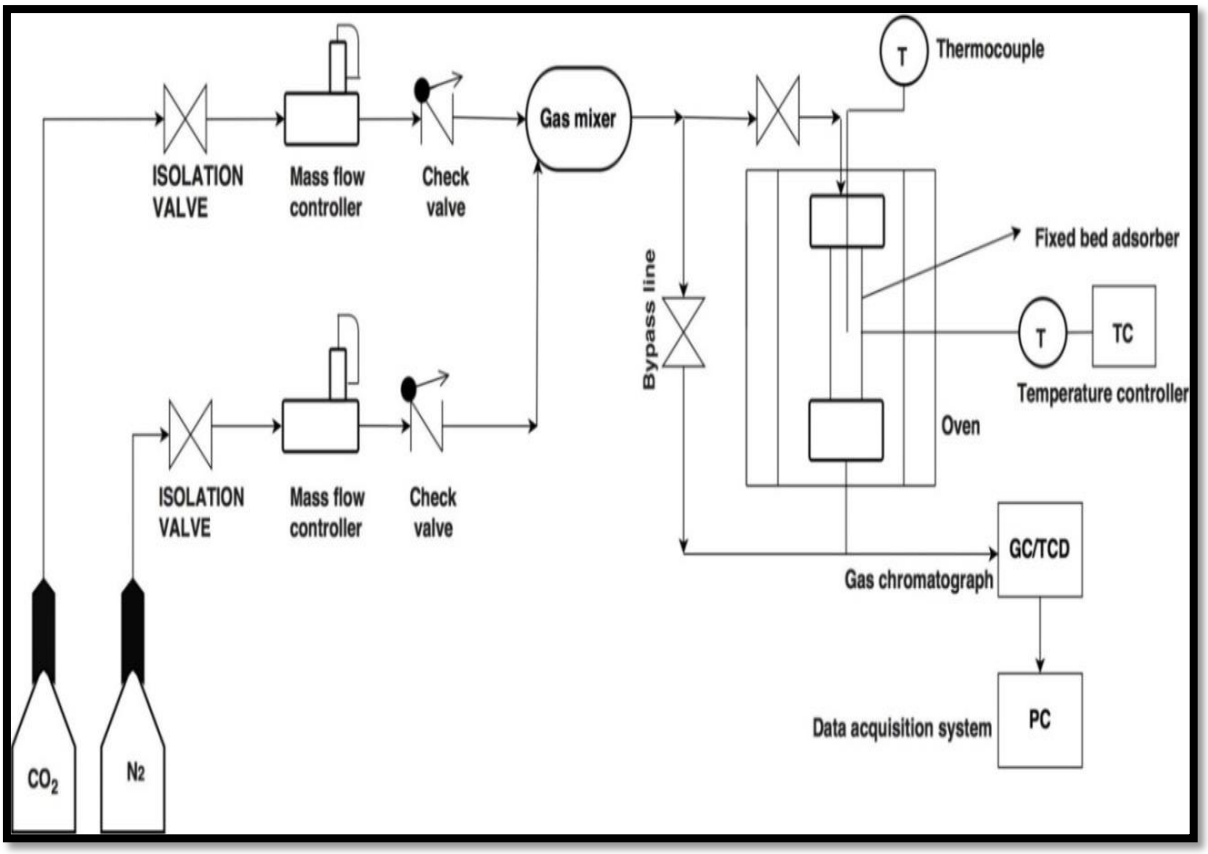

Fig. 3.1 Schematic of the fixed bed CO_2 adsorption/desorption system (reproduced from J Taiwan Inst Chem Eng., 89, 140–150, 2018)

3.4 Adsorption kinetic study

Under the operating conditions during CO_2 adsorption, fast kinetics exhibited by the adsorbents represents its adsorption efficiency towards CO_2. So, the kinetic study is a very essential part of the adsorption process which provides the ability of the adsorbents efficiency towards the high adsorbate flow and gives the information for predicting adsorption rates [142]. In the present study, CO_2 adsorption kinetics of the adsorbents was investigated by using the following kinetic models with the rate equations as follows:

3.4.1 Pseudo-first order model [143]:

In 1898, Lagergen explained about the solid-liquid phase adsorption systems, which included the adsorption of oxalic and malonic acid onto charcoal. The Lagergren's first order rate equation which has been also called the Pseudo-first-order equation, was one of the equations in early time which explained the adsorption rate based on the adsorption capacity.

From the more than five decades, this equation has been widely applied by the many researchers to determine the adsorption kinetics [144].

$$q_t = q_e\,(1 - e^{-k_1 t}) \qquad (3.2)$$

Where, q_e and q_t are the amounts of CO_2 adsorbed (mmol g^{-1}) on the adsorbent at equilibrium and at time t, respectively and k_1 is the first order rate constant (min^{-1}).

3.4.2 Pseudo-second order model [145]:

In the middle of 80's, pseudo second order kinetics was introduced and Ho and McKay [145] investigated number of experimental results taken from literature. They concluded that the ''for all of the systems studied, [...] the pseudo-second order reaction kinetics provide the best correlation of the experimental data"[146]. If the pseudo-second order kinetics fitted best in the adsorption system, then the the adsorption mechanism is chemically rate controlling it is a chemisorption process. The advantage of this equation is that, for estimating qe values, is its small sensitivity to the influence of random experimental errors.

$$q_t = \frac{k_2 q_e^2 t}{1 + k_2 q_e t} \qquad (3.3)$$

Where, k_2 (g mmol $^{-1}$ min $^{-1}$) is the pseudo–second order rate constant.

3.4.3 Fractional order model [147]:

The semiemperical kinetic equation was proposed by Heydari-Gorji and Sayari to describe the CO_2 adsorption rate on amine functionalized adsorbents [147]. The adsorption rate was presumed to be propotional to the mth power of the adsorption time and nth power of the driving force. The kinetic equation represented as follows:

$$\frac{\partial q_t}{\partial t} = k_n\, t^{m-1}\,(q_e - q_t)^n \qquad (3.4)$$

where m, n, and k_n are the fractional order kinetic model constants. This represents the complexity in the reaction mechanism which involves more than one reaction pathways [148]. The parameter k_n could be an overall parameter that may couple various adsorption related factors. Integrating the above-mentioned boundary conditions gives the equation 3.5. If the adsorption mechanism follows this kinetic order model, the process is favorably physiosorption.

$$q_t = q_e - \frac{1}{\left[\left((n-1)k_n/m\right)t^m + \left(1/q_e^{n-1}\right)\right]^{1/n-1}} \quad (3.5)$$

Where, k_n is the rate constant, m and n are the model constants.

3.4.4 Error calculation

In addition, the accuracy of each kinetic model is predicted by R^2 (linear regression coefficient) and error % values which are given by:

$$Error\ (\%) = \sqrt{\frac{\sum\left[\left(q_{t(exp)} - q_{t(pred)}\right)/q_{t(exp)}\right]^2}{N-1}} \times 100 \quad (3.6)$$

Where, $q_{t(exp)}$ and $q_{t(pred)}$ are the experimental and predicted CO_2 loading, respectively and N is the number of experimental points.

3.5 Adsorption isotherm study

To predict the adsorption mechanism and know about the adsorbate and adsorbent interaction, adsorption isotherm study is very useful. In this regard, CO_2 experimental adsorption data were fitted to three standard isotherm models having equations as follows:

3.5.1 Langmuir isotherm model

The Langmuir adsorption isotherm assumes that the monolayer adsorption occurs at homogeneous sites of the adsorbent surface with no interaction among the adsorbed molecules. It is known as simplest as well as the most useful method for adsorption isotherm study. The Langmuir equation can be written as [149]:

$$q_e = \frac{q_m K_L P}{1 + K_L P} \quad (3.7)$$

Where, q_m (mmol g^{-1}) is the maximum monolayer adsorption capacity at CO_2 partial pressure (P, atm) whereas K_L (atm^{-1}) is Langmuir constant.

3.5.2 Freundlich isotherm model

The Freundlich isotherm model is used to describe the heterogeneous system and valid for the multilayer adsorption over the surface of the adsorbent with a non-uniform distribution of adsorption. The Freundlich equation can be written as [150]:

$$q_e = K_F P^{1/n} \quad (3.8)$$

Where, K_F (mmol g^{-1} atm $^{-1/n}$) and n are Freundlich constants indicating adsorption capacity and intensity respectively.

3.5.3 Temkin isotherm model

The Temkin isotherm model assumes that the adsorption energy decreases linearly by increasing surface coverage and illustrates the heterogeneous surfaces of the adsorbent. The Temkin equation can be presented as [151]:

$$q_e = B\, ln(K_T P) \tag{3.9}$$

Where, K_T (atm^{-1}) is the Temkin constant and B is the constant related to heat of adsorption. B = RT/b [(b is Temkin constant related to heat of sorption ($Jmol^{-1}$) and R is the universal gas law constant = 8.314 J $mol^{-1}K^{-1}$].

3.6 Thermodynamic study

3.6.1 Thermodynamic parameters

The change in Gibbs free energy ΔG^0 (kJ mol^{-1}), standard molar adsorption enthalpy ΔH° (kJ mol^{-1}) and ΔS^0 (kJ mol^{-1} K^{-1}) has been evaluated by the equations (3.9 and 3.10) as follows:

$$\Delta G^0 = -RT \ln(K_{eq}) \tag{3.10}$$

$$\frac{\mathrm{d}\ln(K_{eq})}{\mathrm{d}T} = \frac{\Delta H^\circ}{RT^2} \tag{3.11}$$

Where, K_{eq} is the equilibrium constant. ΔH^0 and ΔS^0 values are calculated from Van't Hoff plot by using the equation (3.10).

3.6.2 Energy duty for desorption

Another important aspect of the thermodynamic study is the energy requirement for the regeneration process. The desorption of CO_2 should be calculated for the binary system under dynamic conditions.

The thermal energy input (Q_{th}) can be written as:

$$Q_{th} = Q_{st} + Sensible\ heat \tag{3.12}$$

Sensible heat [152, 153] can be written as:

$$Sensible\ heat = \frac{C_p \Delta T}{adsorption\ capacity} \tag{3.13}$$

Where, C_p is the specific heat capacity of the adsorbent, ΔT is the difference between desorption and adsorption temperatures.

Clausius-Clayperon equation [154] has been used to determine the isosteric heat of adsorption (Q_{st}, kJ mol^{-1}) by using the following equation:

$$Q_{st} = -R\left[\frac{\partial \ln P}{\partial\left(\frac{1}{T}\right)}\right]_{q_e} \quad (3.14)$$

Where, Q_{st} (kJ mol^{-1}) is the isosteric heat of adsorption, q_e is the adsorption capacity (mmol g^{-1}) at temperature T (K).

3.7 Software used

OriginPro 8 software was used for fitting various kinetic and adsorption isotherm models to the experimental data by nonlinear regression.

Chapter 4 – Oxygen Enriched Nanocasted Carbon Monoliths for Carbon Dioxide Adsorption

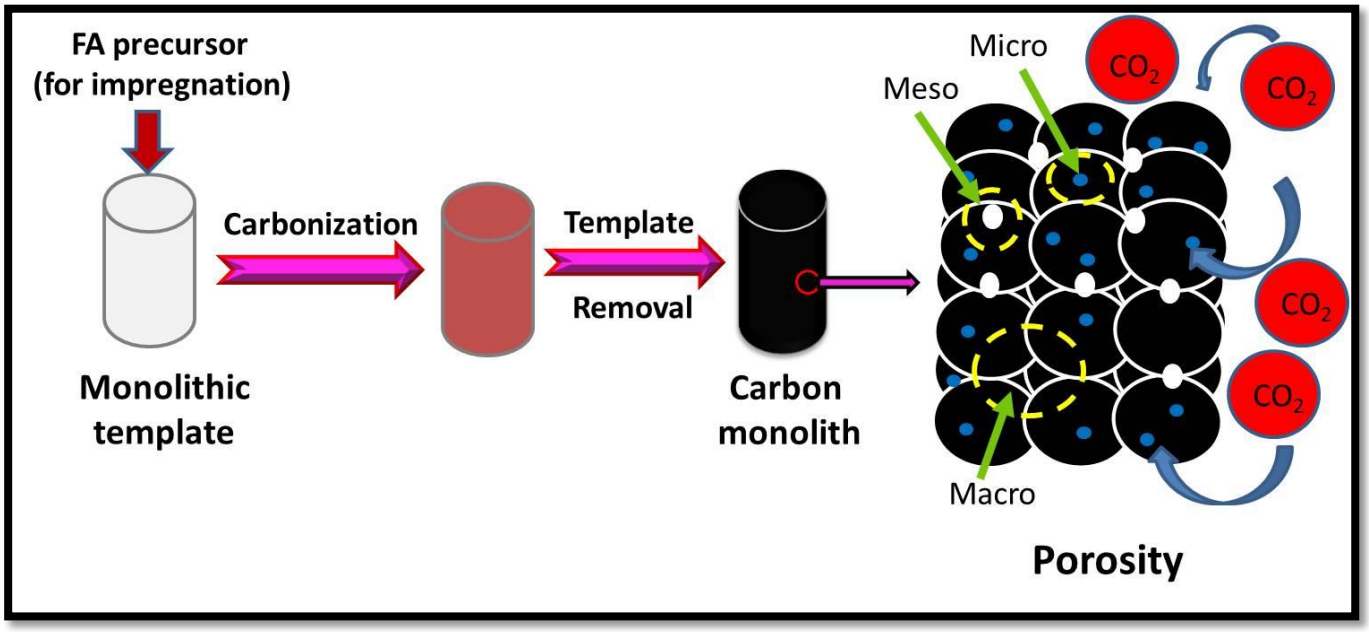

Highlights

- Synthesis of oxygen enriched porous carbon monoliths (CMs) using nanocasting method.
- High CO_2 uptake of 1.0 mmol g^{-1} was observed by CM950 adsorbent.
- Kinetics of CO_2 adsorption follow fractional order kinetic model.
- Heterogeneous nature was found for the synthesized adsorbents.
- CMs exhibit stable and easy regenerability.

4.1 Synthesis of carbon monoliths

4.1.1 Synthesis of silica monoliths

The preparation of the silica monolith (SM) was done by the sol-gel method [155]. Initially, nitric acid was added in the solution of PEG and water. TEOS was inserted after the dissolution and stirred the solution for 10-15 min at room temperature until it became translucent. Then, CTAB surfactant was dissolved into the solution with continuous stirring. The molar ratio of H_2O: HNO_3: TEOS: PEG: CTAB was taken 16.5: 0.53: 2.2: 9.5 $\times 10^{-4}$: 0.2 for the synthesis of SM. The achieved sol was shifted to microplates and kept for 72 h at 40 °C for sol to gel formation. Then, the monoliths were soaked in NH_4OH solution (1M) at 90 °C for 9 h followed by the acidification with 0.1 M nitric acid solution. Later, monoliths were washed with water 5-7 times and kept for drying at 40 °C for 4 days. SMs were obtained after calcination at 550 °C (5 h).

4.1.2 Wet impregnation using furfuryl alcohol

The hard template silica monoliths were degassed under vacuum for 5h and then impregnated with precursor solution (furfuryl alcohol, oxalic acid, and trimethyl benzene where FA: oxalic acid = 250, by molar ratio) for 15 h. The resulted monoliths found to be translucent and then kept in oven at 50 °C for 24 h followed by 90 °C for another 24 h.

4.1.3 Carbonization at different temperatures

The impregnated monoliths were carbonized under an N_2 atmosphere (60 ml min^{-1}) at various temperatures from 550 to 950 °C for 4 h with the heating ramp of 2 °C min^{-1} after isothermal at 150 °C for 3 h.

4.1.4 Removal of the template

The silica-carbon monolith composites were treated with 10 % HF (by volume) for 24 h. The monoliths were washed 5-6 times with H_2O and then kept in an oven at 90 °C for 10 h. The resulted monoliths were assigned as CMT, where T stands for carbonization temperature (550-950 °C). The block flow diagram for the synthesis of carbon monoliths with the parent silica is represented in Fig. 4.1. Firstly, HF is the tremendous toxic acid and strongly corrosive. Therefore, it should be handled with extreme care. HF is usually used for the removal of SiO_2 but after the nanostructures is dried after the etching, the capillary forces

due to the surface tension leads to cause the stiction of freestanding structures to each other. Moreover, the incomplete removal of HF may results in the presence of residual contaminants left behind after drying.

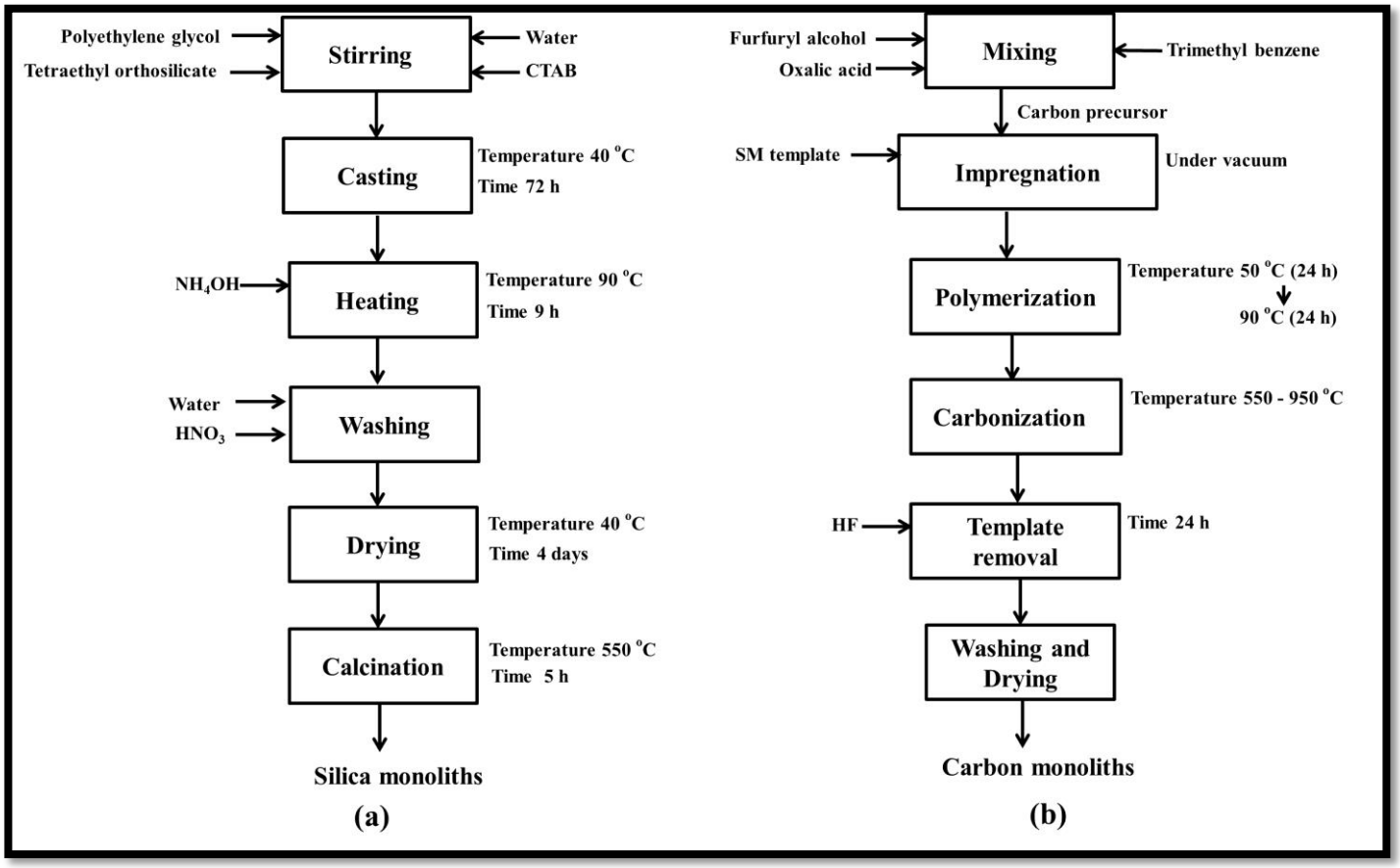

Fig. 4.1 Block flow diagram for the synthesis of (a) silica monolith and (b) carbon monolith (reproduced from J IND ENG CHEM.., 60, 321-332, 2018)

4.2 Characterization of monoliths

4.2.1 Surface area and pore size distribution

The N_2 adsorption-desorption isotherms of the monoliths are given in Fig. 4.2 (a). All the CM samples show both type I and type IV isotherms and H_4 hysteresis loop shows the presence of micropores as well as mesopores. SM sample shows type IV isotherm and H_2 hysteresis loop, illustrates the existence of mesopores [156]. Fig. 4.2(b) depicts the micropore size distribution of the carbon monoliths and exhibits the average pore size of 1-2 nm which verifies the development of microporous adsorbent. The figure in the inset of Fig. 4.2(b), demonstrates the BJH plot of the carbon monoliths confirming the presence of mesopores in the monolithic structure.

It can be seen from Table 4.1, with the increase of carbonization temperature from 550 °C to 950 °C, the surface area and total pore volume gradually increase from 1166.5 m^2 g^{-1} to 1225.1 m^2 g^{-1} and 1.01 cm^3 g^{-1} to 1.26 cm^3 g^{-1} respectively. The t-plot method was used to calculate the micropore volume whereas, the mesopore volume was calculated from the BJH plot. The highest surface area of 1225.1 m^2 g^{-1} was shown by the carbon monolith CM950 that indicates that the carbonization at 950 °C promotes the monoliths towards good textural properties and porosity. It is thus achievable to get good textural properties and porosity of the monoliths at higher carbonization temperatures. On the other side, SM shows lower surface area (760 m^2 g^{-1}) than the CMs but higher pore volume (1.42 cm^3g^{-1}) because of the basic treatment of silica monoliths during synthesis was performed at a temperature above 80 °C for 9 h which results in the large pore volume. After analyzing the results of Table 4.1, it can be concluded that CMs show good textural properties as compared to SM which favorably promote the faster diffusion of CO_2 molecules on the surface, thus significantly improving their CO_2 adsorption capacity.

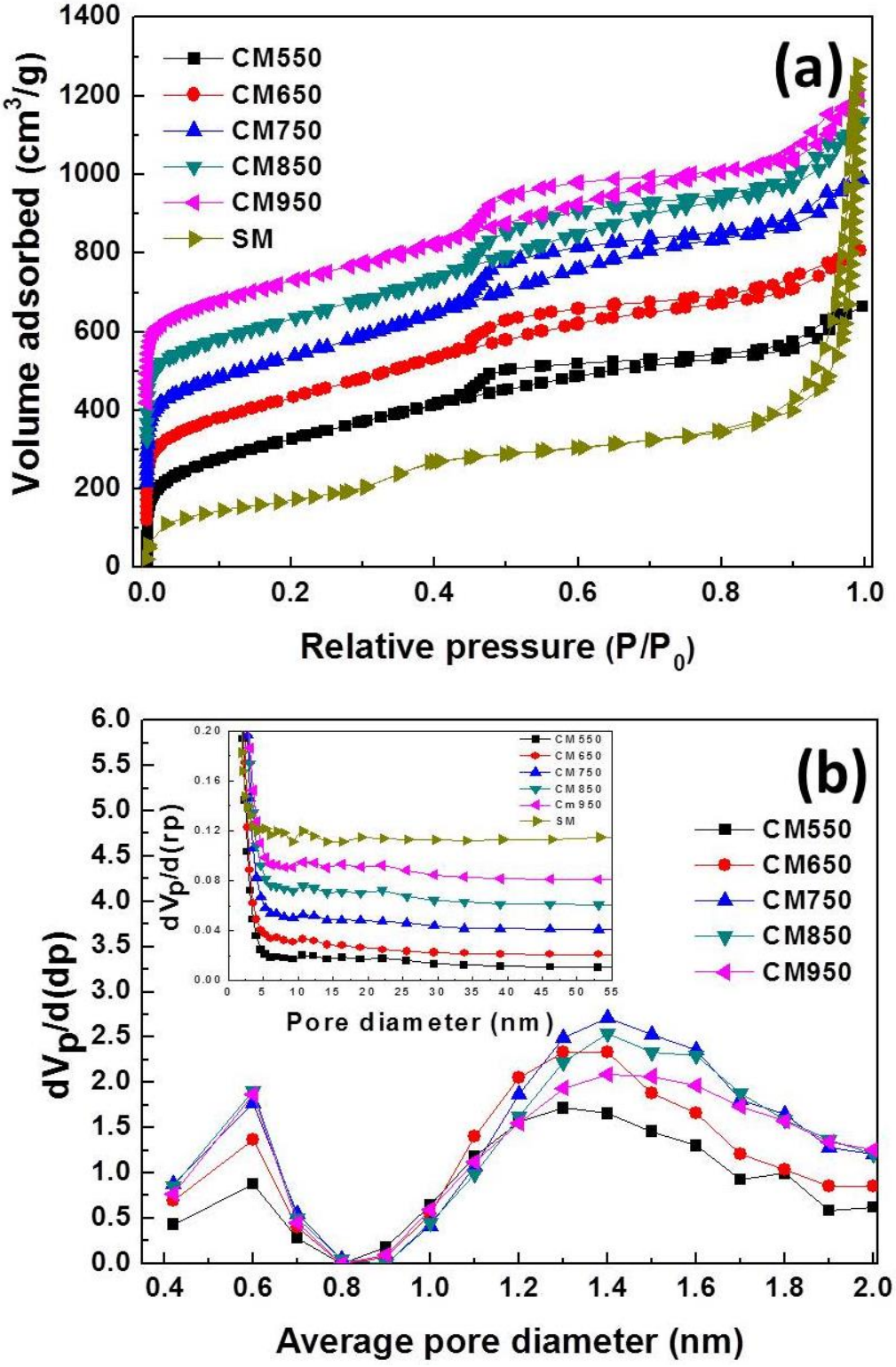

Fig. 4.2 (a) N_2 sorption isotherms and (b) PSD curves of the monoliths (inset shows the BJH plot for mesoporosity) (reproduced from J Taiwan Inst Chem Eng 89, 140–150, 2018)

Table 4.1 Textural parameters of the monoliths

Sample	Surface area (m^2 g^{-1})	Total pore volume (cm^3 g^{-1})	Pore diameter (nm)	Micropore volume (cm^3 g^{-1})	Mesopore volume (cm^3 g^{-1})
CM550	1166.5	1.01	3.46	0.75	0.26
CM650	1178.3	1.08	3.60	0.76	0.32
CM750	1203.6	1.19	3.9	0.80	0.39
CM850	1211.8	1.20	4.21	0.81	0.39
CM950	1225.1	1.26	4.13	0.85	0.41
SM	760	1.42	6.40	0.16	1.26

4.2.2 XRD analysis

Fig. 4.3 shows the XRD peaks of the carbon adsorbents at the 2Θ values of 25° and 44°, which correspond to (002) and (101) diffraction planes respectively, signifying the semi-graphitic carbon like structure [157]. The broadening of peaks confirms the existence of an amorphous carbon phase as well as the development of nanostructured carbon materials [158].

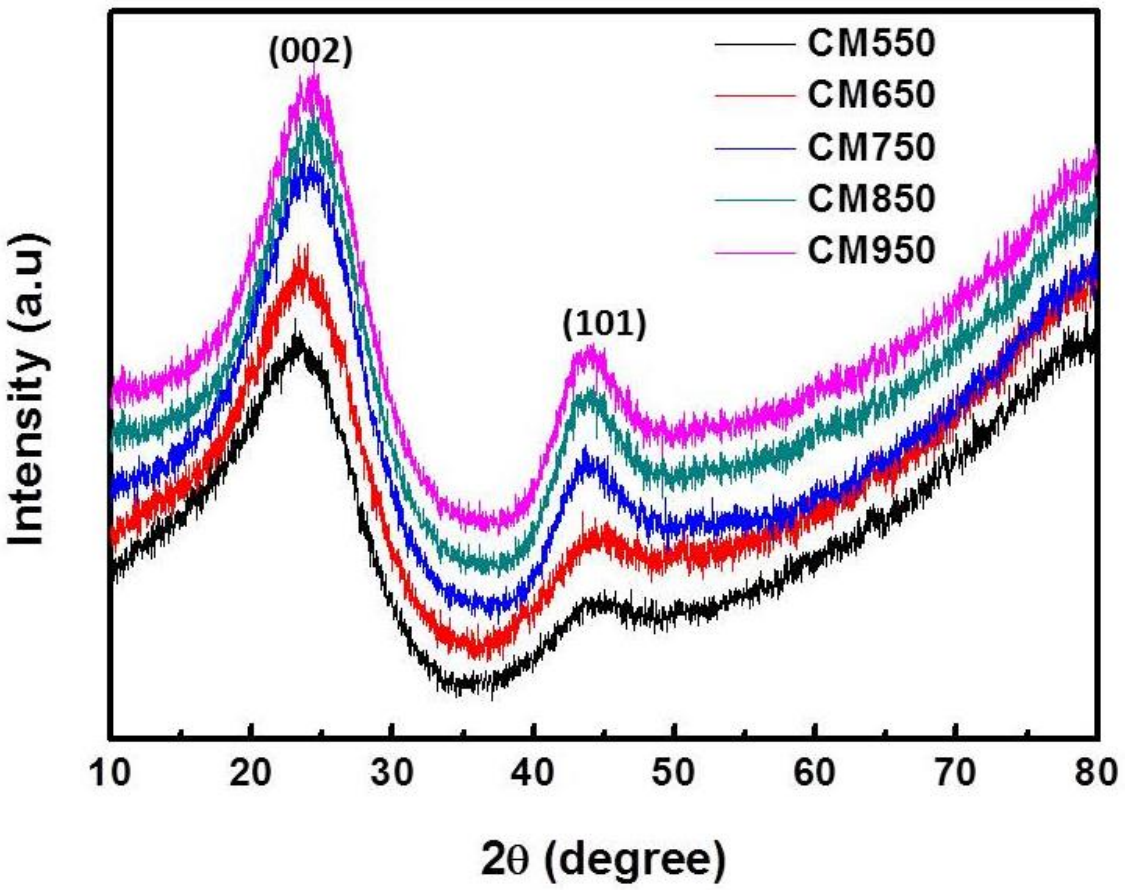

Fig. 4.3 XRD patterns of the carbon monoliths (reproduced from J Taiwan Inst Chem Eng 89, 140–150, 2018)

4.2.3 SEM analysis

Fig. 4.4 (a-f) shows the SEM micrographs of the monoliths. The silica monolith (Fig. 4.4a) consists of interconnected spherical shape fragments which form macropores [159]. The spherical shape of carbon monoliths (Fig. 4.4b-f) indicates that there is no change in the macroscopic appearance of the carbon after the removal of silica template during nanocasting. This is evident that the carbon monoliths are negative replica of parent silica monoliths. Carbon monoliths show more interconnected networking structure as compared to silica monoliths that resulted in the large surface area of 1225.1 m^2 g^{-1} and form abundant meso/macropores in the framework. Both these two factors play an important role on CO_2 adsorption capacity by allowing easy diffusion of CO_2 molecules on the surface. The shrinkage of the carbon particles in case of CM950 (Fig. 4.4f) is due to the sintering at higher carbonization temperature.

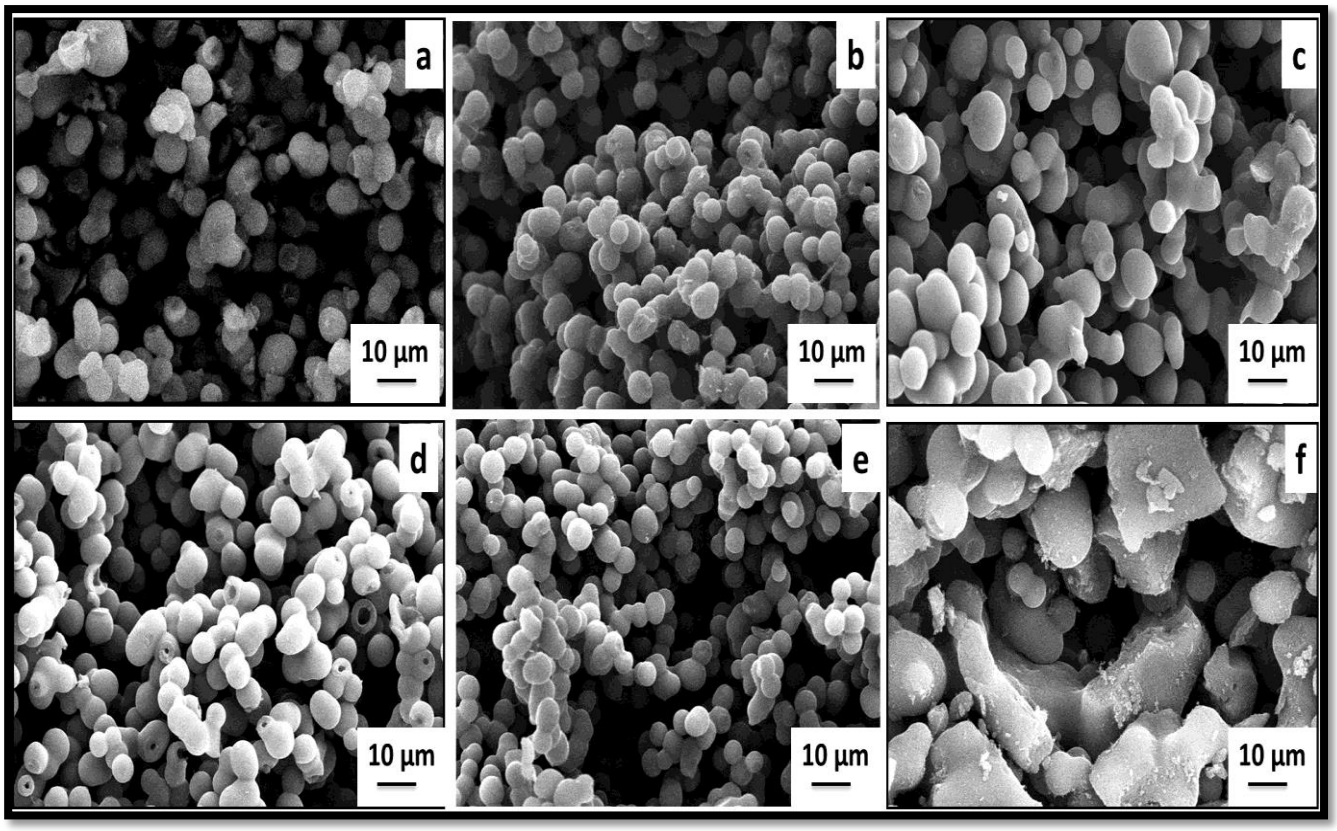

Fig. 4.4 SEM micrographs of (a) SM, (b) CM550, (c) CM650, (d) CM750, (e) CM850, and (f) CM950 monoliths (reproduced from J Taiwan Inst Chem Eng. 89, 140–150, 2018)

4.2.4 TEM analysis

Fig. 4.5 shows the TEM images for the CM950 monolith which indicates that the micropore (within the spherical particle) lies in between 1 to 2 nm. So, it can be said that the carbon monoliths contain micropores which help for better CO_2 adsorption. Micropores and mesopores are the most suitable for CO_2 trapping [131]. Based on the SEM and TEM results, it is confirmed that CMs possess porosity i.e. contain micropores as well as macropores which are beneficial for adsorption of CO_2. Micropores are most suitable for traping of CO_2 whereas macropores provided the low resistant pathways for diffusion of CO_2 molecules [131]. These results also reveal the highly interconnected structure of the monoliths which is reflected to its higher mechanical stability.

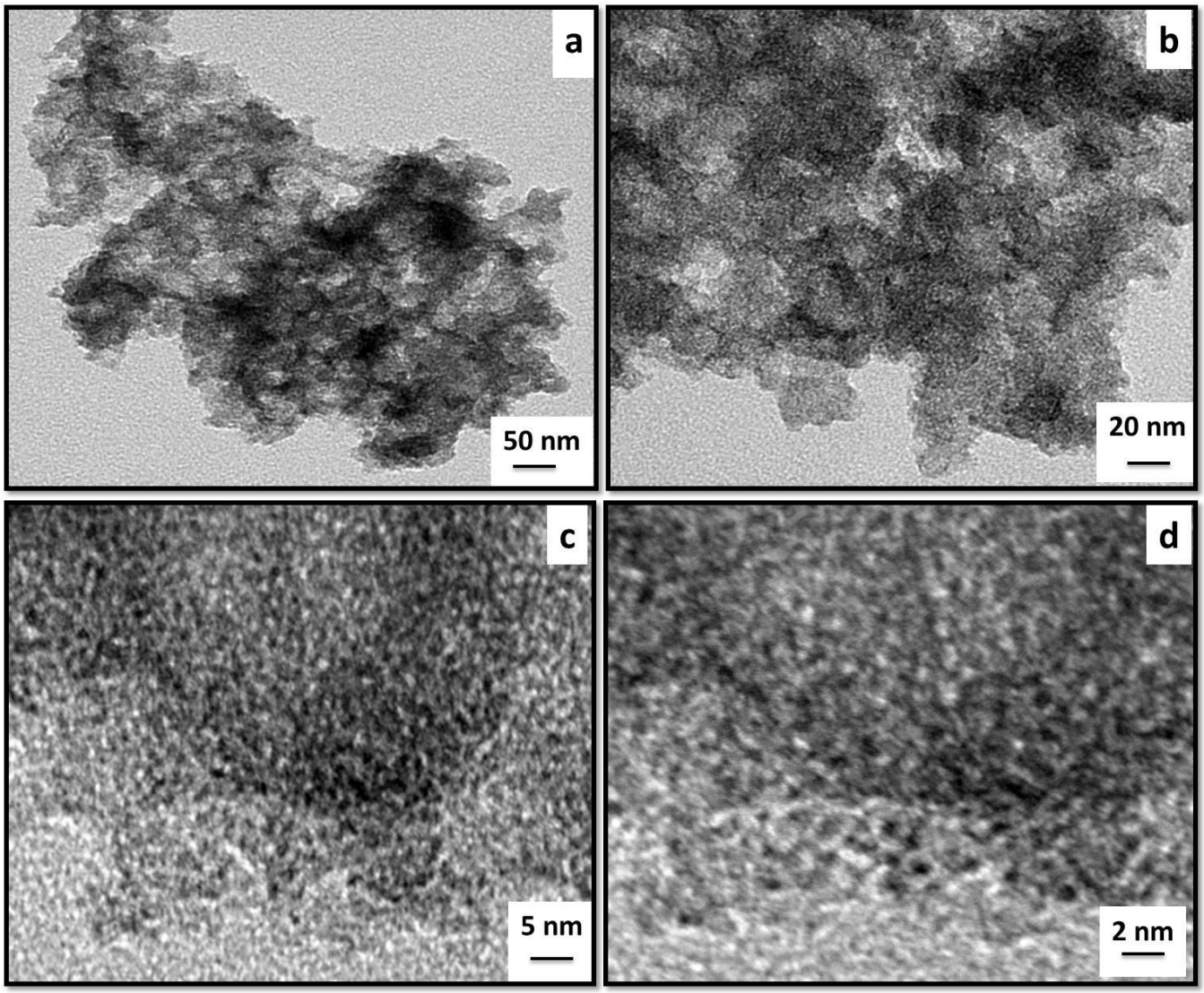

Fig. 4.5 TEM images of CM950 monolith at different magnifications (reproduced from J Taiwan Inst Chem Eng. 89, 140–150, 2018)

4.2.5 TG analysis

The TGA and DTG curves of the CMs and SM in the nitrogen atmosphere are shown in Fig. 4.6. All the monoliths exhibited a slight weight loss of approximately 3 % with different rates of weight loss from 30 °C to 100 °C due to the elimination of moisture via dehydration process. The TGA and DTG curves show the decomposition of the carbon monoliths starting at nearly 500 °C, and the maximum weight lost (ca. 20 %) occurred between 500 °C to 900 °C due to the decomposition of oxygen functionalities. Whereas, there is not so much effect of temperature on the silica monoliths. CM550 shows a maximum

weight loss of 21.85 %, while CM-950 shows the weight loss of only 15.16 % which indicates the low content of oxygen or volatile substance and exhibit good thermal stability as compared to CMs. The order of weight loss is as follows: CM550 > CM650 > CM750 > CM850 > CM950 > SM.

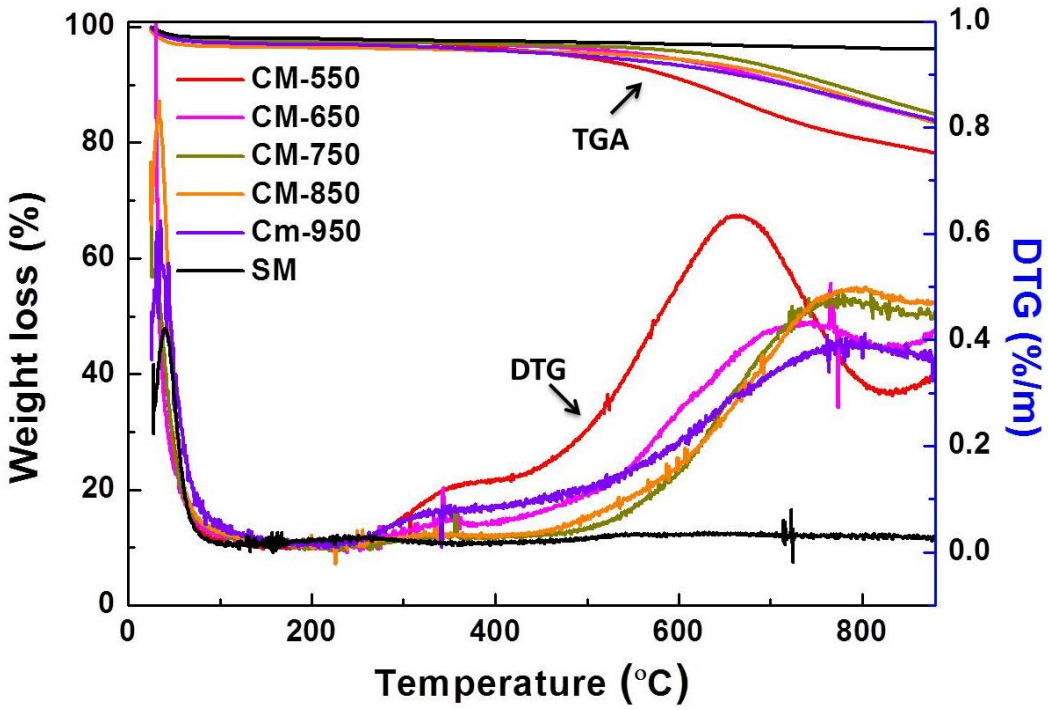

Fig. 4.6 TGA and DTG plots for the monoliths (reproduced from J IND ENG CHEM., 60, 321-332, 2018)

4.2.6 Elemental analysis

Fig. 4.7 shows the elemental composition of the monoliths. The carbon content increases from 78.9 % to 85 % with the increase of carbonization temperature. However, the oxygen content is maximum (18.92 %) at a carbonization temperature of 550 °C and gets reduced to 14.38 % with the increase in carbonization temperature to 950 °C due to the decomposition of oxygen functionalities present in the adsorbents. Also, the hydrogen content shows the same trend of decreasing from 2.12 % to 0.59 % by increasing carbonization temperature from 550 °C to 950 °C, which may be due to the cleavage and breakage of weak bonds present within the furfuryl alcohol structure [160].

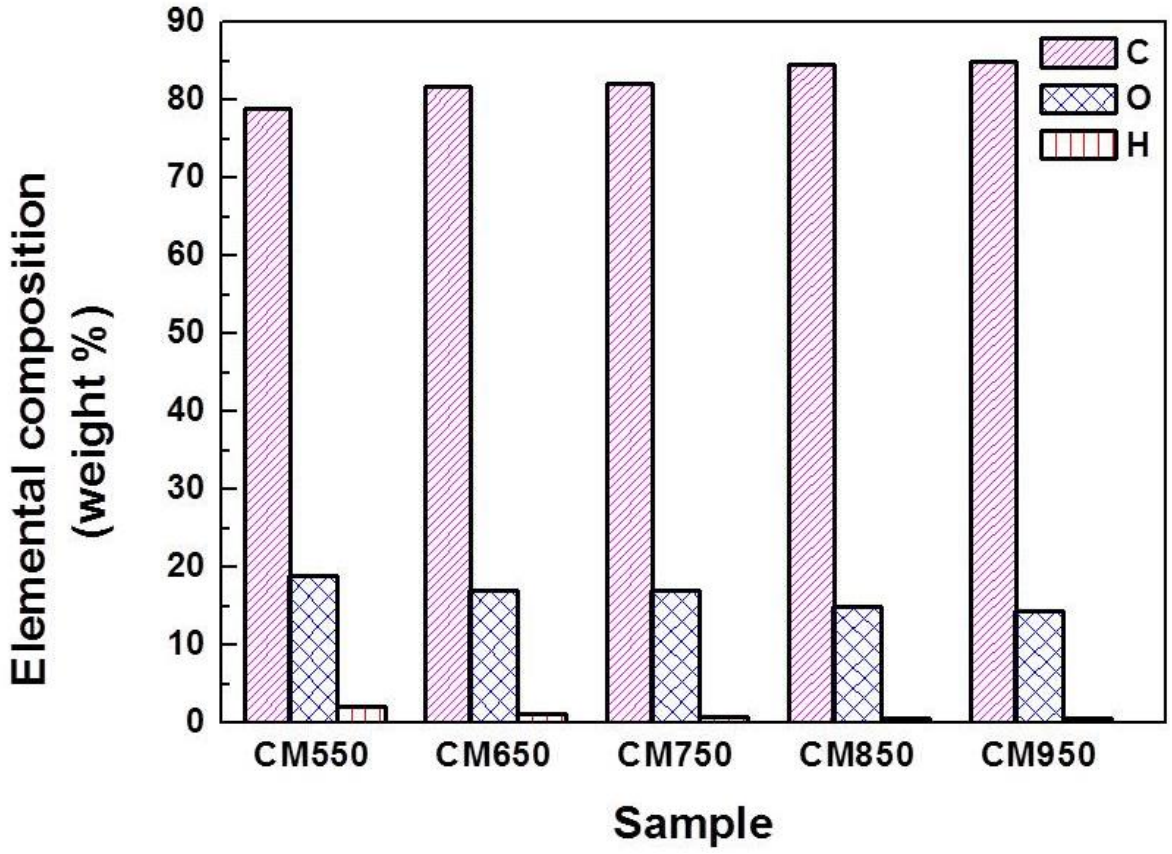

Fig. 4.7 Elemental composition of carbon monoliths (reproduced from J Taiwan Inst Chem Eng. 89, 140–150, 2018)

4.2.7 FTIR analysis

The FTIR spectra of the monoliths can be seen in Fig. 4.8. The peaks at 1700 cm^{-1} and 1527 cm^{-1} are assigned to the stretching of C=O and C=C respectively. Whereas, peaks at 3612 cm^{-1} and 3736 cm^{-1} show the -OH stretching frequencies. The existence of the oxygen functional groups on the surface of the adsorbents as confirmed from FTIR analysis, helps to provide the Lewis basic sites for efficient CO_2 adsorption.

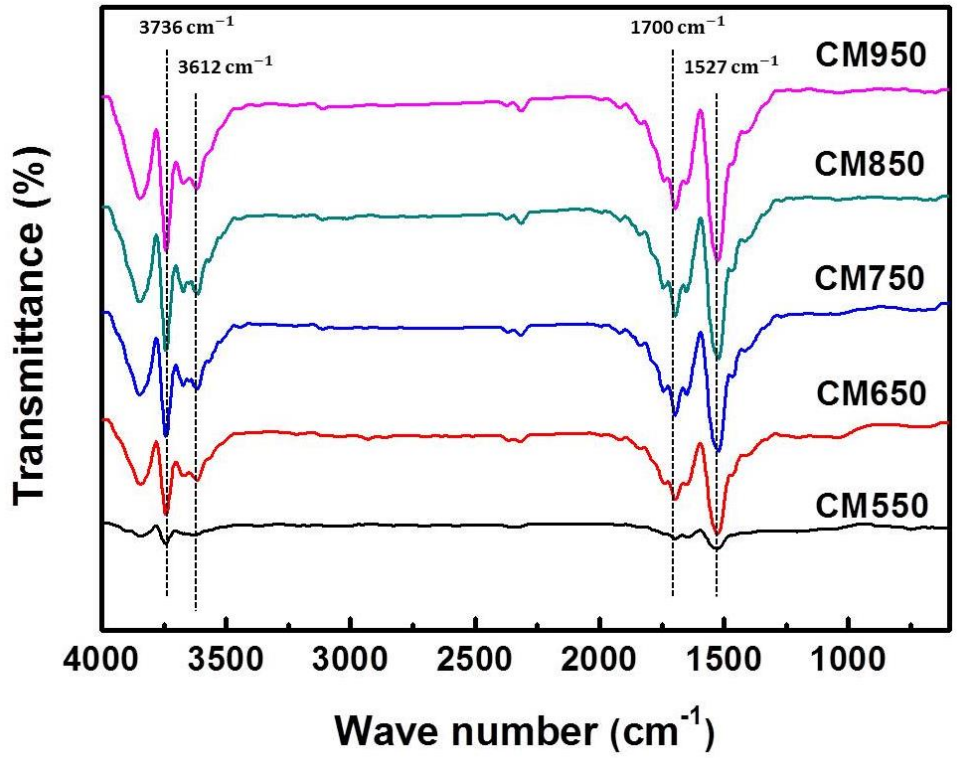

Fig. 4.8 FTIR spectra of the adsorbents (reproduced from J Taiwan Inst Chem Eng. 89, 140–150, 2018)

4.2.8 XPS analysis

XPS spectra of the CM950 clearly show the presence of carbon and oxygen species (Fig. 4.9a). In Fig. 4.9 (b), the deconvoluted XPS peaks of C1s centered at 285.6, 284.5 and 284 eV are ascribed to the C-O (C1), C-C (C2) and C=C (C3) respectively [161-164]. The oxygen functionalities increase the Lewis basic character of the adsorbent via the addition of various basic functionalities on the adsorbent surface and are beneficial to capture CO_2. For O1s spectra, the three peaks with the binding energies of 533.2, 532.3 and 531.2 eV assigned to oxygen in water (O1), C-OH (O2) and C=O (O3) groups respectively are shown in Fig. 4.9 (c). The major contribution is ascribed to oxygen (42 %) presents in the form of C-OH (O2) which represents the basic character of CM950 monolith [161].

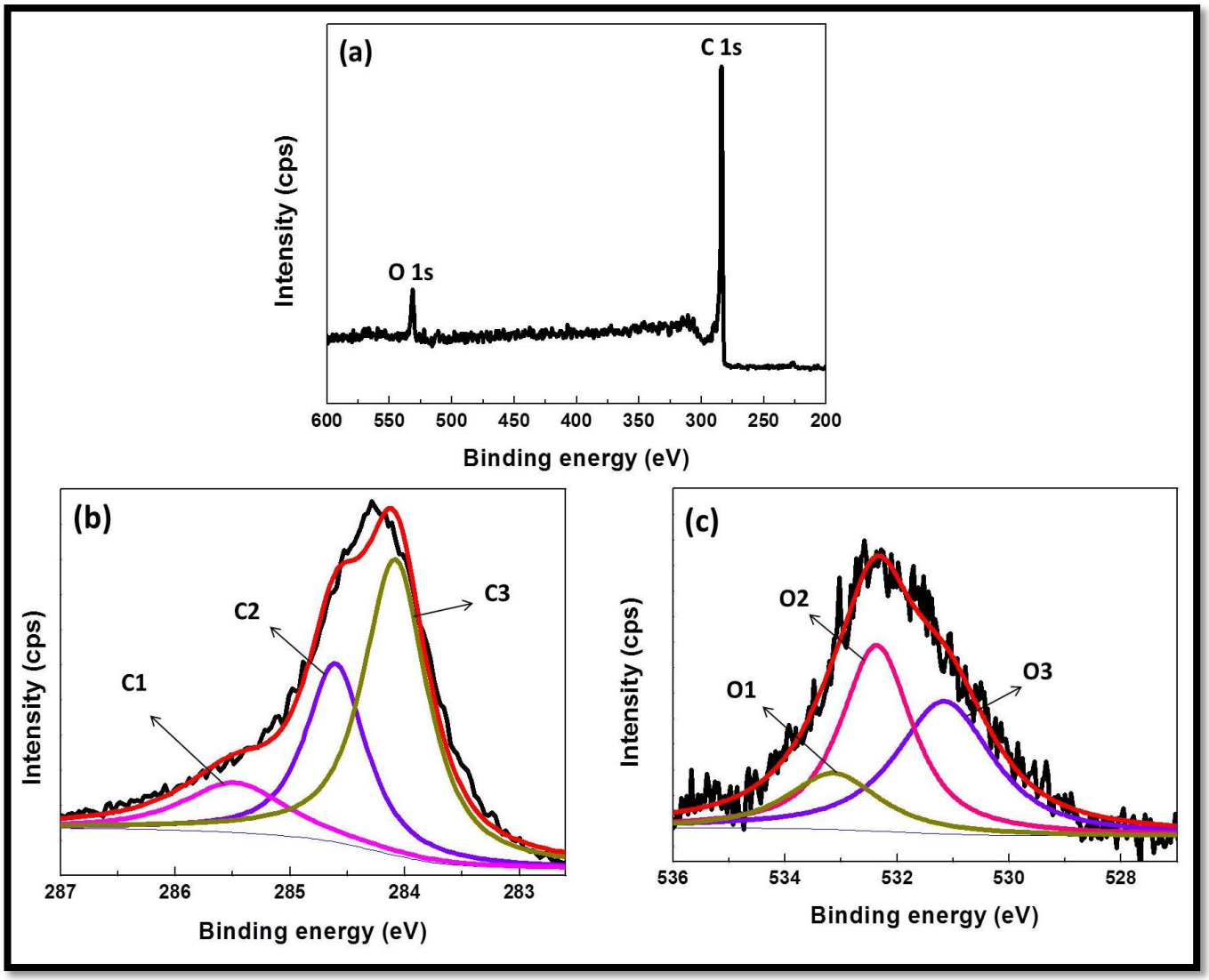

Fig. 4.9 (a) Full range XPS spectra, (b) C1s, and (c) O1s spectra of CM950 monolith (reproduced from J Taiwan Inst Chem Eng. 89, 140–150, 2018)

4.3 CO_2 adsorption performance

4.3.1 Effect of carbonization temperature

Fig. 4.10 shows the breakthrough curves and CO_2 adsorption capacity of the monoliths at 30 °C and 12.5 % CO_2 concentration. The area above the breakthrough curves was integrated for the estimation of CO_2 uptake capacity. CO_2 was not found in the effluent stream initially because of the higher adsorption rate of CO_2 molecules. But after 1 min time, the effluent stream showed the CO_2 appearance, as the mass transfer zone attains the bed outlet. The CO_2 uptake capacity increases from 0.42 to 1.0 mmol g^{-1} with the increase in carbonization temperature from 550 to 950 °C due to the development of the textural

properties and the existence of basic oxygen functional groups on the adsorbent's surface. Pevida *et al.* [165] also observed similar kind of results. The CO_2 adsorption capacity follows the order of CM950 > CM850 > CM750 > CM650 > CM550 > SM. On the other hand, silica monoliths prepared by sol-gel method shows the least adsorption capacity in comparison to other carbon monoliths due to its inferior textural properties. Since CM950 exhibited the best CO_2 capture performance as compared to the other prepared adsorbents in terms of CO_2 uptake capacity, so we considered CM950 as a model adsorbent for further CO_2 uptake studies.

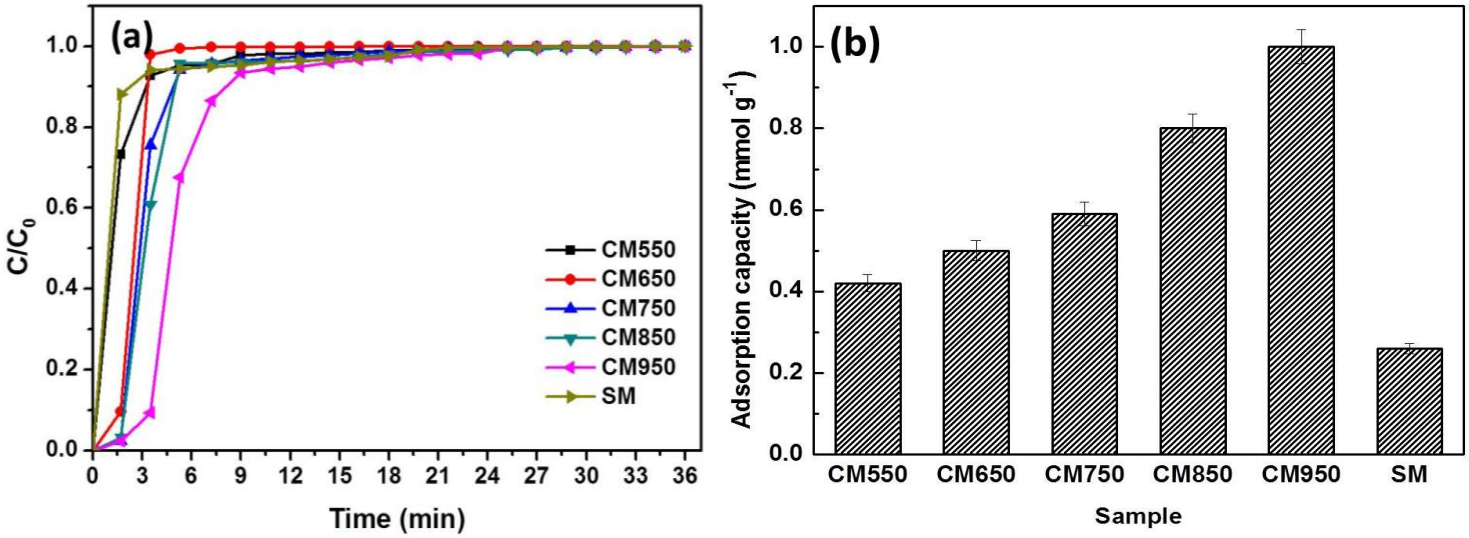

Fig. 4.10 (a) CO_2 Breakthrough curves and (b) CO_2 adsorption capacity of monoliths at 30 °C (reproduced from J Taiwan Inst Chem Eng. 89, 140–150, 2018)

4.3.2 Effect of CO_2 feed concentration and adsorption temperature

Fig. 4.11 shows the CO_2 adsorption breakthrough curves of CM950 at different CO_2 feed concentration (5-12.5 %) and temperature (30-100 °C). The adsorption capacity of CM950 increased from 0.33 to 1.0 mmol g^{-1} by increasing CO_2 concentration from 5 to 12.5 % at 30 °C (Fig. 4.12). The same trend of increasing adsorption capacity with CO_2 concentration was observed at all adsorption temperatures due to earlier bed saturation at higher concentrations. On the other hand, the saturation stage for the adsorbents reached early by an increase in temperature from 30 to 100 °C. Also, with the increase in temperature, breakpoint time become shorter which signifies a loss in the adsorption capacity at a higher temperature. The decreasing trend of adsorption capacity for all CO_2 feed concentrations by increasing temperature confirms the exothermic process. As we can see from Fig. 4.12, for 12.5 % CO_2, the capacity decreases from 1.0 mmol g^{-1} to 0.49 mmol g^{-1} with the increase in

temperature from 30 °C to 100 °C. This is because of increasing surface energy and CO_2 diffusion rate by elevating the adsorption temperature which leads to reduced stability of CO_2 molecules.

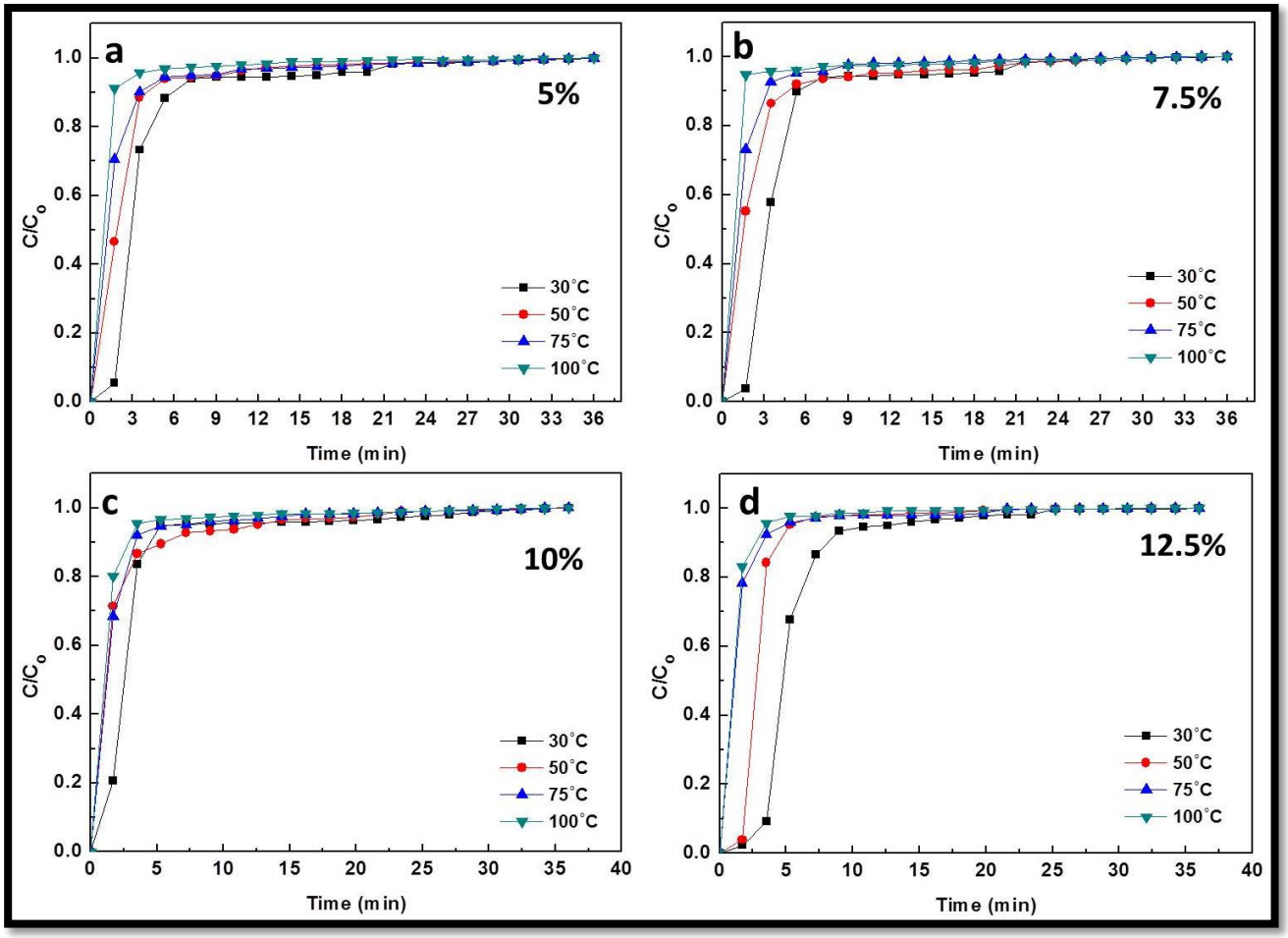

Fig. 4.11 Breakthrough curves at various operating conditions (reproduced from J Taiwan Inst Chem Eng. 89, 140–150, 2018)

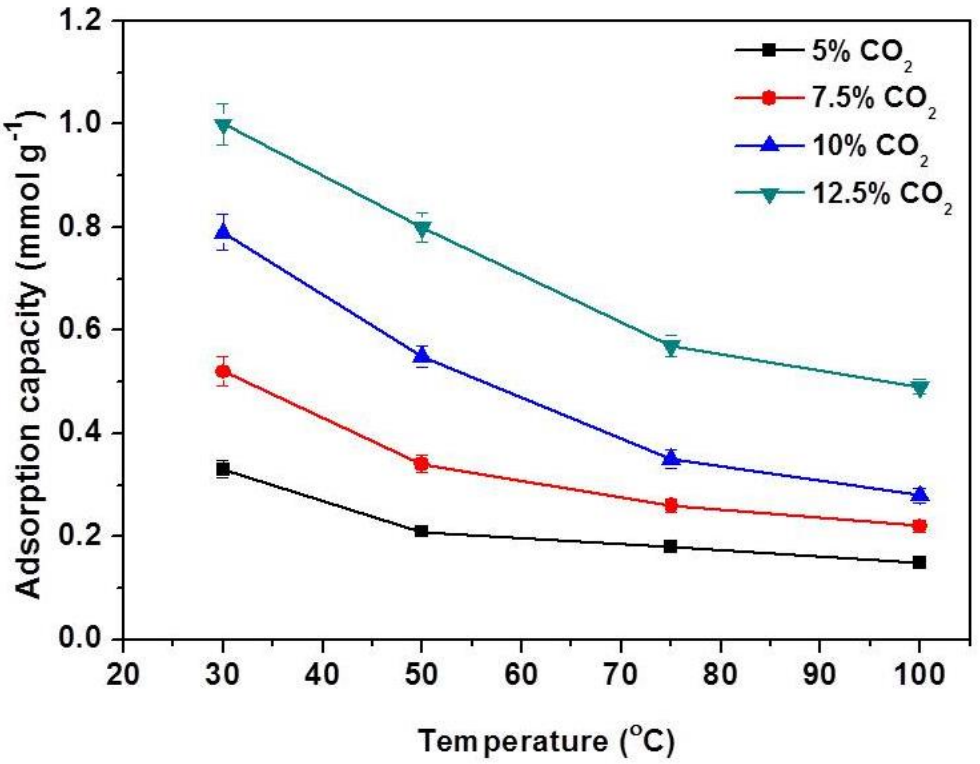

Fig. 4.12 CO_2 uptake capacity of CM950 monolith at various operating conditions (reproduced from J Taiwan Inst Chem Eng. 89, 140–150, 2018)

4.3.3 CO_2 selectivity

Fig. 4.13 shows the breakthrough curves of CO_2/N_2 at different adsorption temperatures (30 and 50 °C) under 12.5 % CO_2 concentration. N_2 detected immediately in the bed outlet indicating that N_2 uptake capacity is very low. From Fig. 4.13, it is observed that the initial (C/C_0) value for $N_2 > 1$ indicates the higher occupancy of N_2 on the active sites of the sample initially. However, the N_2 had been replaced by CO_2 with time which shows the higher affinity for CO_2. The same kind of pattern was reported by Goel *et al.*[166].

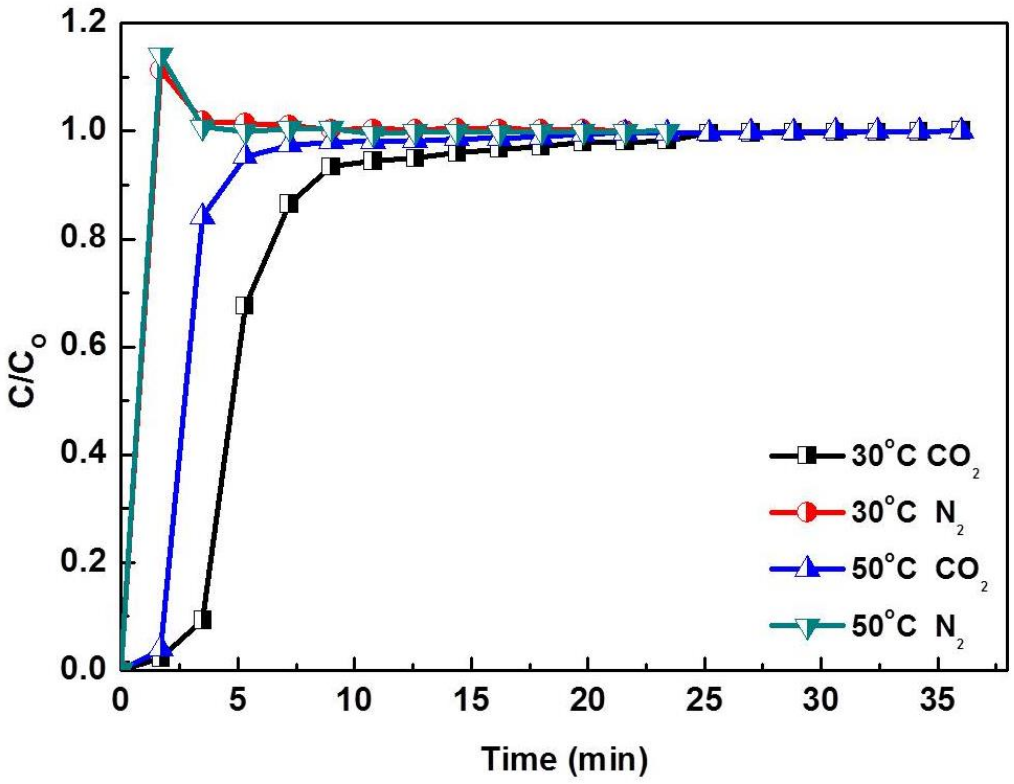

Fig. 4.13 Breakthrough curves of CO_2 and N_2 for 12.5 % CO_2 rest N_2 on CM950 monolith at 30 °C, and 50 °C (reproduced from Journal of the Taiwan Institute of Chemical Engineers 89, 140–150, 2018)

4.3.4 Regeneration study

A series of five consecutive cycles of adsorption-desorption experiments was conducted to evaluate the regenerability of the monoliths. Fig. 4.14(a) shows the adsorption-desorption of CM950 monolith at 12.5 % CO_2 and 30 °C. It can be seen that the sudden fall of C/C_o value on desorption at 200 °C confirms the easy desorption of CO_2 from the adsorbent surface. As a result of this, there is no change in the adsorption capacity over five cycles at different adsorption temperatures (Fig. 4.14(b)), indicating the excellent regenerablity of the monoliths.

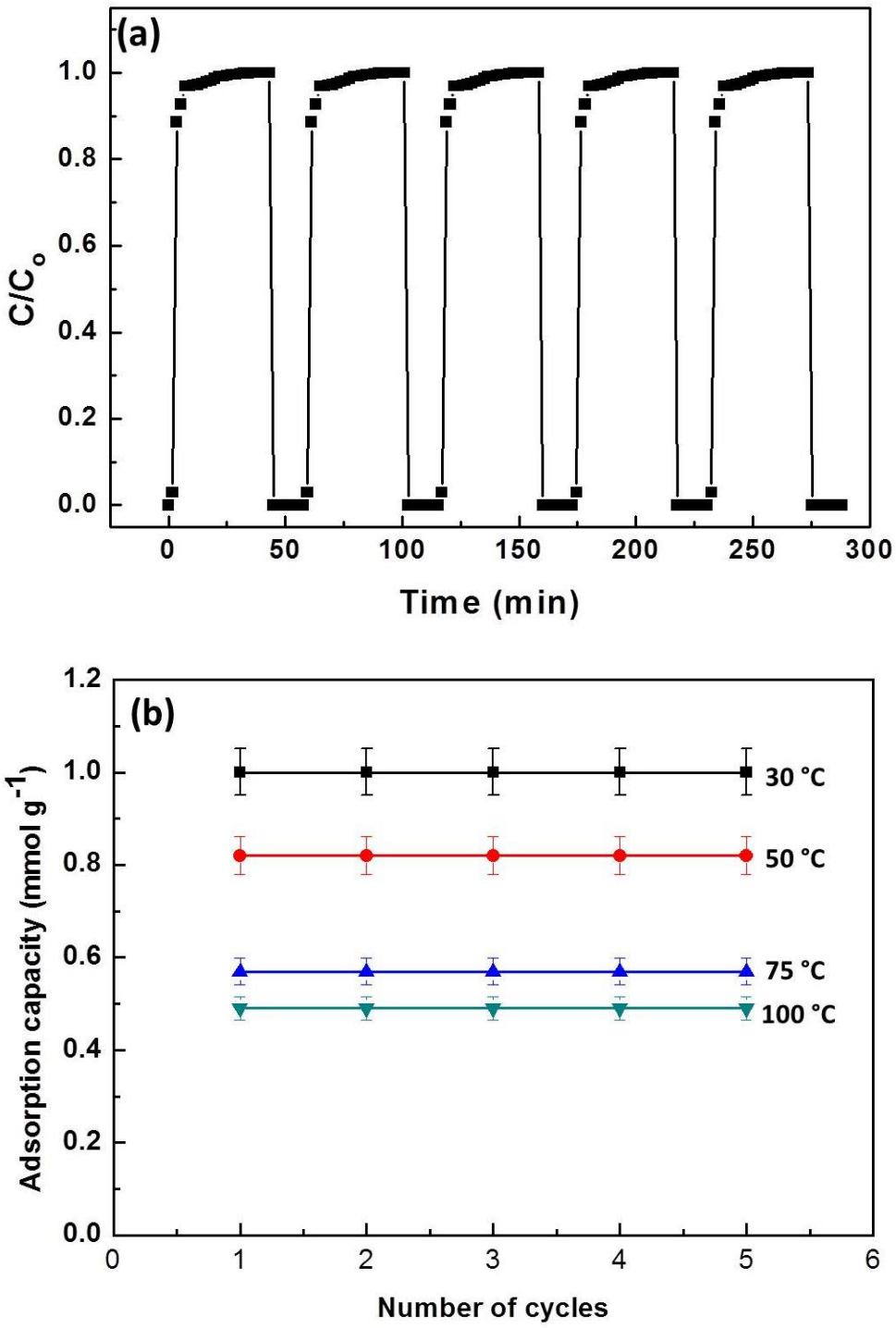

Fig. 4.14 (a) Multiple adsorption-desorption cycles at 30 °C and (b) multiple cycle CO_2 capture capacity at various temperatures for CM950 monolith at 12.5 % CO_2 concentration (reproduced from J Taiwan Inst Chem Eng. 89, 140–150, 2018)

The comparison of the CO_2 uptake capacities of the monoliths in this study with the reported literature results is shown in Table 4.2. Under the dynamic conditions, the synthesized monolith in the present study has shown the outstanding adsorption capacities in

comparison to the other adsorbents. Thus, the prepared monoliths exhibit the efficient and stable adsorption capacity which makes them superior monolithic adsorbents for CO_2 adsorption applications.

Table 4.2 CO_2 capture capacities of the various adsorbents

Adsorbent	Experimental conditions		CO_2 uptake	Ref.
	CO_2 (vol. %)	Temperature (^oC)	(mmol g^{-1})	
CM950	12.5	30	1.0	Present work
CM950	12.5	50	0.82	Present work
Activated carbon (AC)	17	55	0.25-0.8	[167]
Wood ash based activated carbon	10	60	0.54	[168]
Nitrogen enriched carbons	12.5	30	0.68	[169]
Coal tar pitch/Furfural activated carbon	15	30	0.61	[170]
Carbon monolith	100	120	0.62	[131]
Carbon monolith	15	30	0.52	[133]
Carbon adsorbents	15	100	0.16	[171]
Carbon adsorbents	12.5	50	0.66	[166]
Carbon adsorbents	100	30	0.79	[172]
Carbon adsorbents	12.5	30	0.65	[8]
Carbon adsorbents	12.5	30	0.76	[123]
Carbon adsorbents	12.5	50	0.59	[173]

4.3.5 TPD study

Fig. 4.15 shows the TPD profile of CM950. The broadest peak lies in between 50-100 °C and the maximum is at 70 °C. This is due to the removal of CO_2 molecules which are physically adsorbed on the carbon surface. The longest tail present beyond 250 °C indicates some contribution of chemisorption nature of the adsorbent.

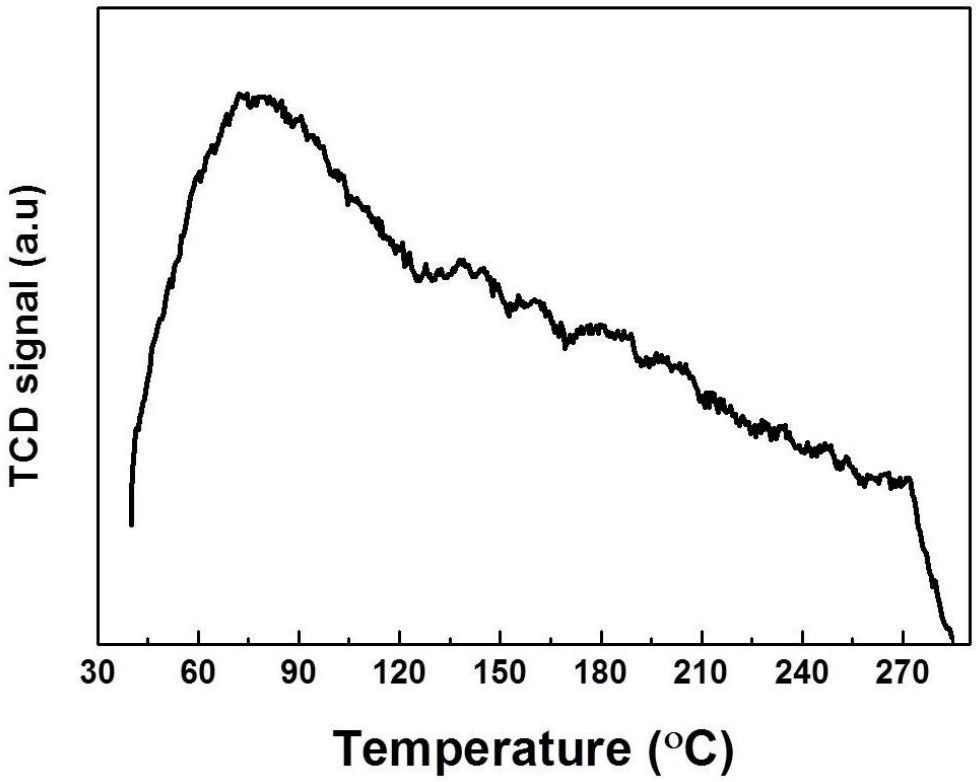

Fig. 4.15 TPD profile of CM950 for CO_2

4.4 Adsorption kinetic study

The experimental data with the predicted CO_2 uptake for CM950 monolith with the time are represented in Fig. 4.16. As ca. 90 % of the adsorption takes place within 10 min time and then it gets slow down to reach the equilibrium. This is due to the enhancement in diffusion resistance as well as a reduction in the unoccupied active sites [174]. Table 4.3 shows the kinetic parameter values for the kinetic models. Based on the R^2 value (0.99) and error (maximum 1.81 %), the fractional order model describes the adsorption process best as compared to other kinetic models.

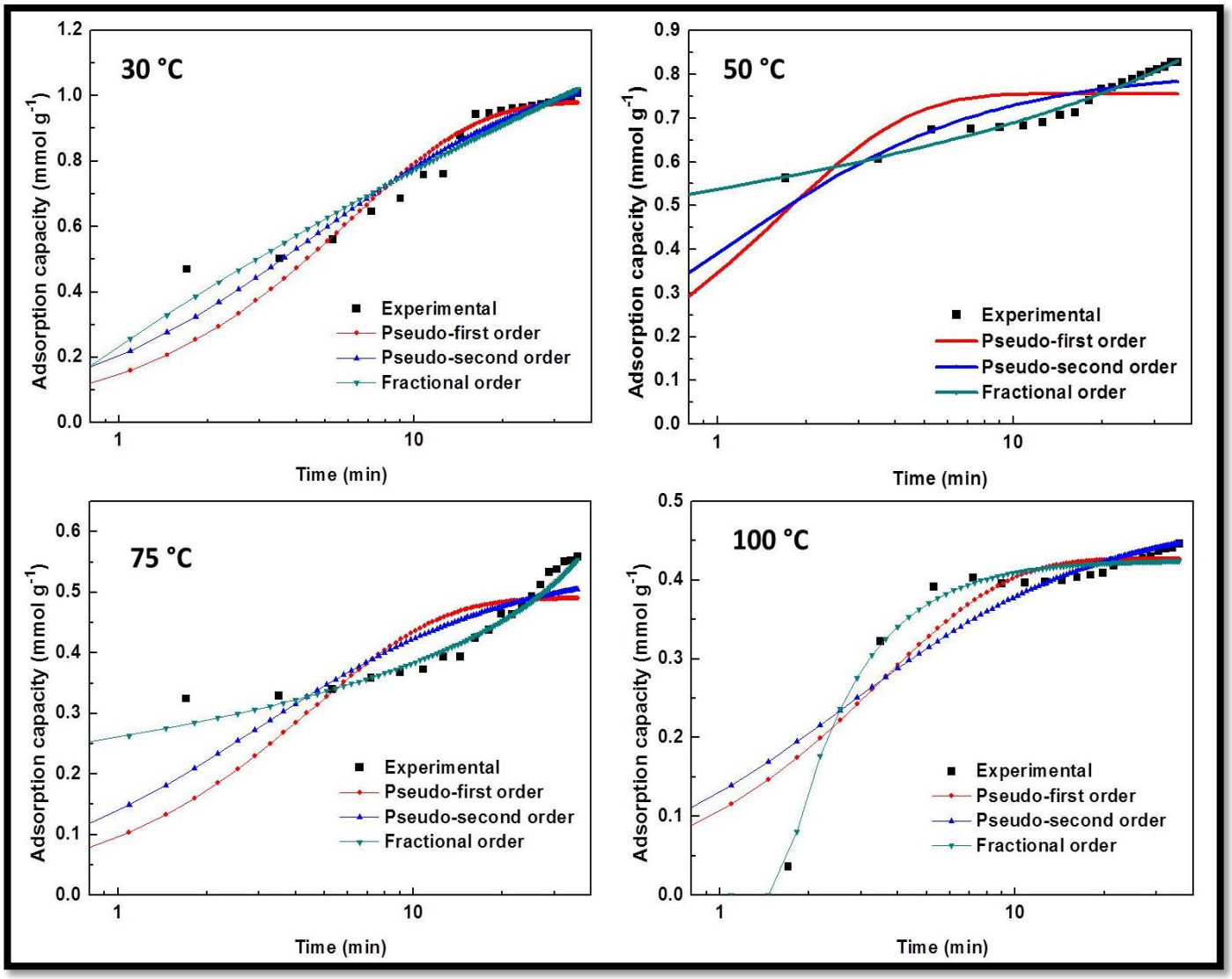

Fig. 4.16 CO_2 uptake kinetics on CM950 (reproduced from Journal of the Taiwan Institute of Chemical Engineers 89, 140–150, 2018)

Table 4.3 Kinetic parameters for CM950

Model	Parameters	Temperature			
		30 °C	50 °C	75 °C	100 °C
Pseudo-first-order					
	k_1	0.60	1.39	1.0	0.68
	q_e	0.91	0.78	0.52	0.38
	R^2	0.89	0.99	0.96	0.91
	Error %	7.57	0.39	4.19	7.06
Pseudo-second-order					
	k_2	1.16	0.12	4.94	3.83
	q_e	0.89	0.84	0.47	0.31
	R^2	0.95	0.95	0.98	0.96
	Error %	4.99	1.36	2.55	4.46
Fractional-order					
	k_n	0.43	0.20	0.22	0.30
	q_e	1.02	0.76	0.60	0.46
	n	3.13	6.17	2.40	2.51
	m	5.28	15.80	0.16	0.23
	R^2	0.99	0.99	0.99	0.99
	Error %	1.61	0.38	1.18	1.81

4.5 Adsorption isotherm study

Fig. 4.17 illustrates the isotherm models fitting with the experimental data for CM950 adsorbent. The adsorption isotherm parameters were calculated using the Langmuir, Freundlich and Temkin isotherm equations (eqns. 3.7 - 3.9). The isotherm parameters are reported in Table 4.4 and based on the R^2 values, the Temkin isotherm model shows a good fit to the experimental results which indicate the heterogeneous surface of CM950 monolith. Also, physisorption process can be verified by the decrease in K_F value with the adsorption temperature.

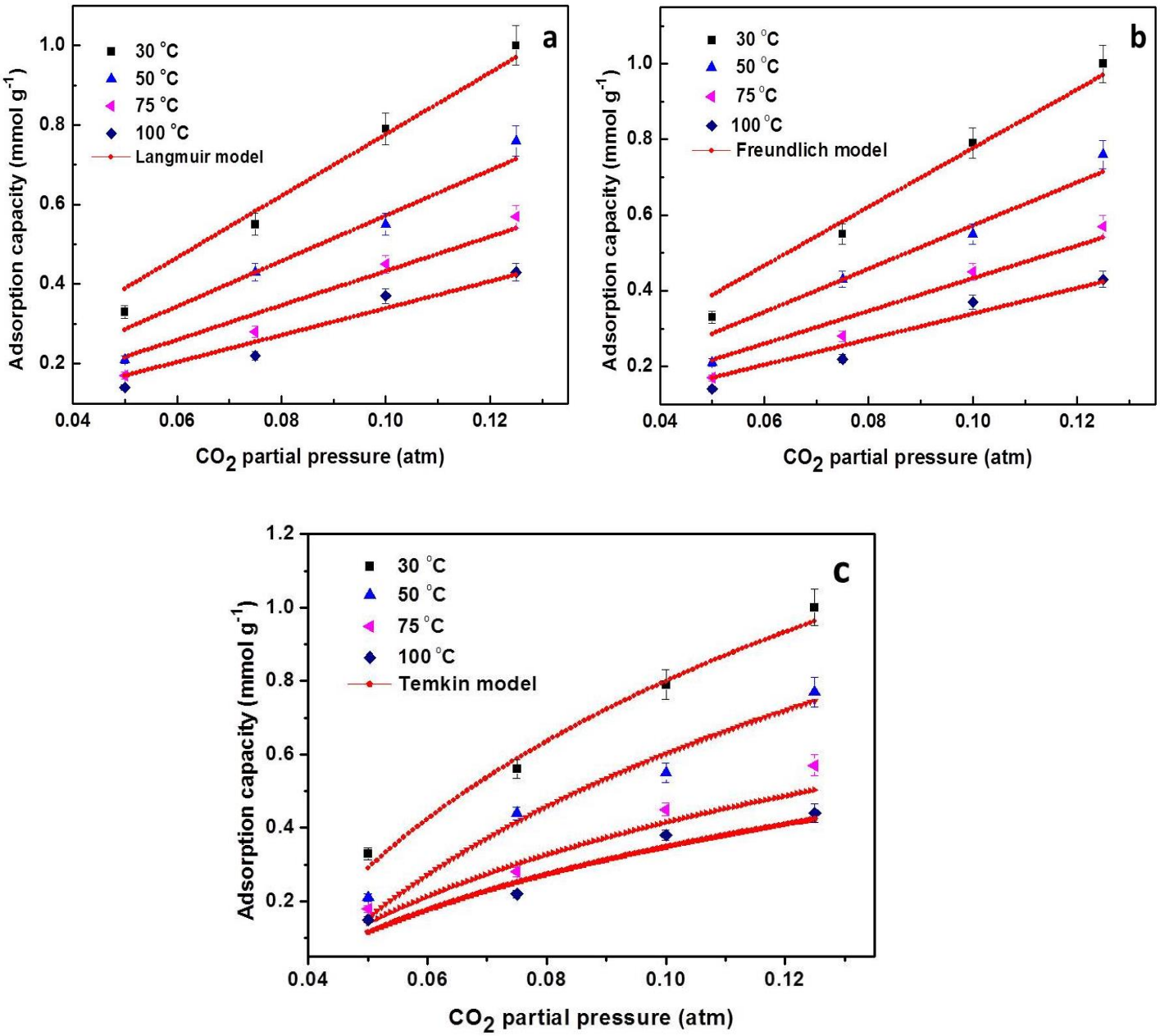

Fig. 4.17 Langmuir (a), Freundlich (b) and Temkin (c) isotherm models fitting with the experimental data for CM950 adsorbent

Table 4.4 CO_2 adsorption isotherm parameters

Model	Parameters	Temperature (°C)			
		30	50	75	100
Langmuir					
	q_m	5.21	4.5	4.22	0.73
	K_L	1.52	1.12	0.88	5.6
	R^2	0.99	0.98	0.98	0.97
Freundlich					
	K_F	3.99	3.46	1.92	1.55
	n	1.12	1.06	1.30	1.32
	R^2	0.98	0.97	0.99	0.93
Temkin					
	K_T	33.99	37.87	38.21	52.10
	b	4.84	7.45	11.12	19.38
	R^2	0.99	0.99	0.99	0.99

4.6 Thermodynamic study

4.6.1 Thermodynamic parameters

Thermodynamic parameters for CO_2 uptake on CM950 are calculated using eqns.3.10 and 3.11 and are reported in Table 4.5. The adsorption process is spontaneous as confirmed by negative ΔG° values. Whereas, ΔH° value of -5.092 kJ mol^{-1} indicates the exothermic nature of the adsorption process.

Table 4.5 Thermodynamic parameters of CO_2 adsorption on CM950

Temperature (°C)	$\Delta G°$ (kJ mol^{-1})	$\Delta H°$ (kJ mol^{-1})	$\Delta S°$ (kJ mol^{-1})
30	-8.86	-5.092	0.0458
50	-9.74		
75	-10.53		
100	-12.24		

Isosteric heat of adsorption values (Fig. 4.18) for CM950 were calculated using the eqn. 3.14 and the corresponding parameters can be seen in Table 4.6. The Q_{st} value ranged from 10.03 to 10.93 kJ mol^{-1} indicating the physisorption process. The Q_{st} has the average value of |10.61| kJ mol^{-1} which is lower than that of activated carbon i.e. |20.3| kJ mol^{-1} [175]. The random trend found by the Q_{st} values indicates the heterogeneity of the carbon surface.

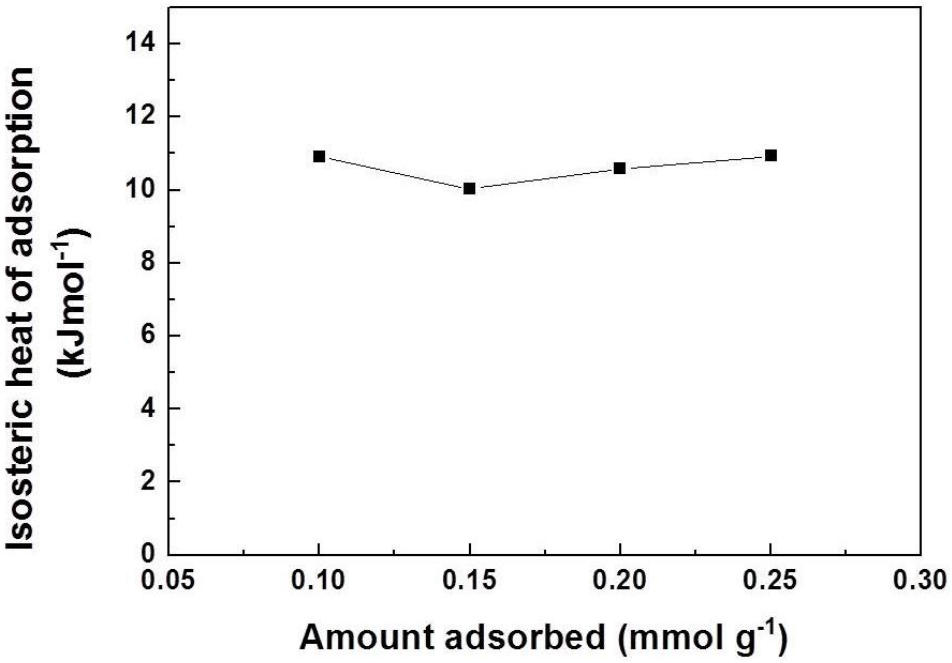

Fig. 4.18 Isosteric heat of adsorption for CM950

Table 4.6 Isosteric heat of adsorption values for CM950

CO_2 uptake (mmol g^{-1})	Q_{st} (kJ mol^{-1})
0.1	10.91
0.15	10.03
0.2	10.58
0.25	10.93
Average	10.61

4.6.2 Energy duty for desorption of CO_2

C_P value for CM950 = 1.2 J g^{-1} K^{-1} (assumed)

Adsorption temperature is 30 °C and desorption temperature is 200 °C

Temperature difference, ΔT = (200-30) °C = 170 °C.

Adsorption capacity of CM950 = 1.0 mmol CO_2/g adsorbent

= 1.0 * 10^{-3} mol CO_2/g adsorbent = 0.044 kg CO_2/kg adsorbent.

Therefore, sensible heat = $\frac{1.2 \times 170}{1.0 * 10-3}$ J per mole CO_2 = 204 kJ per mole CO_2.

Net sensible heat needed is 25 % of 204 kJ per mole CO_2, assuming 75 % heat recovery.

Sensible heat = 51 kJ per mole CO_2.

Isosteric heat of adsorption, Q_{st} = 10.61 kJ per mole CO_2

Thermal energy input = (51 + 10.61) kJ per mole CO_2 = 61.61 kJ per mole CO_2

= 1.40 MJ per kg CO_2

Assuming, 0.0884 kg CO_2 per MJ generated on using bituminous coal (as fossil fuel) for energy production.

Therefore, for desorption of 1.0 mmol g^{-1} of CO_2 (0.044 kg kg^{-1}), the energy required is 0.0616 MJ.

Thus, CO_2 created to produce 0.0616 MJ energy for desorption = 0.00544 kg CO_2.

Therefore, energy penalty = $\frac{0.00544}{0.044}$x 100= 12.36 %

4.7 Conclusions

Effective porous carbon monoliths have been synthesized using nanocasting method for highly effective CO_2 adsorption. The monolith, prepared at 950 °C exhibits the highest dynamic CO_2 capture capacity (1.0 mmol g^{-1}) at 12.5 % CO_2 due to the higher surface area and presence of basic oxygen functionalities on its surface. The CO_2 adsorption process onto carbon monoliths is entirely physisorption. Adsorbent follows the adsorption capacity order of CM950> CM850> CM750> CM650> CM550> SM. Also, after five adsorption-desorption

cycles, the adsorbent exhibits good regenerability and stability. Moreover, fractional order kinetic model gives the best fit with the adsorption data. The heterogeneity was found for the monoliths by appropriate fitting of Temkin isotherm model. Thermodynamic studies depict the exothermic, spontaneous as well as the feasible adsorption process. The thermal energy required for CO_2 desorption after adsorption is ca. 1.40 MJ per kg of CO_2. The energy penalty for CO_2 capture by adsorption on CM950 is ca. 12.36 %.

Chapter 5 – Activated Carbon Adsorbents Synthesized from Polyacrylonitrile for Carbon Dioxide Adsorption

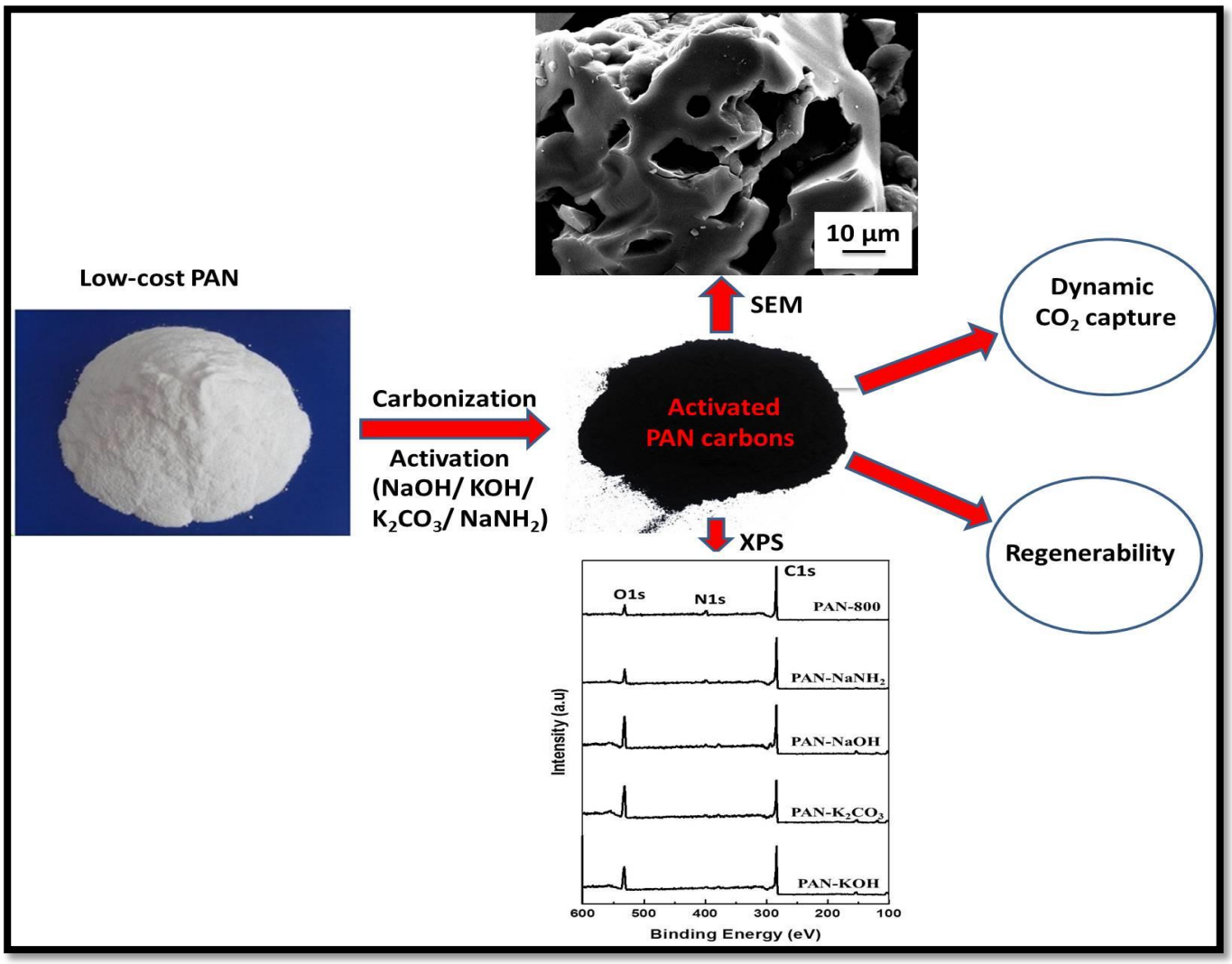

Highlights

- Preparation of activated carbons from PAN via carbonization followed by chemical activation.
- Role of various activating agents towards CO_2 uptake was evaluated.
- Maximum dynamic CO_2 uptake (1.2 mmol g^{-1}) was obtained under 12.5 % CO_2 flow.
- CO_2 adsorption process has been found to be exothermic.
- Carbons show easy regeneration over multiple adsorption/desorption cycles.

5.1 Preparation of activated carbon adsorbents

5.1.1 Carbonization of PAN

PAN polymer was used for the synthesis of activated carbons. PAN was firstly carbonized in a tubular furnace for 1.0-2.5 h from 600-900 °C using the heating rate of 10 °C min^{-1} and the N_2 flow of 50 ml min^{-1}. The sample was represented as PAN-x for simplification, where x signifies the carbonization temperature. The block flow diagram for the preparation of carbon adsorbent using direct carbonization is shown in Fig. 5.1. The samples carbonized at different temperatures were evaluated for CO_2 adsorption. PAN-800 was found to have maximum adsorption capacity. Therefore, PAN-800 was selected for further studies.

5.1.2 Chemical activation with various chemical activating agents

The optimized carbonized sample i.e. PAN-800 was chemically activated by various activating agents (Fig. 5.2). The activation of PAN-800 by NaOH, K_2CO_3, and KOH was executed as follows: 2 g of PAN-800 was mixed with the selected activator (6 g) aqueous solution (10 ml water) in a crucible and kept overnight at 100 °C, then carbonized at 800 °C (2 h). In the case of $NaNH_2$, 2 g of PAN-800 was mixed manually with 6 g of $NaNH_2$ in a crucible and then carbonized at 800 °C for 2 h. Then, the resulted carbons were treated with 2M HCl for the removal of K^+ ions and then washed repeatedly (4-5 times) with water. After that, the samples were kept for drying at 120 ºC for 15 h. The collected activated PANs were named as PAN-y, where, y is the applied activating agent i.e K_2CO_3, $NaNH_2$, NaOH or KOH.

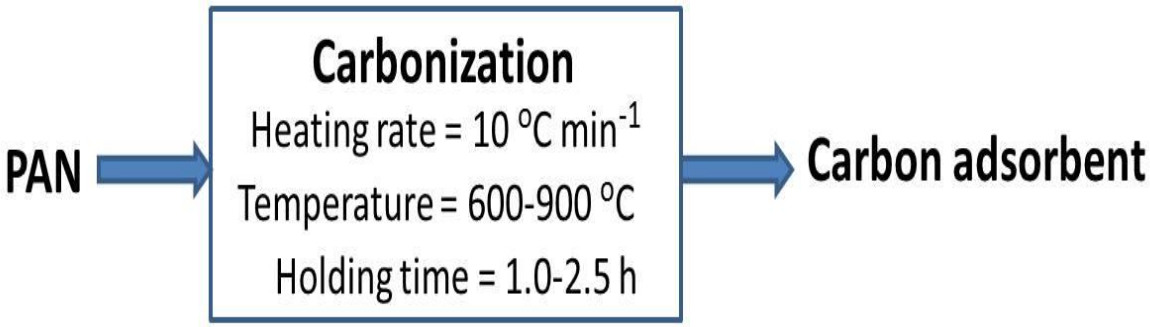

Fig. 5.1 Block diagram for the preparation of carbons via direct carbonization

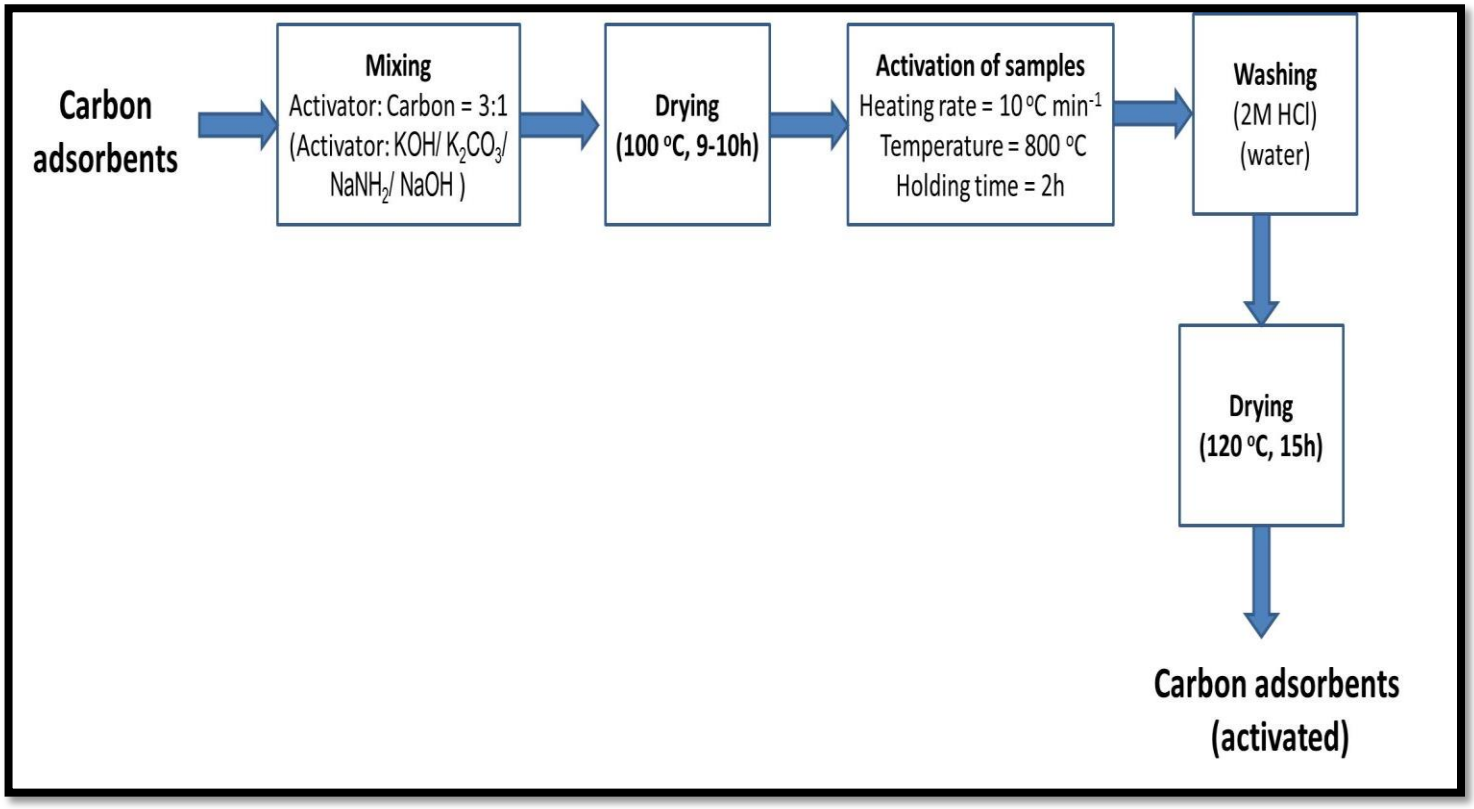

Fig. 5.2 Block diagram for the activation of carbon adsorbent(s)

5.2 Characterization of adsorbents

5.2.1 Surface area and pore size distribution

Fig. 5.3(a) represents the N_2 sorption isotherms of the synthesized carbons. Due to the negligible surface area of directly carbonized PAN samples, the instrument could not provide the accurate measurement. Whereas, PAN-activated carbons showed the type-I isotherms, suggesting the existence of micropores. Fig. 5.3(b) shows the PSD curves for the carbons which clearly indicate the presence of 0.4-2.0 nm pore size. The surface area and total pore volume values are 833-1890 $m^2\ g^{-1}$ and 0.36-1.47 $cm^3\ g^{-1}$, respectively (Table 5.1). The higher surface area of KOH activated samples are due to the gasification. At higher temperature, it forms metallic K which reacts with carbon to generate the mesopores as well as micropores in the framework. Also, the HCl washing during the synthesis of resulted carbons leads to produce the highly porous structure because it removes the intercalated free metals. The significant difference in the surface area between the PAN-KOH and other samples confirms the development of textural properties with the KOH activation and indicate the KOH superiority over $NaNH_2$, NaOH and K_2CO_3 activating agents.

The significant difference in the surface area along with porous properties between the PAN-KOH and other samples confirms the development of porosity by using the synthesis technique of KOH activation after the carbonization. Comparatively, the effectiveness of various activators towards PAN follows the order: $NaNH_2$< NaOH< K_2CO_3< KOH. Thus, it can be concluded that activating agents play the major function in the enhancement of textural properties of the carbons.

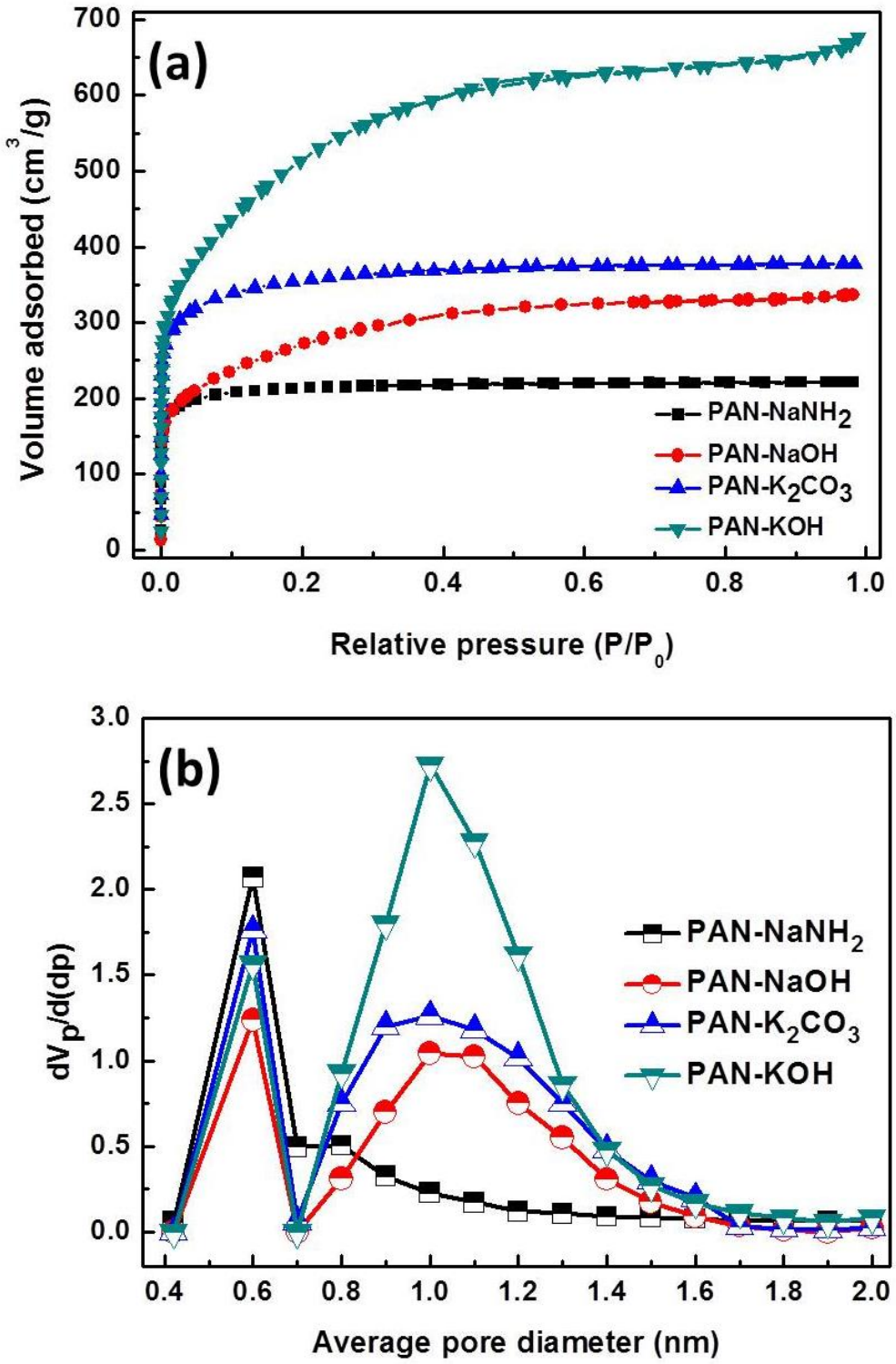

Fig. 5.3 (a) N_2 sorption isotherms and (b) PSD curves for the prepared carbons (reproduced from reference [42])

Table 5.1 Textural properties calculated from nitrogen sorption

Adsorbent	S_{BET} ($m^2\ g^{-1}$)	V_{total} ($cm^3\ g^{-1}$)	V_{meso} ($cm^3\ g^{-1}$)	V_{micro} ($cm^3\ g^{-1}$)
PAN-800	-	-	-	-
PAN-$NaNH_2$	833	0.36	0.02	0.34
PAN-NaOH	1020	0.55	0.02	0.53
PAN-K_2CO_3	1250	0.64	0.07	0.57
PAN-KOH	1890	1.47	0.48	0.99

5.2.2 XRD analysis

For all the adsorbents, XRD peaks at 2Θ value of 25° and 43° have been seen (Fig. 5.4), which are indexed to (002) and (100) planes, respectively. These are indicating the existence of graphitic carbon [176]. The (002) d-spacing is 3.43 which shows that the graphene layers have the turbostactic ordering of the atoms [103].

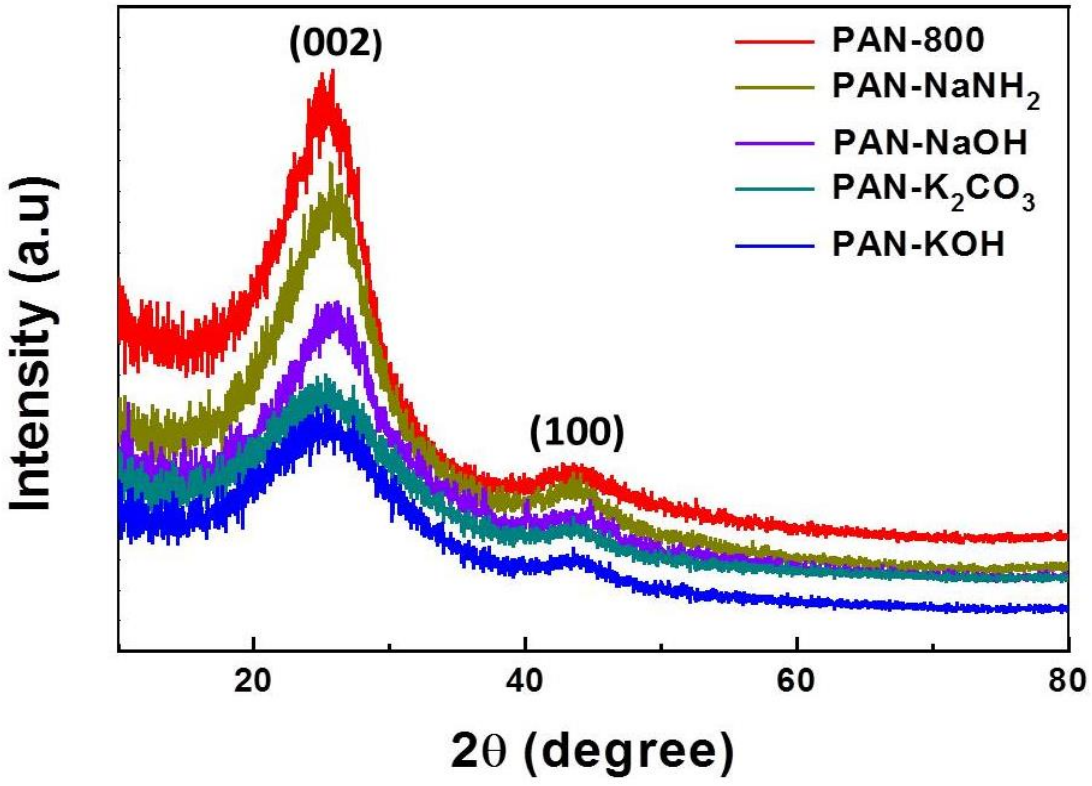

Fig. 5.4 XRD patterns of adsorbents (reproduced from reference [42])

5.2.3 SEM analysis

Fig. 5.5 illustrates the surface morphology of PAN-800 and activated PAN adsorbents. The PAN activated adsorbents (Fig. 5.5b, c, d, and e) show the pores as well as small pits and cracks on the surface whereas, the carbonized PAN (Fig. 5.5 (a)) shows the smooth surface with no cracks or defects. This difference in surface morphology is due to the decomposition of volatile compounds during the activation with the various activators which generates numerous pores on the carbon surface.

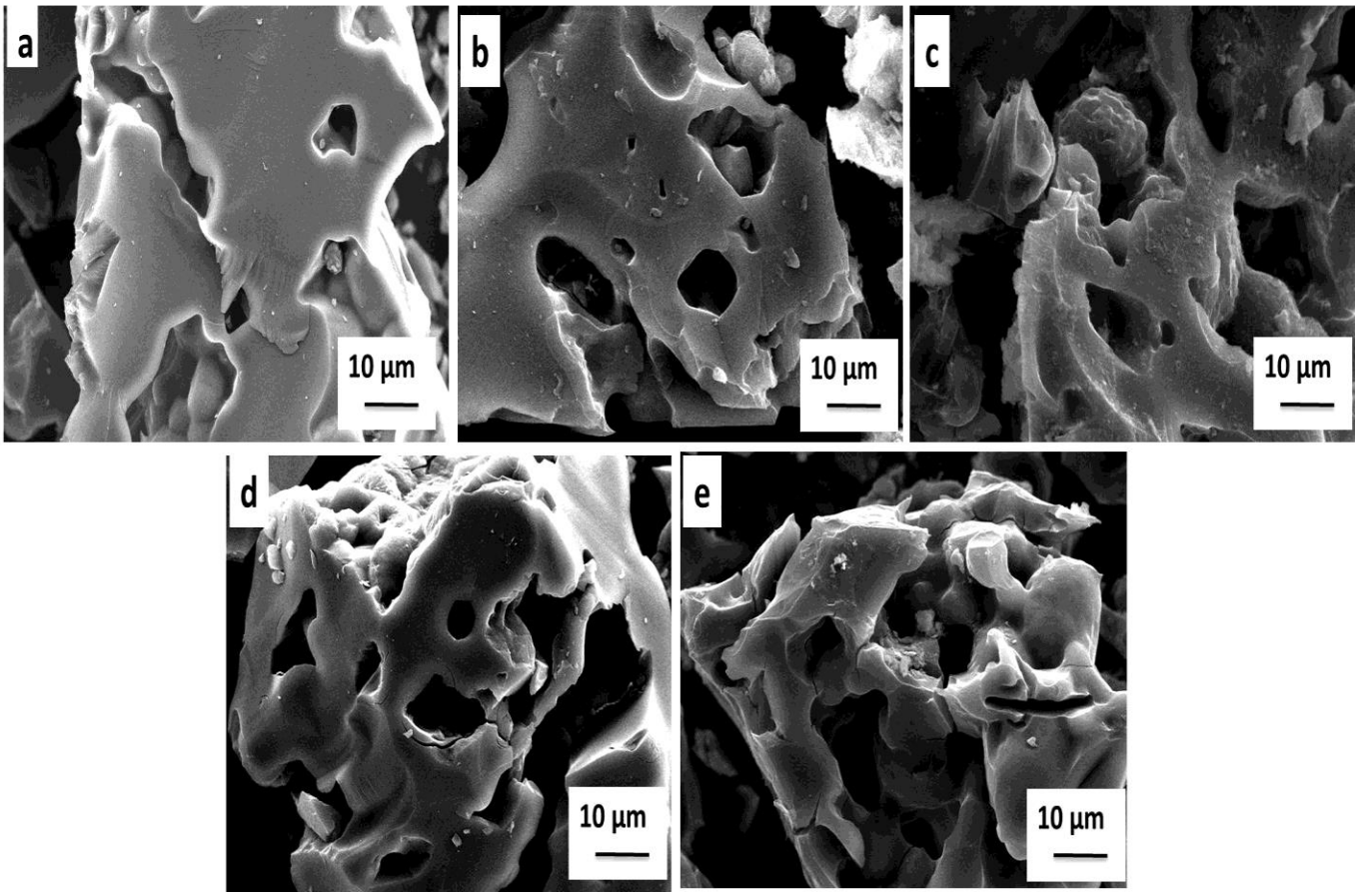

Fig. 5.5 SEM images of (a) PAN-800, (b) PAN-$NaNH_2$, (c) PAN-NaOH, (d) PAN-K_2CO_3 and (e) PAN-KOH adsorbents (reproduced from reference [42])

5.2.4 TEM analysis

From the TEM images, graphite-like layer and non-porous structure of PAN-800 can be seen (Fig.5.6a) whereas, activated carbons show the presence of micropores in the framework (Fig. 5.6 b-e). Therefore, the SEM and TEM results confirm an improvement in the surface morphology and inner structure of PAN activated samples with an enhancement in porosity through chemical activation which is beneficial for CO_2 capture.

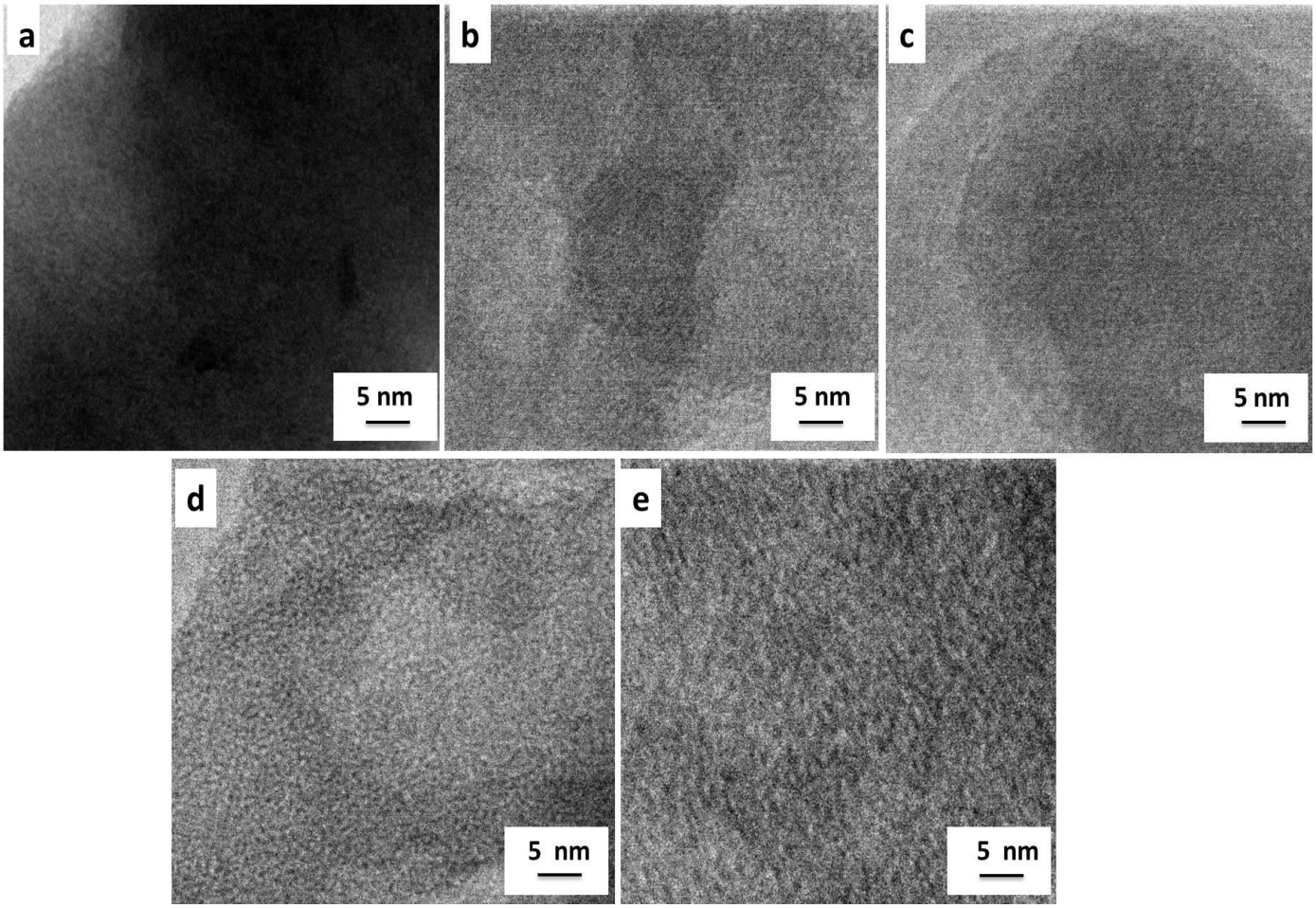

Fig. 5.6 Transmission electron micrographs of carbon adsorbents (reproduced from reference [42])

5.2.5 TG analysis

Fig. 5.7 represents the comparison of TGA and DTG curves for the different carbons. All the samples exhibited weight loss during the rise in temperature from ca. 20 to 100 ºC due to the removal of unwanted moisture. After that, the weight loss occurs in 500-800 ºC probably due to the oxidation and decomposition of the nitrogen as well as oxygen moieties

present in the samples. The order for the weight loss follows: PAN-K_2CO_3 (38 %) > PAN-NaOH (34 %) > PAN-$NaNH_2$ (25 %) > PAN-KOH (24 %) > PAN-800 (9 %). It was observed that PAN-KOH is most thermally stable as compared to other activated carbons.

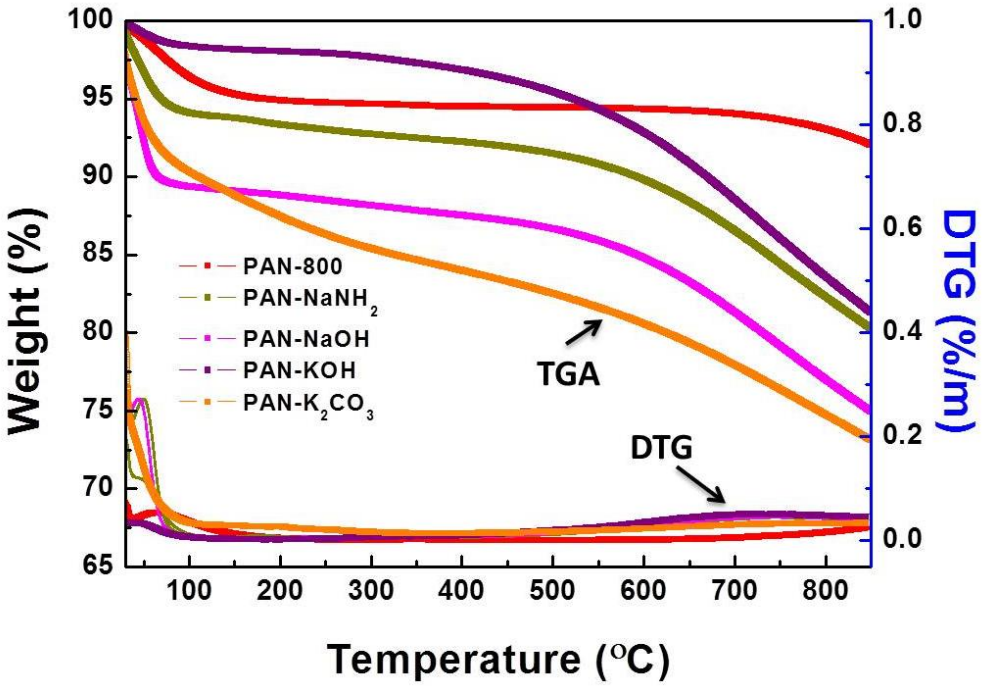

Fig. 5.7 Thermogravimetric profiles of the prepared adsorbents (reproduced from reference [42])

5.2.6 Elemental analysis

The CHN analysis verifies the existence of a different amounts of elements in the adsorbents (Table 5.2). All the adsorbents are rich in the carbon content which is good for the CO_2 capture [177]. The sample PAN-800 shows the highest nitrogen content of 13.62 % which varied with the chosen activating agent, indicated the degradation of the nitrogen species during activation. Whereas, PAN activated samples exhibit the nitrogen content in between 1.73-5.64 % indicating the insertion or decomposition of the various nitrogen species during the chemical activation process using $NaNH_2$, NaOH, K_2CO_3, and KOH activating agents.

Table 5.2 CHN analysis of the synthesized adsorbents

Adsorbent	Carbon (%)	Hydrogen (%)	Nitrogen (%)
PAN-800	72.0	0.83	13.62
PAN-$NaNH_2$	63.54	1.44	5.64
PAN-NaOH	54.4	2.75	4.90
PAN-K_2CO_3	62.04	1.91	1.73
PAN-KOH	74.47	0.69	2.52

5.2.7 X-ray photoelectron spectroscopy

The full range XPS spectra of the carbon adsorbents indicate the existence of carbon, nitrogen and oxygen species as shown in Fig 5.8. The deconvoluted O1s spectra into various peaks with different binding energies (B.Es.) representing various oxygen functionalities on the adsorbent's surface (Fig. 5.9). The peak with B.E at 531.2 eV (O1) corresponds to the ketone, carbonyl, and lactone; 532.04 eV (O2) for alcohol, ether and 533.3 eV (O3) for ether oxygen in anhydrides and esters [178, 179]. From Table 5.3, the maximum relative area percentage (A%) (50.97%) in the PAN-KOH sample for O1 indicates the major existence of ketone, carbonyl, and lactone functional groups on its surface. The three major peaks for the N1S spectrum with the B.E of 398.3 eV (N1) ascribes to pyridinic-N, 399.7 eV (N2) for pyrrolic and/ or pyridone-N and 400.7 eV (N3) for quaternary-N, respectively [94, 178] (Fig.5.10). The respective FWHM and area percentage (A%) for the peaks are shown in Table 5.3. All these N-functionalities play a significant role to enhance the basicity of samples and advantageous for the CO_2 adsorption [180]. The C1S spectrum deconvoluted into four peaks with the B.E of 284.39 eV (C1) ascribed to sp^2/sp^3 carbon atoms, 284.97 eV (C2) for C-H bond of ether and/or C=N bond, 285.85 eV (C3) for the carbonyl groups and/or C-N bond, 288.75 eV (C4) for C=O functional groups [181, 182] (Fig. 5.11). It was observed that the relative area percentage (A %) for C1S increased after activation suggesting the enhanced graphitization nature of the carbons (Table 5.4).

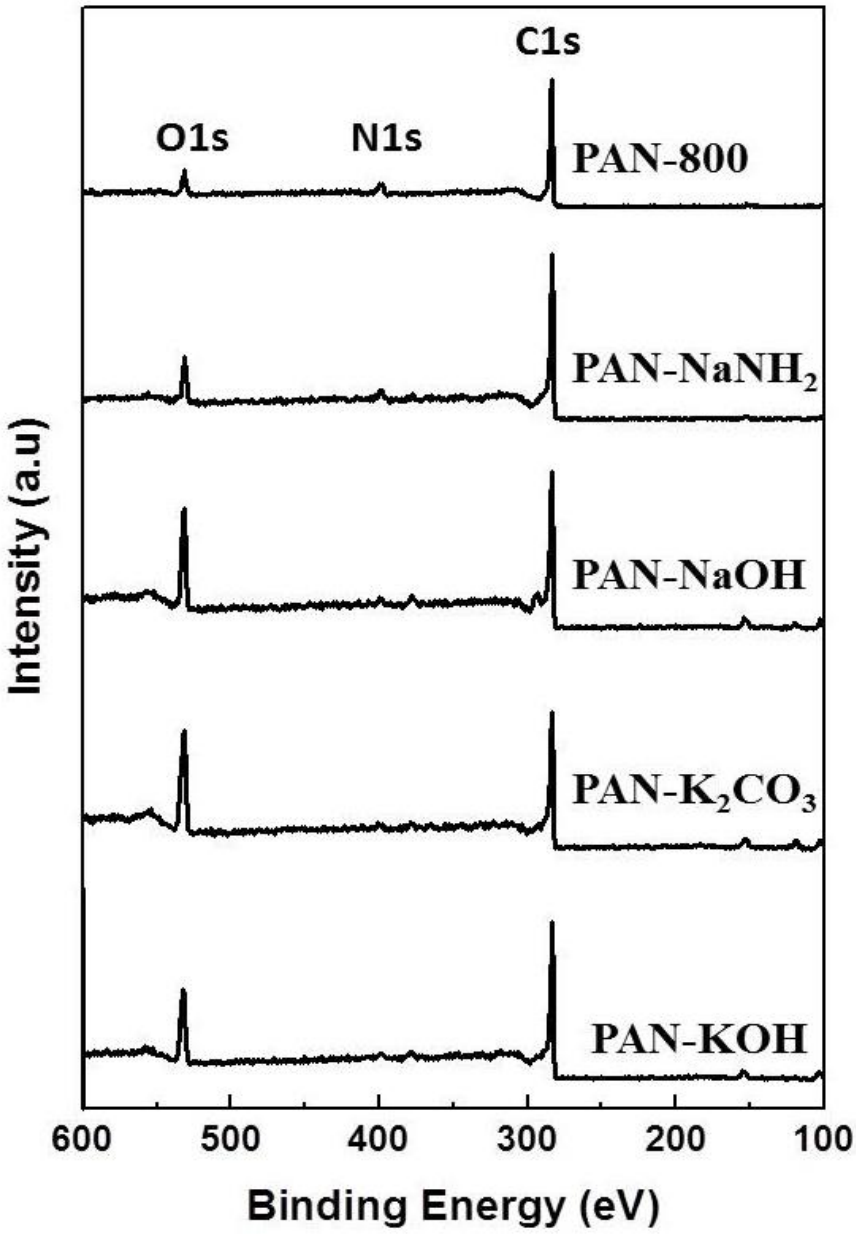

Fig. 5.8 Full range XPS spectra for the adsorbents

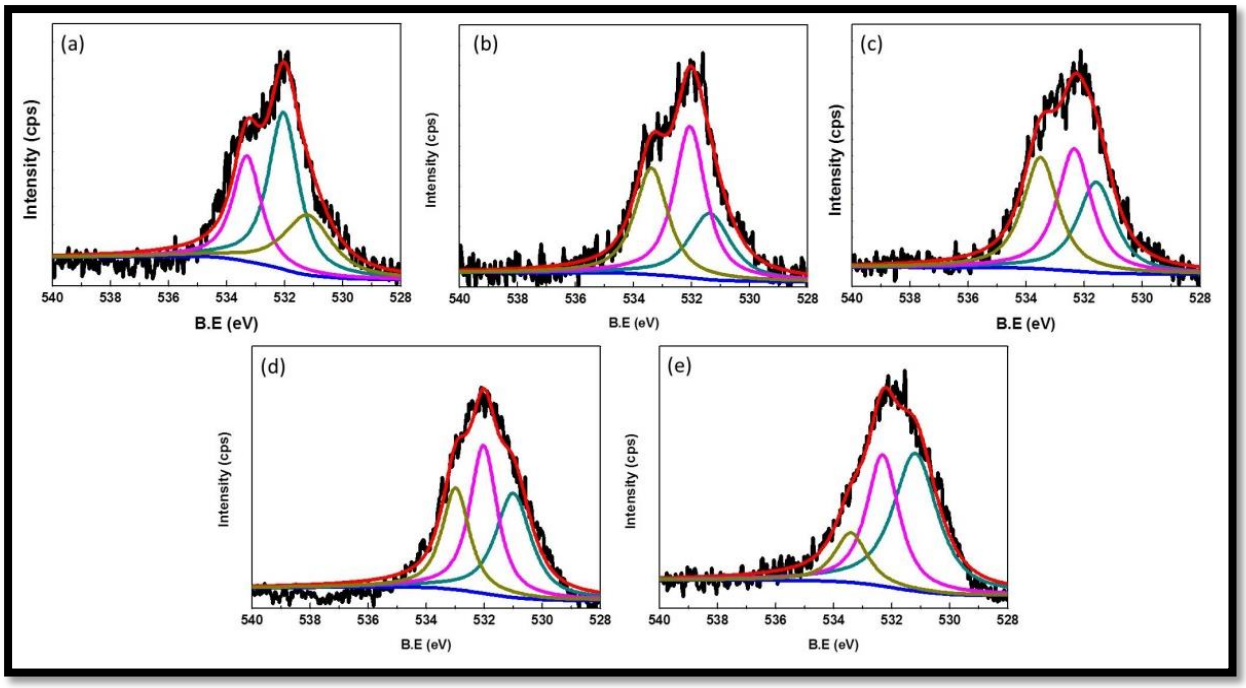

Fig. 5.9 Deconvoluted XPS spectra of O1S for (a) PAN-800 (b) PAN-$NaNH_2$ (c) PAN-NaOH (d) PAN-K_2CO_3 and (e) PAN-KOH adsorbents (reproduced from reference [42])

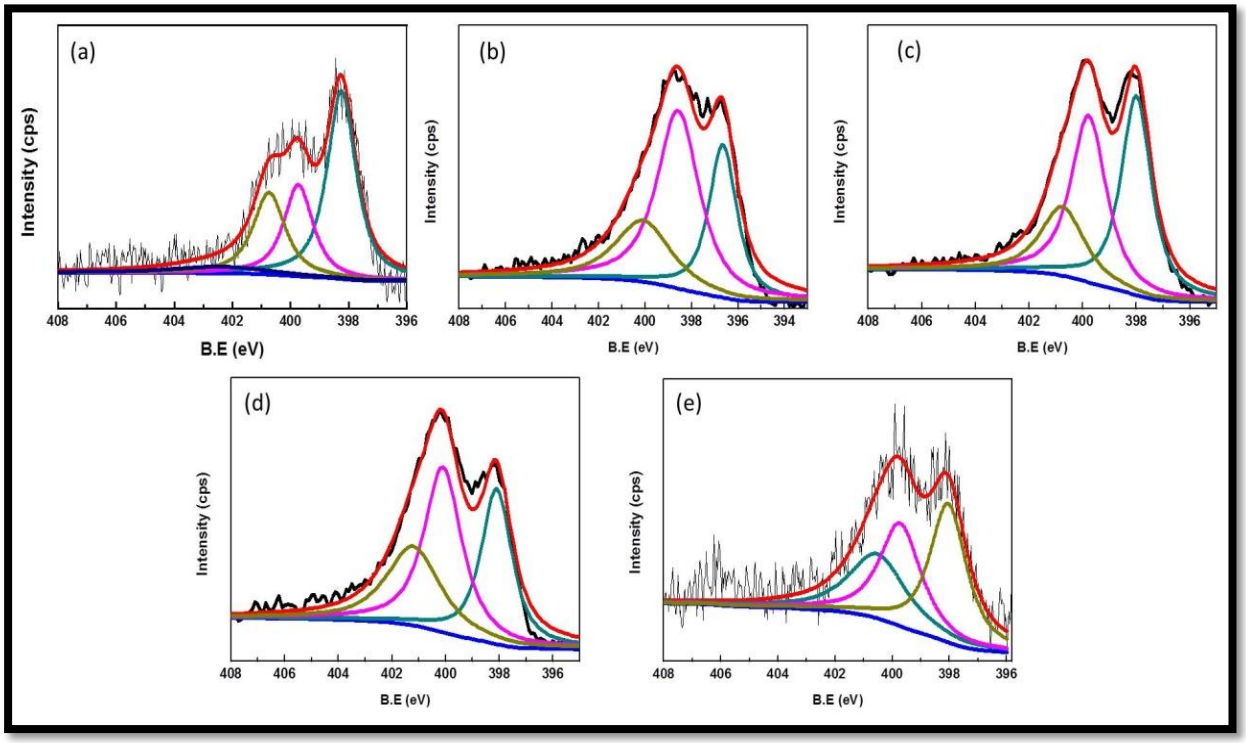

Fig. 5.10 Deconvoluted XPS spectra of N1S for (a) PAN-800 (b) PAN-$NaNH_2$ (c) PAN-NaOH (d) PAN-K_2CO_3 and (e) PAN-KOH adsorbents (reproduced from reference [42])

Table 5.3 O1s and N1s XPS data for the carbon adsorbents

Sample		O1	O2	O3	N1	N2	N3
PAN-800							
	BE	531.2	532.0	533.3	398.3	399.7	400.7
	FWHM	1.980	1.250	1.150	1.189	1.198	1.313
	A %	27.19	44.97	27.83	47.93	23.52	23.07
PAN-$NaNH_2$							
	BE	531.3	532.06	533.3	396.6	398.5	400.08
	FWHM	1.7	1.2	1.3	1.43	2.16	2.86
	A %	25.10	43.0	31.87	28.19	49.33	22.47
PAN-NaOH							
	BE	531.5	532.3	533.5	398.0	399.7	400.75
	FWHM	1.54	1.40	1.44	1.35	1.57	1.94
	A %	29.48	36.45	34.06	40.48	39.38	20.13
PAN-K_2CO_3							
	BE	531.0	532.02	532.98	398.1	400.10	401.2
	FWHM	1.46	1.12	1.12	1.38	1.67	2.38
	A %	35.17	38.48	26.34	31.56	40.72	27.70
PAN-KOH							
	BE	531.18	532.31	533.40	398.04	399.7	400.5
	FWHM	1.81	1.33	1.32	1.54	1.72	2.38
	A %	50.97	35.57	13.45	39.20	32.56	28.23

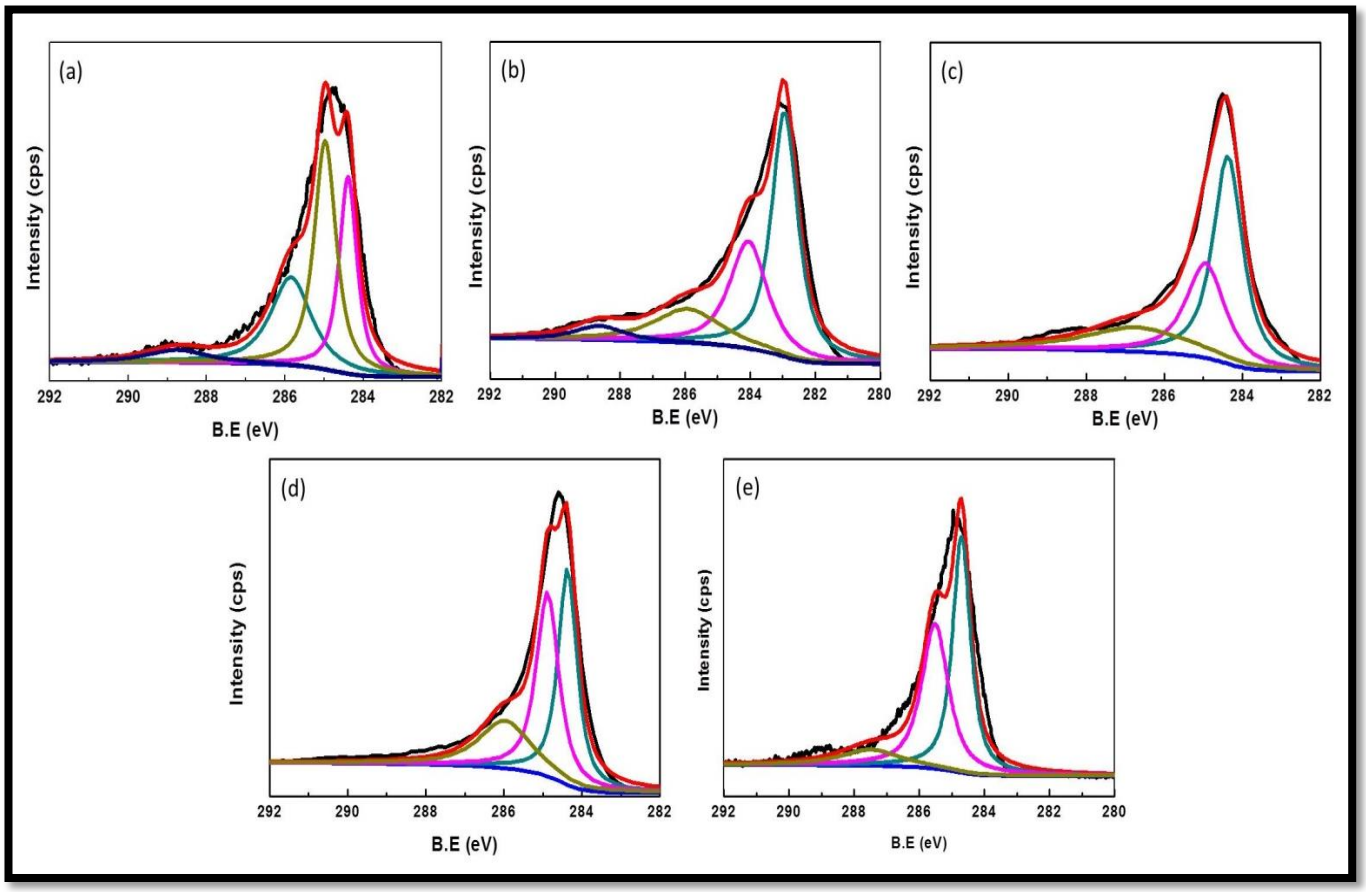

Fig. 5.11 Deconvoluted XPS spectra of C1s for (a) PAN-800 (b) PAN-$NaNH_2$ (c) PAN-NaOH (d) PAN-K_2CO_3 and (e) PAN-KOH adsorbents (reproduced from reference [42])

Table 5.4 C1s XPS data for the adsorbents

Adsorbent		C1	C2	C3	C4
PAN-800					
	BE	284.3	284.9	285.8	288.7
	FWHM	0.545	0.668	1.230	1.860
	A %	27.36	38.63	27.66	5.95
PAN-$NaNH_2$					
	BE	282.94	284.05	285.92	288.63
	FWHM	0.95	1.38	2.44	1.82
	A %	47.74	30.07	16.92	5.25
PAN-NaOH					
	BE	284.3	284.9	286.7	-
	FWHM	0.91	1.20	3.19	-
	A %	49.68	29.80	20.50	-
PAN-K_2CO_3					
	BE	284.3	284.8	285.9	-
	FWHM	0.57	0.68	1.56	-
	A %	38.34	38.71	22.93	-
PAN-KOH					
	BE	284.701	-	285.51	287.49
	FWHM	0.66	-	0.98	2.21
	A %	46.85	-	42.47	10.67

5.3 Dynamic CO_2 adsorption performance

5.3.1 Effect of carbonization temperature

To investigate the effect of carbonization temperature on the CO_2 uptake performance of PAN, it was carbonized at different temperatures from 600 to 900 °C. CO_2 capture capacity increases with the increase in temperature from 600 to 800 °C (Fig. 5.12). The maximum CO_2 uptake of 0.32 mmol g^{-1} was obtained with the same carbonized at 800°C. However, it decreased to 0.25 mmol g^{-1} for 900 °C sample. This may be due to the blockage of pores at a higher temperature. Therefore, the optimum carbonization temperature of 800 °C was chosen for further studies.

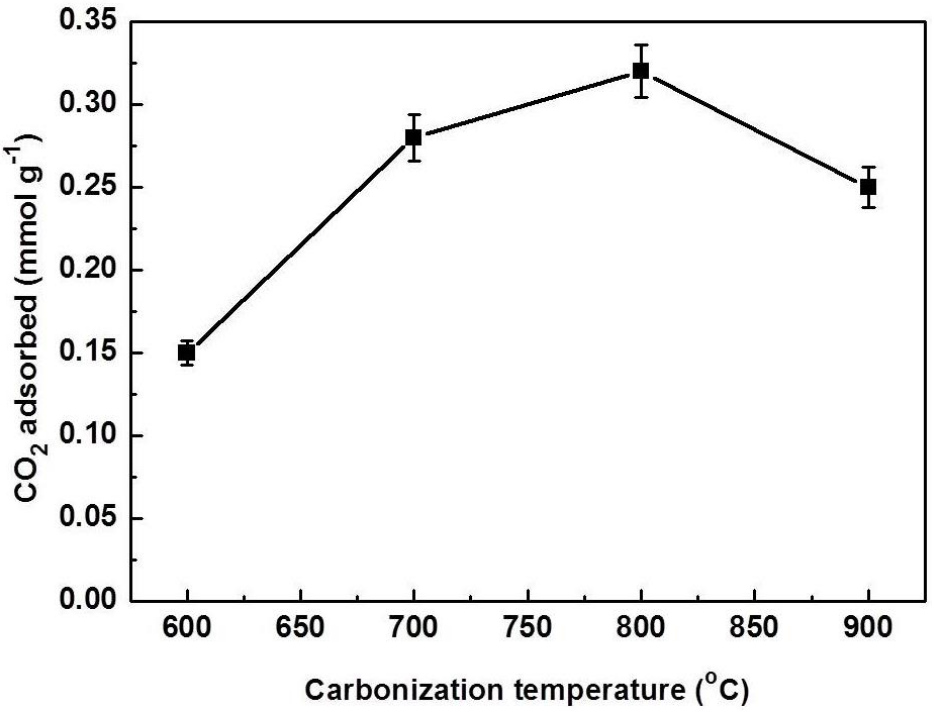

Fig. 5.12 Influence of carbonization temperature on the CO_2 adsorption capacity of the adsorbents at 30 °C and 12.5 % CO_2 concentration

5.3.2 Effect of activation time

The CO_2 capture capacity was different at different activation times at 800 °C (Fig. 5.13). The CO_2 uptake capacity gets enhanced by increasing the treatment time from 1.0 to 2 h. Afterward, the adsorption capacity has decreased. Therefore, the treatment time of 2h was considered for the present study.

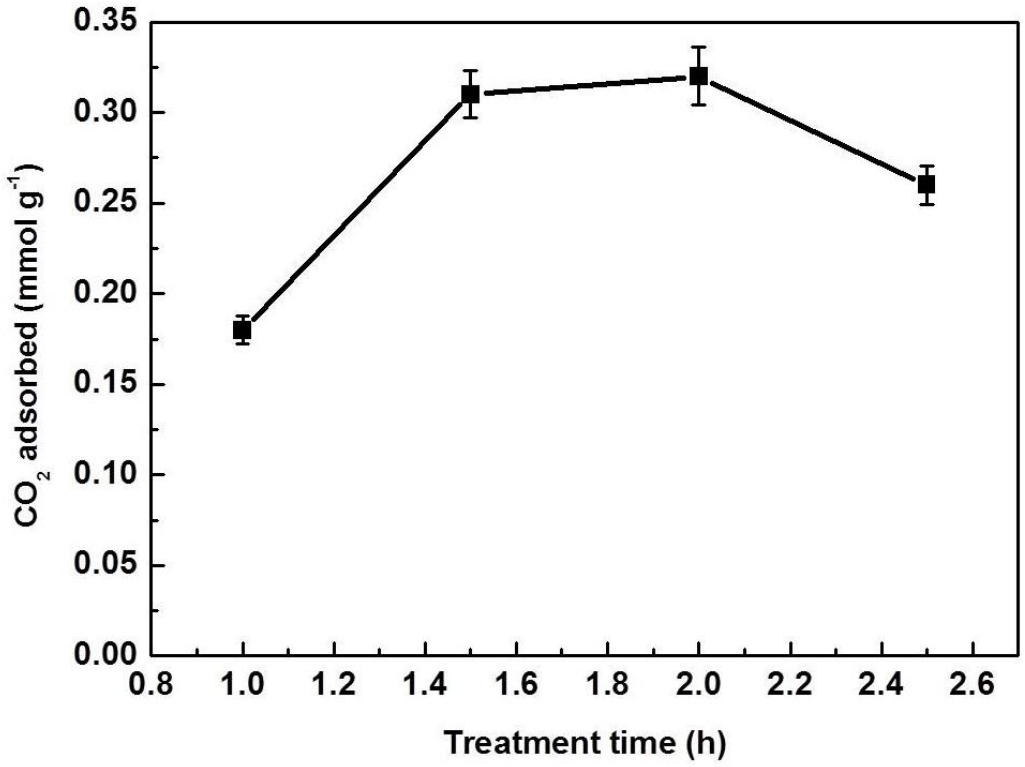

Fig. 5.13 Influence of activation time on the CO_2 capture capacity of PAN at 30 °C and 12.5 % CO_2

5.3.3 Influence of chemical activation

Fig. 5.14 compares the obtained CO_2 breakthrough curves of different carbon samples at 30 °C. CO_2 was not detected in the bed outlet initially because the bed was not completely saturated by CO_2 adsorption. However, CO_2 started appearing after 1 min at the bed outlet. The sample, PAN-KOH shows the broadest breakthrough curve whereas PAN-800 shows the steepest breakthrough curve. The adsorption capacity of PAN-KOH is maximum i.e 1.2 mmol g^{-1} due to the highest surface area (1890 m^2 g^{-1}) and of a large amount of basic oxygen and nitrogen functionalities on its surface as compared to PAN-$NaNH_2$ (0.57 mmol g^{-1}), PAN-NaOH (0.68 mmol g^{-1}) and PAN-K_2CO_3 (0.91 mmol g^{-1}). Besides, PAN sample synthesized by direct carbonization exhibits the least adsorption capacity (0.32 mmol g^{-1}) as compared to other activated carbons due to its inferior surface and textural properties. Tiwari *et al.* [183] also noticed a similar kind of observations in their CO_2 adsorption study. The adsorbents are in the following order in terms of CO_2 uptake: PAN-KOH > PAN-K_2CO_3 > PAN-NaOH > PAN-$NaNH_2$ > PAN-800. Therefore, it can be concluded that not only the textural properties affect the CO_2 uptake capacity but also, the presence of oxygen and

nitrogen species have a considerable impact on it. Among all the synthesized adsorbents, PAN-KOH has good performance for CO_2 capture, so we take this as a model adsorbent for study.

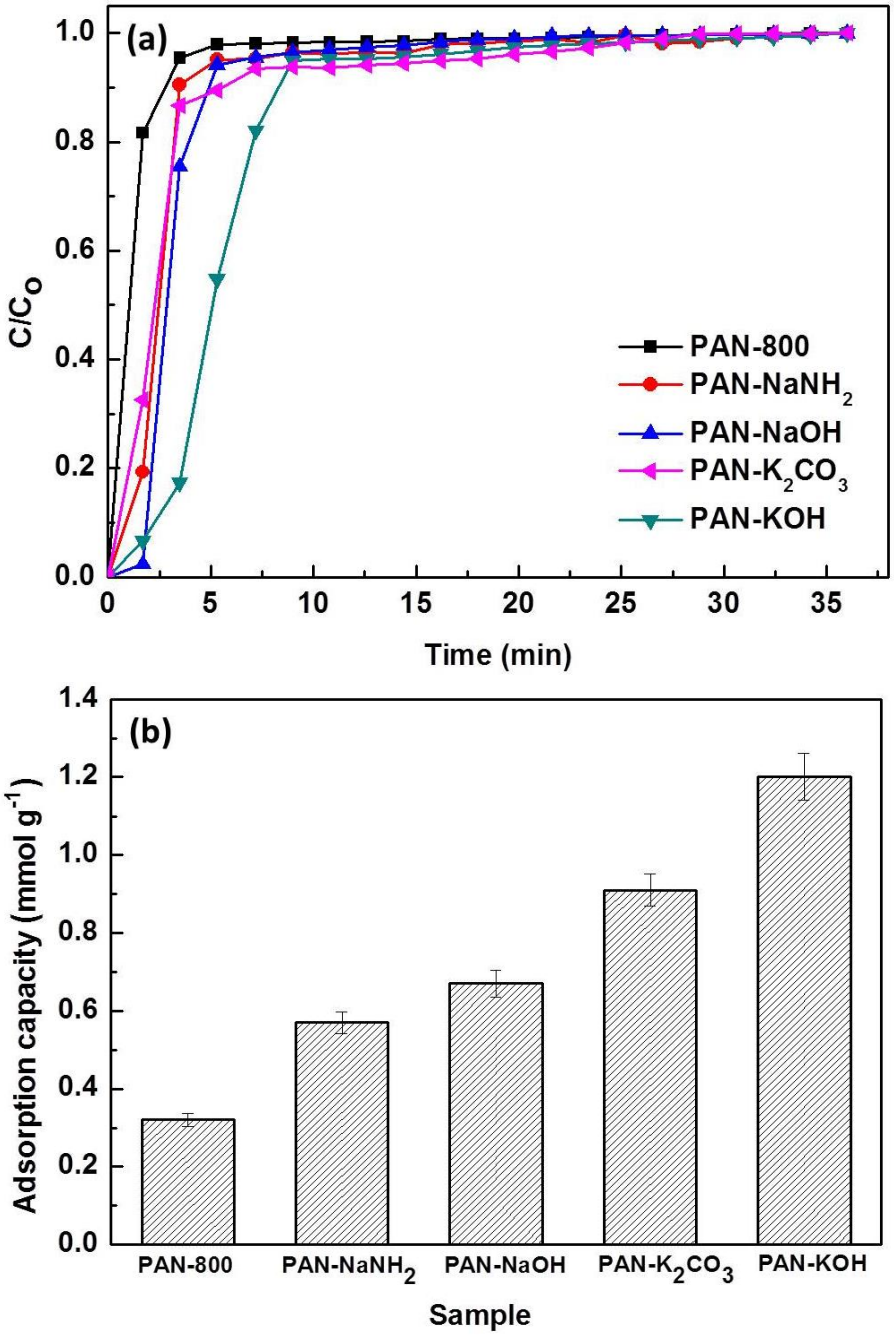

Fig. 5.14 (a) Carbon dioxide adsorption breakthrough curves and (b) CO_2 capture capacity of the carbons at 30 °C at 12.5 % CO_2 flow (reproduced from reference [42])

5.3.4 Influence of adsorption temperature and CO_2 feed concentration

Fig. 5.15 shows the CO_2 adsorption breakthrough curves for the PAN-KOH sample under various CO_2 concentrations. It is noticed that the uptake capacity increases from 0.52 to 1.2 mmol g^{-1} by increasing the CO_2 concentration (5 to 12.5 %) at 30 °C as shown in Fig. 5.16. The similar kind of increasing trend in CO_2 capture capacity with the increase in CO_2 concentration was noticed at all other temperatures. The adsorbent gets saturated early by increasing the temperature (Fig. 5.15). As a result, the movement of breakpoint shifted towards lesser time and became shorter with the increase in temperature which implies the loss in the CO_2 uptake capacity. The adsorption capacity decreases from 1.2 mmol g^{-1} to 0.44 mmol g^{-1} with the increase in the temperature from 30 to 100 °C at a fixed CO_2 concentration (12.5 %) as shown in Fig. 5.16. This decreasing trend in the adsorption capacity represents the physisorption nature of the adsorbents. At higher temperatures, due to the high surface energy the molecular diffusion on the surface enhances, which makes CO_2 adsorption to be unstable and enhances the desorption process.

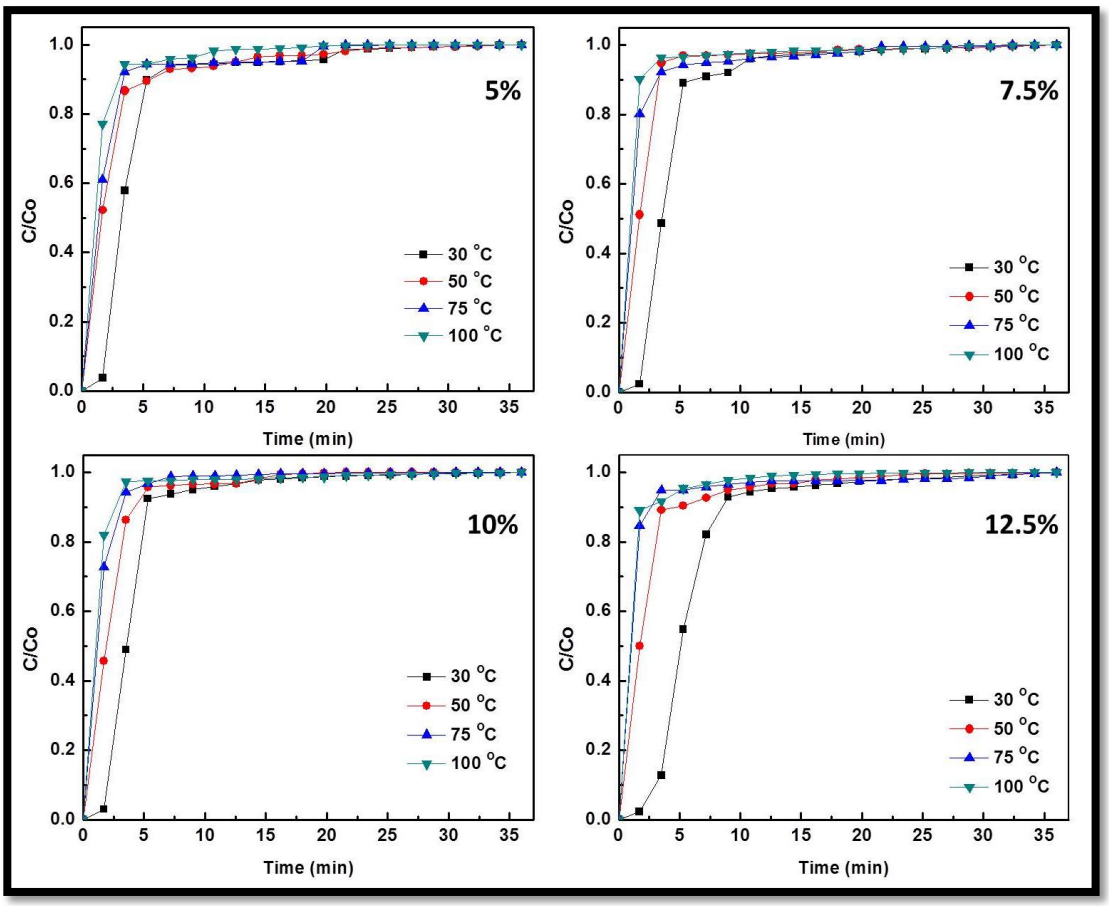

Fig. 5.15 Breakthrough curves for the CO_2 adsorption on PAN-KOH (reproduced from reference [42])

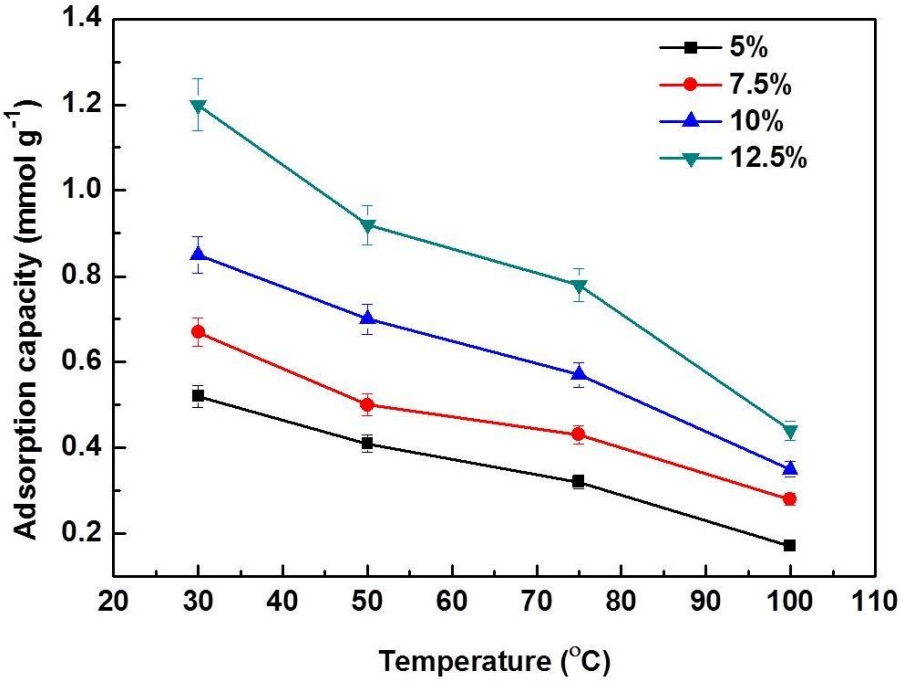

Fig. 5.16 CO_2 adsorption capacities of the PAN-KOH at different CO_2 concentrations (%)

5.3.5 CO_2 selectivity

The CO_2/N_2 breakthrough curves for the PAN-KOH adsorbent under 12.5 % CO_2 concentration can be seen in Fig. 5.17. It was observed that N_2 detected immediately whereas CO_2 started coming out in the effluent after some time. This confirms the lower uptake capacity of N_2 in comparison to CO_2. As can be seen in Fig. 5.17, the initial value of C/C_0 for N_2 >1 which shows occupation of N_2 on the adsorbent active sites at the initial stage. However, N_2 gets replaced by CO_2 with the time indicating that the adsorbent has a higher affinity towards CO_2. Goel *et al*. [166] also observed a similar pattern in their study.

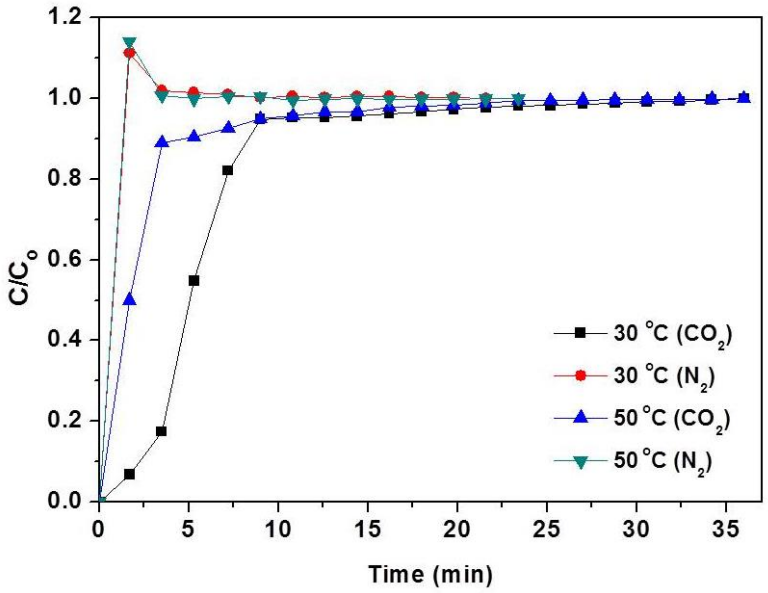

Fig. 5.17 Breakthrough curves of CO_2 and N_2 for 12.5 % CO_2 rest N_2 on PAN-KOH at 30 °C, and 50 °C (reproduced from reference [42])

5.3.6 Regeneration study

Easy regeneration is a significant characteristic of effective adsorbent with its higher adsorption capacity. In this regard, the adsorption capacity of PAN-KOH was tested at 30 °C for five adsorption/desorption cycles and the sudden fall of C/C_o value was noticed for all the cycles on desorption at 200 °C which indicates the easy CO_2 desorption from the adsorbent (Fig. 5.18a). In a similar way, the adsorbent exhibits stable CO_2 adsorption capacity over repetitive cycles at various temperatures (Fig. 5.18b) and hence, indicating its good regenerability. Therefore, the developed activated adsorbent is effective as well as promising one for reducing the CO_2 emissions.

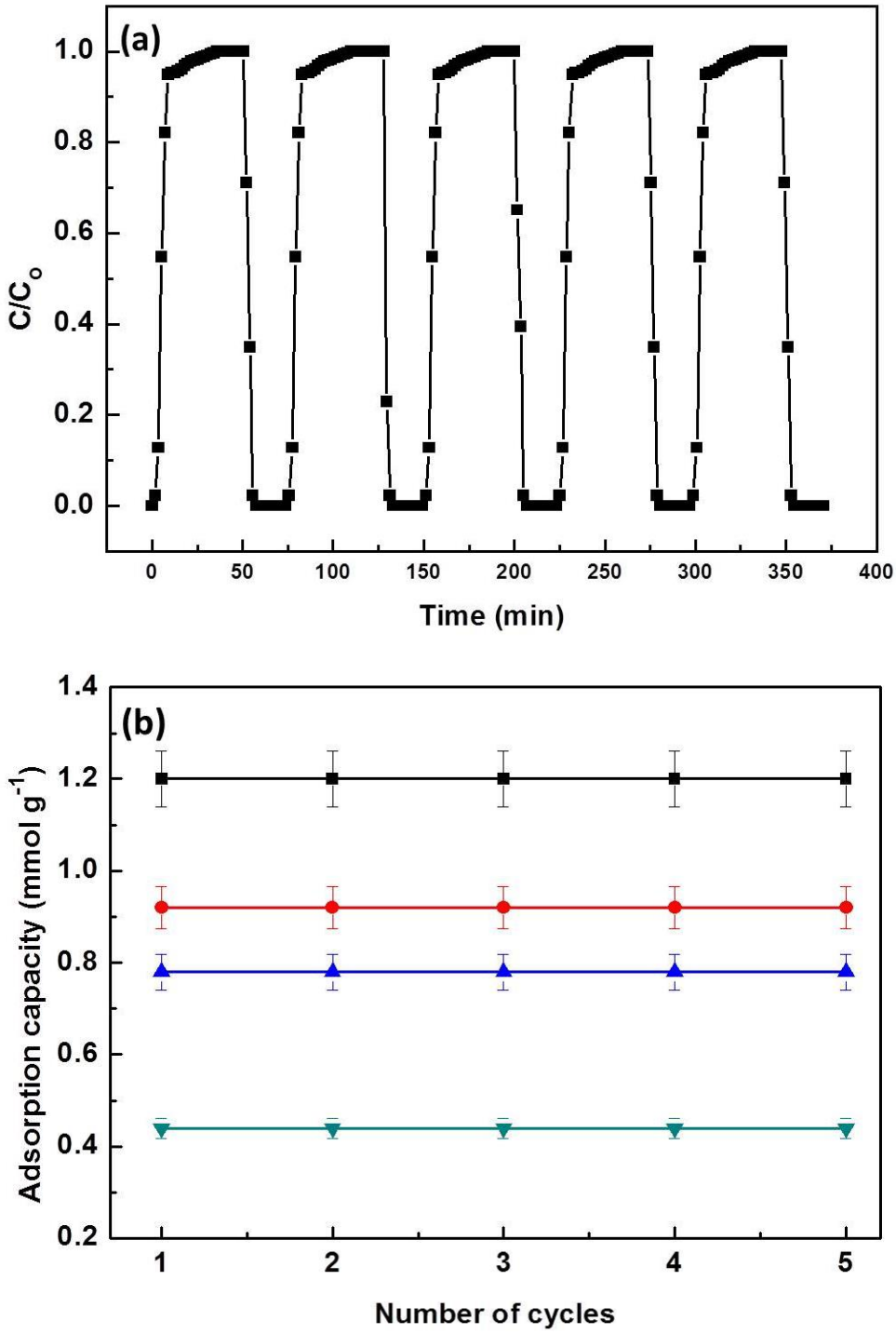

Fig. 5.18 (a) Multiple adsorption-desorption cycles at 30 °C and (b) multiple cycles CO_2 adsorption capacities of PAN-KOH at different adsorption temperatures (reproduced from reference [42])

The dynamic CO_2 adsorption capacities found in the present study has been compared with the reported values for various activated carbons (Table 5.5). The adsorbents synthesized in this study show superior adsorption capacities than the other carbon-based adsorbents in the dynamic conditions.

Table 5.5 CO_2 adsorption performance of PAN-KOH and other carbon adsorbents

Adsorbent	Treatment method	Experimental conditions		CO_2 capture capacity (mmol g^{-1})	References
		CO_2 (vol. %)	Temp. (°C)		
PAN-KOH*	Chemical/KOH (800 °C)	12.5	30	1.2*	Present study
PAN-KOH*	Chemical/KOH (800 °C)	12.5	50	0.92*	Present study
PAN fibers	Chemical/KOH (750 °C)	100	25	0.76	[116]
Soybean	Chemical/$ZnCl_2$ (600 °C) then, Physical/CO_2 (800 °C)	15.4	30	0.93	[110]
Fly ash	Chemical/KOH (700 °C)	100	25	0.6	[184]
Carbon monolith*	Chemical/KOH (R.T)	15	30	0.66*	[185]
Urea-based AC*	Chemical/KOH (700 °C)	15	50	0.93*	[183]
Rice Husk	Chemical/$ZnCl_2$(700 °C)	100	25,75	1.3, 0.5	[186]
PAN activated carbon	Chemical/KOH (850 °C)	100	25	1.3	[117]
Potassium based AC*	Chemical/K_2CO_3 (R.T)	0.5	20	0.87*	[187]
N-containing resin	Chemical/K_2CO_3 (700 °C)	100	25	1.9	[188]
Anthracite	Physical/Steam (800 °C)	100	30	1.5	[189]

*performance evaluation under dynamic conditions

5.3.7 Temperature programed desorption

Fig. 5.19 presents the TPD profile for the PAN-KOH adsorbent. The broad peak was found to be in between 60-130 ºC indicating the CO_2 removal from the carbon surface. Also, the CO_2 signal was found in between 275 to 300 ºC which indicates the involvement of smaller contribution of the chemisorption process.

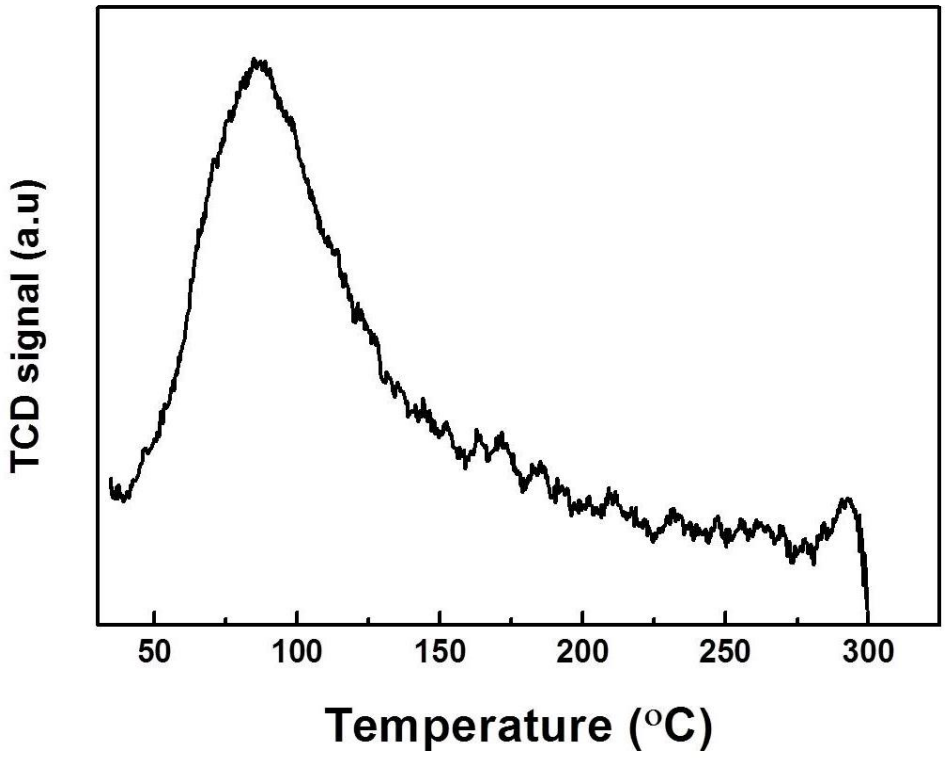

Fig. 5.19 Temperature programmed desorption curve for the PAN-KOH sample (reproduced from reference [42])

5.4 Adsorption kinetic study

The experimental adsorption data fitting with the predicted CO_2 adsorption capacities by respective kinetic models for PAN-KOH at various adsorption temperatures with respect to time is displayed in Fig. 5.20. It is observed that 90 % of the adsorption occurs in ca. 10 min and then it slows down to reach the equilibrium as the active sites are occupied during first few minutes [174]. The calculated kinetic parameters for the models along with the error % values are summarized in Table 5.6. Larger values of R^2 and error % less than 3 signifies the best fitting of fraction order kinetic model with all the adsorption data.

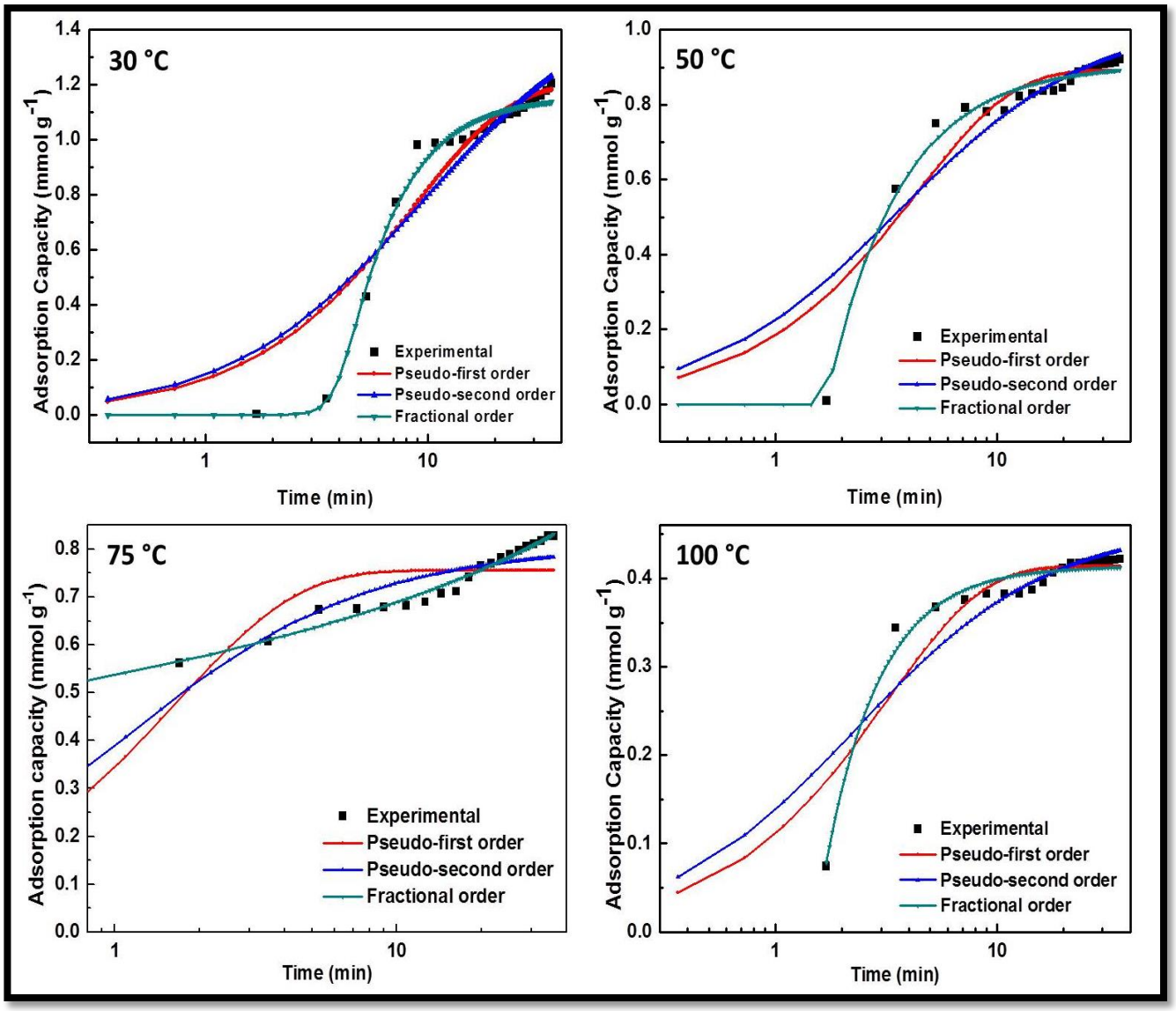

Fig. 5.20 CO_2 uptake kinetics on PAN-KOH (reproduced from reference [42])

Table 5.6 Kinetic parameters of PAN-KOH at different adsorption temperatures

Model	Parameters	Temperature (°C)			
		30	50	75	100
Pseudo first order					
	q_e	0.114	0.23	0.72	0.41
	k_1	1.2	0.89	0.14	0.31
	R^2	0.91	0.91	0.95	0.92
	Error %	9.56	8.12	3.0	2.3
Pseudo second order					
	k_2	0.65	9.27	0.17	0.94
	q_e	1.55	1.02	0.87	0.45
	R^2	0.96	0.95	0.97	0.96
	Error %	8.83	3.26	2.01	1.05
Fractional order					
	k_n	0.15	0.20	0.35	0.51
	q_e	1.16	0.90	0.98	0.41
	n	9.67	14.28	75.5	109.8
	m	6.35	113.94	176.93	63.7
	R^2	0.98	0.99	0.98	0.98
	Error %	1.9	1.65	2.16	2.0

5.5 Adsorption isotherm study

Fig. 5.21 shows different isotherm models fitting with the experimental data for PAN-KOH. The isotherm parameters were calculated using the eqns. 3.7-3.9. The highest R^2 values (Table 5.7) proving the best result found with the Freundlich isotherm model. Also, K_F value decreases with the temperature signifying the physisorption process and n>1 signifies that the adsorption of CO_2 onto adsorbent is favorable [190].

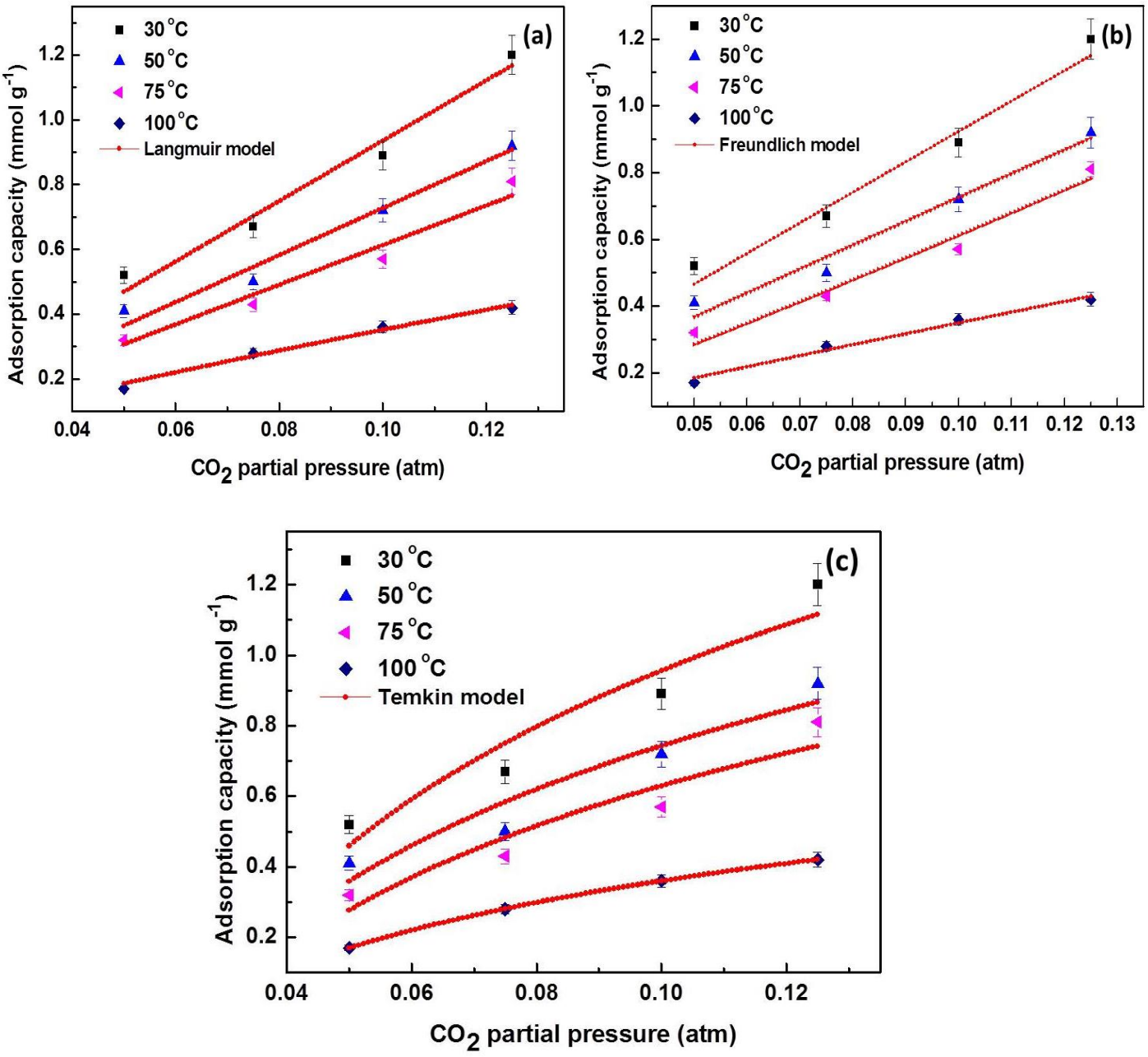

Fig. 5.21 Langmuir (a), Freundlich (b) and Temkin (c) isotherm models fitting with the experimental data for PAN-KOH adsorbent

Table 5.7 Isotherm parameters

Isotherm Model	Parameters	Temperature			
		30 °C	50 °C	75 °C	100 °C
Langmuir	K_L	8.03	6.02	5.8	1.15
	q_m	2.67	2.35	1.7	0.81
	R^2	0.93	0.95	0.94	0.98
Freundlich	n	1.9	1.7	1.5	1.8
	K_F	8.96	6.94	7.71	2.29
	R^2	0.98	0.99	0.97	0.98
Temkin	b	0.699	0.55	0.508	0.27
	K_T	38.48	38.16	34.44	37.22
	R^2	0.96	0.96	0.95	0.97

5.6 Thermodynamic study

5.6.1 Thermodynamic parameters

The thermodynamic parameters calculated using eqns. 3.10 and 3.11 for the CO_2 adsorption on PAN-KOH are presented in Table 5.8. The negative ΔG° values at all the temperatures indicate the spontaneous and feasible nature of the adsorption process whereas, ΔH° value of -6.49 kJ mol^{-1} reveals the exothermic nature. ΔS° is found to be positive (0.09 kJ mol^{-1}) which confirms the high CO_2 affinity and enhancement of randomness at the interface. The calculated Q_{st} values for PAN-KOH at different q_e are shown in Fig. 5.22, which is in between 24.39 kJ mol^{-1} to 41.39 kJ mol^{-1} (Table 5.9). The increase in Q_{st} values with the surface coverage indicates the adsorbent's surface heterogeneity. Also, the calculated Q_{st} values are much greater than the reported values (28.4-10.5 kJ mol^{-1}) in the literature [191], implying relatively the stronger affinity towards CO_2.

Table 5.8 Parameters obtained from the thermodynamic study of the adsorption process

Temperature (°C)	$\Delta G°$ (kJ mol^{-1})	$\Delta H°$ (kJ mol^{-1})	$\Delta S°$ (kJ mol^{-1})
30	-4.77	-6.49	0.09
50	-5.3		
75	-8.0		
100	-12.08		

Table 5.9 Calculated Q_{st} values for PAN-KOH

Adsorption capacity (mmol g^{-1})	Q_{st} (kJ mol^{-1})
0.3	24.39
0.35	30.17
0.4	32.88
0.45	34.93
0.5	41.39
Average	32.75

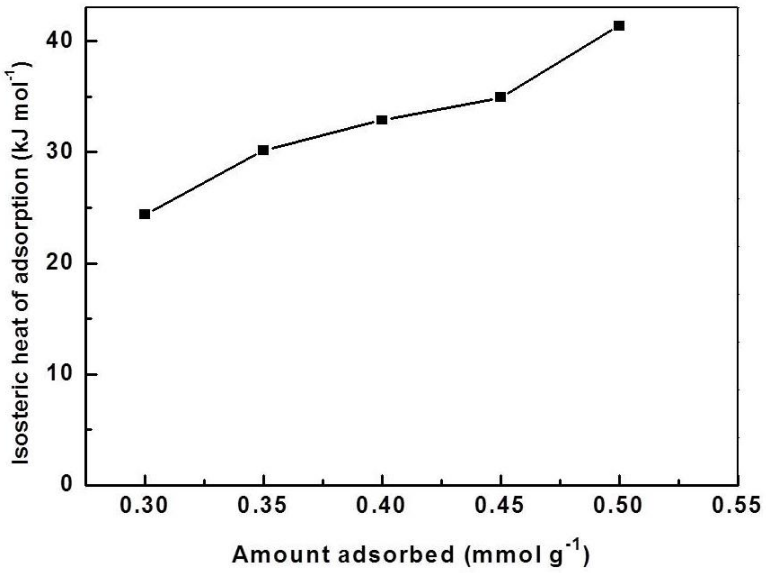

Fig. 5.22 Plot of Q_{st} values against surface loading (q_e) for CO_2 adsorption on PAN-KOH (reproduced from reference [42])

5.6.2 Energy duty for desorption of CO_2

C_P value for PAN-KOH = 1.2 J g^{-1} K^{-1} (assumed)

Adsorption temperature was 30 °C whereas, desorption for CO_2 was carried out at 200 °C.

Temperature difference, ΔT = (200-30) °C = 170 °C.

The adsorption capacity of PAN-KOH = 1.2 mmol CO_2/g adsorbent

= 1.2 * 10^{-3} mol CO_2/g adsorbent = 0.0528 kg CO_2/kg adsorbent.

Therefore, sensible heat = $\frac{1.2 \times 170}{1.2 * 10-3}$ J per mole CO_2 = 170 kJ per mole CO_2.

Net sensible heat needed is 25 % of 170 kJ per mole CO_2, assuming 75 % heat recovery.

Sensible heat = 42.5 kJ per mole CO_2 and

As Q_{st} is 32.75 kJ per mole CO_2

Thermal energy input = (42.5 + 32.75) kJ per mole CO_2 = 75.25 kJ per mole CO_2

= 1.71 MJ per kg CO_2

Assuming, 0.0884 kg CO_2 per MJ generated on using bituminous coal (as fossil fuel) for energy production.

Therefore, for desorption of 1.2 mmol g^{-1} of CO_2 (0.0528 kg kg^{-1}), the energy required is 0.0633 MJ.

Thus, CO_2 created to produce 0.0633 MJ for the desorption of 0.00559 kg CO_2.

Therefore, energy penalty (%) = $\frac{0.00559}{0.0528}$x 100= 10.58 %

5.7 Conclusions

In this study, nitrogen and oxygen containing activated PAN adsorbents have been prepared via carbonization and chemical activation process for its use in the CO_2 capture. The synthesized adsorbents exhibited a substantial enhancement in the surface morphology and textural properties with the chemical activation of PAN derived carbons. The adsorption process was undoubtedly exothermic and showed physisorption nature. The adsorbent, PAN-KOH showed the maximal capacity of 1.2 mmol g^{-1} under dynamic conditions at 30 °C. Furthermore, the adsorbent showed the good regenerability over 5 adsorption-desorption cycles and thus it could be reused for many times for CO_2 capture process. In addition, the adsorption data were fitted best with the fractional order kinetic models. The thermodynamic study indicated the spontaneous, feasible as well as exothermic process. Furthermore, the thermal energy needed for the desorption of CO_2 is ca.1.71 MJ per kg of CO_2. The energy penalty for CO_2 capture by adsorption on PAN-KOH is ca. 10.58 %.

Chapter 6 - Conclusions and Recommendations for Future Work

6.1 Conclusions

Porous carbon monoliths were synthesized via nanocasting technique, using silica monolith as hard template and impregnated with the furfuryl alcohol followed by carbonization at different temperatures. The obtained carbon monoliths showed highly porous nature with high surface area (1166-1225 m^2 g^{-1}) and pore volume (1.01-1.26). The oxygen content decreases from 18.92 to 14.38% with the temperature from 550 to 950 °C. The oxygen functional groups present in the monoliths acted as Lewis base sites on its pore wall to bind acidic CO_2 molecules during the CO_2 adsorption process.

Both textural and surface chemistry found to be effective for the variation in the CO_2 capture capacity of the monoliths. The monolithic adsorbent, CM-950 (carbonization temperature of 950 °C) exhibits the CO_2 uptake of 1.0 mmol g^{-1} due to the superior textural properties. The monoliths showed excellent stability over multiple regeneration cycles. Moreover, the fractional-order kinetic model was perfectly fitted among all the kinetic models at various adsorption temperatures. The heterogeneous nature of the monoliths was indicated by the appropriate fitting of the Temkin isotherm model. The thermodynamic parameters confirmed the spontaneous, exothermic and feasible nature of the process.

High nitrogen-containing PAN polymer using chemical activation with the various chemical activating agents i.e K_2CO_3, NaOH, $NaNH_2$, and KOH, results in the development of activated carbons with excellent textural properties. The pore volume and surface area of the adsorbents lie in between the range of 0.36–1.47 cm^3 g^{-1} and 833-1890 m^2 g^{-1} respectively. Both of the properties of microporosity and functional groups explicate the high CO_2 capture performance of the carbons under dynamic conditions. KOH activated carbon exhibited maximum dynamic capacity (1.2 mmol g^{-1}) as compared to NaOH (0.68 mmol g^{-1}), K_2CO_3 (0.91 mmol g^{-1}) and $NaNH_2$ (0.57 mmol g^{-1}) activated carbons respectively at 30 °C. The synthesized carbons can be regenerated and reused multiple times without loss in the adsorption performance. Moreover, good cyclic stability along with regenerability over five consecutive adsorption-desorption cycles was achieved for the adsorbents. The fractional order kinetic and Freundlich isotherm models fitted best with the adsorption data. A

heterogeneous interaction between CO_2 and the surface of carbons was confirmed by Qst values.

Direct carbonization of the carbon precursors leads to develop the carbon adsorbents of poor textural properties and exhibiting the least CO_2 adsorption capacity. This confirms the implementation of nanocasting method and chemical activation to produce superior textural properties and CO_2 uptake performance of the carbon adsorbents which makes it effective and promising in the CO_2 capture practical applications.

The nature of the precursor with the presence of heteroatoms has a crucial role in the involvement of various functionalities on the adsorbent surface and their existence affects the CO_2 uptake capacity. The existence of the oxygen and nitrogen functionalities on the carbon surface defines its acidity or basicity. So, the basic functional groups increase the Lewis basic character of the adsorbents and help in efficient CO_2 adsorption.

In summary, the present work is a comprehensive study of developing the nanostructured carbon adsorbents from nanocasting, direct carbonization followed by chemical activation using effective chemical activating agents and performance evaluation for CO_2 adsorption under dynamic conditions along with the kinetics, isotherm and thermodynamic studies.

6.2 Recommendations for future work

- Synthesis of carbon monoliths can be carried out by using different carbon precursors and various monolithic templates like zeolite for CO_2 adsorption.
- The chemical activation of the carbon monoliths with different activating agents and activating conditions should be investigated.
- The CO_2 capture performance of the developed carbon adsorbents should be evaluated at high-pressure conditions.
- Effect of impurities like SO_x and NO_x on CO_2 adsorption performance can be evaluated for complete overview of the adsorption process.

Appendix

OriginPro 8 software was used to calculate all the crucial parameters in section 3.4 and 3.5. All the kinetic and isotherm model equations were firstly feed in the software. Onwards, the parameters in the model equations were obtained through non-linear fitting the experimental data. For example:

$$q_t = q_e (1 - e^{-k_1 t})$$

1. Firstly the above first pseudo-first-order equation feed in the OriginPro 8 software by following these steps: **Analysis→ Non-linear fit→ Origin basic function→ New.**
2. After compile the equation, the raw data fitted with the non-linear curve fitting using the feed equation.
3. The values of the k_1 and q_e parameters along with the R^2 are automatically generated by the software.

References

[1] S.A. Montzka, E.J. Dlugokencky, J.H. Butler, Non-CO_2 greenhouse gases and climate change, Nature, 476 (2011) 43.

[2] A. Al-Mamoori, A. Krishnamurthy, A.A. Rownaghi, F. Razeai, Carbon capture and utilization update, Energy Technology, 5 (2017) 834-849.

[3] P. Puthiaraj, W.-S. Ahn, Facile synthesis of microporous carbonaceous materials derived from a covalent triazine polymer for CO_2 capture, Journal of Energy Chemistry, 26 (2017) 965-971.

[4] R. Zhong, X. Yu, W. Meng, S. Han, J. Liu, Y. Ye, C. Sun, G. Chen, R. Zou, A solvent 'squeezing'strategy to graft ethylenediamine on Cu_3 $(BTC)_2$ for highly efficient CO_2/CO separation, Chemical Engineering Science, 184 (2018) 85-92.

[5] R. Muraleedharan, A. Mondal, B. Mandal, Absorption of carbon dioxide into aqueous blends of 2-amino-2-hydroxymethyl-1, 3-propanediol and monoethanolamine, Separation and Purification Technology, 94 (2012) 92-96.

[6] S. Anantharaj, S.R. Ede, K. Sakthikumar, K. Karthick, S. Mishra, S. Kundu, Recent trends and perspectives in electrochemical water splitting with an emphasis on sulfide, selenide, and phosphide catalysts of Fe, Co, and Ni: a review, ACS Catalysis, 6 (2016) 8069-8097.

[7] M.A. Hassaan, A. El Nemr, Health and environmental impacts of dyes: Mini review, American Journal of Environmental Science and Engineering, 1 (2017) 64-67.

[8] D. Tiwari, C. Goel, H. Bhunia, P.K. Bajpai, Novel nanostructured carbons derived from epoxy resin and their adsorption characteristics for CO_2 capture, RSC Advances, 6 (2016) 97728-97738.

[9] F. Perera, Pollution from fossil-fuel combustion is the leading environmental threat to global pediatric health and equity: Solutions exist, International Journal Of Environmental Research and Public Health, 15 (2017) 16.

[10] A.B. Robinson, N.E. Robinson, W. Soon, Environmental effects of increased atmospheric carbon dioxide, Journal of American Physicians and Surgeons, 12 (2007) 79-90.

[11] A.J. McMichael, A. Haines, R. Slooff, S. Kovats, M.L. Wilson, Climate change and human health, World Health Organization Geneva, 1996.

[12] S.K. Tandon, J. Mallik, Links between energy usage and climate: implications on increasing CO_2 emissions and carbon capture and storage, Current Science 114 (2018) 1430-1437.

[13] B. Ekwurzel, J. Boneham, M. Dalton, R. Heede, R.J. Mera, M.R. Allen, P.C. Frumhoff, The rise in global atmospheric CO_2, surface temperature, and sea level from emissions traced to major carbon producers, Climatic Change, 144 (2017) 579-590.

[14] P. Markewitz, W. Kuckshinrichs, W. Leitner, J. Linssen, P. Zapp, R. Bongartz, A. Schreiber, T.E. Müller, Worldwide innovations in the development of carbon capture technologies and the utilization of CO_2, Energy & Environmental Science, 5 (2012) 7281-7305.

[15] M. Sharma, R.K. Vyas, K. Singh, A review on reactive adsorption for potential environmental applications, Adsorption, 19 (2013) 161-188.

[16] S.I. Plasynski, J.T. Litynski, H.G. McIlvried, R.D. Srivastava, Progress and new developments in carbon capture and storage, Critical Reviews in Plant Sciences, 28 (2009) 123-138.

[17] R. Lal, Sequestering atmospheric carbon dioxide, critical reviews in plant sciences, 28 (2009) 90-96.

[18] U.S.E.P. Agency, Climate change indicators in the United States, 2014, in, 2014.

[19] Y.-C. Chiang, R.-S. Juang, Surface modifications of carbonaceous materials for carbon dioxide adsorption: A review, Journal of the Taiwan Institute of Chemical Engineers, 71 (2017) 214-234.

[20] S. Cha, H.-M. Chae, S.-H. Lee, J.-K. Shim, Effect of elevated atmospheric CO_2 concentration on growth and leaf litter decomposition of *Quercus acutissima* and *Fraxinus rhynchophylla*, PloS one, 12 (2017) e0171197.

[21] G.K. Parshetti, S. Chowdhury, R. Balasubramanian, Biomass derived low-cost microporous adsorbents for efficient CO_2 capture, Fuel, 148 (2015) 246-254.

[22] D.Y. Leung, G. Caramanna, M.M. Maroto-Valer, An overview of current status of carbon dioxide capture and storage technologies, Renewable and Sustainable Energy Reviews, 39 (2014) 426-443.

[23] C. Marchetti, On geoengineering and the CO_2 problem, Climatic change, 1 (1977) 59-68.

[24] IPCC, IPCC special report on carbon dioxide capture and storage, working group III of the Intergovernmental Panel on Climate Change (2005).

[25] S.-Y. Lee, S.-J. Park, A review on solid adsorbents for carbon dioxide capture, Journal of Industrial and Engineering Chemistry, 23 (2015) 1-11.

[26] J.M. Sánchez, M. Maroño, D. Cillero, L. Montenegro, E. Ruiz, Laboratory- and bench-scale studies of a sweet water–gas-shift catalyst for H_2 and CO_2 production in pre-combustion CO_2 capture, Fuel, 114 (2013) 191-198.

[27] S. Danaei Kenarsari, M. Fan, G. Jiang, X. Shen, Y. Lin, X. Hu, Use of a robust and inexpensive nanoporous TiO_2 for pre-combustion CO_2 separation, Energy & Fuels, 27 (2013) 6938-6947.

[28] E.S. Rubin, H. Mantripragada, A. Marks, P. Versteeg, J. Kitchin, The outlook for improved carbon capture technology, Progress in Energy and Combustion Science, 38 (2012) 630-671.

[29] Z.H. Lee, K.T. Lee, S. Bhatia, A.R. Mohamed, Post-combustion carbon dioxide capture: Evolution towards utilization of nanomaterials, Renewable and Sustainable Energy Reviews, 16 (2012) 2599-2609.

[30] B.P. Spigarelli, S.K. Kawatra, Opportunities and challenges in carbon dioxide capture, Journal of CO_2 Utilization, 1 (2013) 69-87.

[31] M.D. Hornbostel, J. Bao, G. Krishnan, A. Nagar, I. Jayaweera, T. Kobayashi, A. Sanjurjo, J. Sweeney, D. Carruthers, M.A. Petruska, Characteristics of an advanced carbon sorbent for CO_2 capture, Carbon, 56 (2013) 77-85.

[32] R. Ben-Mansour, M. Habib, O. Bamidele, M. Basha, N. Qasem, A. Peedikakkal, T. Laoui, M. Ali, Carbon capture by physical adsorption: materials, experimental investigations and numerical modeling and simulations – a review, Applied Energy, 161 (2016) 225-255.

[33] C. Das, S. Bose, Advanced Ceramic Membranes and Applications, CRC Press, 2017.

[34] D. Aaron, C. Tsouris, Separation of CO_2 from flue gas: a review, Separation Science and Technology, 40 (2005) 321-348.

[35] A. Meisen, X. Shuai, Research and development issues in CO_2 capture, Energy Conversion and Management, 38 (1997) S37-S42.

[36] C. Goel, Preparation of Adsorbent(s) using Nano-Casting Technique for Carbon Dioxide Capture from Flue Gases, M.Tech (Chemical Engg.) Thesis, Thapar University, Patiala, 2011.

[37] S.-H. Ho, C.-Y. Chen, D.-J. Lee, J.-S. Chang, Perspectives on microalgal CO_2-emission mitigation systems — a review, Biotechnology Advances, 29 (2011) 189-198.

[38] C. Pevida, T.C. Drage, C.E. Snape, Silica-templated melamine–formaldehyde resin derived adsorbents for CO_2 capture, Carbon, 46 (2008) 1464-1474.

[39] R. Serna-Guerrero, Y. Belmabkhout, A. Sayari, Triamine-grafted pore-expanded mesoporous silica for CO_2 capture: effect of moisture and adsorbent regeneration strategies, Adsorption, 16 (2010) 567-575.

[40] M. Songolzadeh, M.T. Ravanchi, M. Soleimani, Carbon dioxide capture and storage: a general review on adsorbents, World Academy of Science, Engineering and Technology, 70 (2012) 225-232.

[41] H. Zhou, J. Wang, J. Zhuang, Q. Liu, A covalent route for efficient surface modification of ordered mesoporous carbon as high performance microwave absorbers, Nanoscale, 5 (2013) 12502-12511.

[42] J. Singh, S. Basu, H. Bhunia, Dynamic CO_2 adsorption on activated carbon adsorbents synthesized from polyacrylonitrile (PAN): Kinetic and isotherm studies, Microporous and Mesoporous Materials, 280 (2019) 357-366.

[43] G.-P. Hao, W.-C. Li, D. Qian, G.-H. Wang, W.-P. Zhang, T. Zhang, A.-Q. Wang, F. Schuth, H.-J. Bongard, A.-H. Lu, Structurally designed synthesis of mechanically stable poly (benzoxazine-co-resol)-based porous carbon monoliths and their application as high-performance CO_2 capture sorbents, Journal of the American Chemical Society, 133 (2011) 11378-11388.

[44] D. Tiwari, H. Bhunia, P.K. Bajpai, Epoxy based oxygen enriched porous carbons for CO_2 capture, Applied Surface Science, 414 (2017) 380-389.

[45] S. Sridhar, B. Smitha, T. Aminabhavi, Separation of carbon dioxide from natural gas mixtures through polymeric membranes — a review, Separation & Purification Reviews, 36 (2007) 113-174.

[46] Y. Takamura, J. Aoki, S. Uchida, S. Narita, Application of high-pressure swing adsorption process for improvement of CO_2 recovery system from flue gas, The Canadian Journal of Chemical Engineering, 79 (2001) 812-816.

[47] M. Clausse, J. Merel, F. Meunier, Numerical parametric study on CO_2 capture by indirect thermal swing adsorption, International Journal of Greenhouse Gas Control, 5 (2011) 1206-1213.

[48] R.T. Yang, Adsorbents: Fundamentals and Applications, John Wiley & Sons, Inc., 2003.

[49] J. Wang, I. Senkovska, M. Oschatz, M.R. Lohe, L. Borchardt, A. Heerwig, Q. Liu, S. Kaskel, Highly porous nitrogen-doped polyimine-based carbons with adjustable

microstructures for CO_2 capture, Journal of Materials Chemistry A, 1 (2013) 10951-10961.

[50] R. Srivastava, Synthesis and applications of ordered and disordered mesoporous zeolites: Present and future prospective, Catalysis Today, 309 (2018) 172-188.

[51] J. Zhang, R. Singh, P.A. Webley, Alkali and alkaline-earth cation exchanged chabazite zeolites for adsorption based CO_2 capture, Microporous and Mesoporous Materials, 111 (2008) 478-487.

[52] S. Choi, J.H. Drese, C.W. Jones, Adsorbent materials for carbon dioxide capture from large anthropogenic point sources, ChemSusChem, 2 (2009) 796-854.

[53] N. Hedin, L. Andersson, L. Bergström, J. Yan, Adsorbents for the post-combustion capture of CO_2 using rapid temperature swing or vacuum swing adsorption, Applied Energy, 104 (2013) 418-433.

[54] Q. Wang, J. Luo, Z. Zhong, A. Borgna, CO_2 capture by solid adsorbents and their applications: current status and new trends, Energy & Environmental Science, 4 (2011) 42-55.

[55] A. Heydari-Gorji, A. Sayari, CO_2 capture on polyethylenimine-impregnated hydrophobic mesoporous silica: Experimental and kinetic modeling, Chemical Engineering Journal, 173 (2011) 72-79.

[56] A.-H. Lu, G.-P. Hao, Porous materials for carbon dioxide capture, Annual Reports Section" A"(Inorganic Chemistry), 109 (2013) 484-503.

[57] F. Akhtar, Q. Liu, N. Hedin, L. Bergström, Strong and binder free structured zeolite sorbents with very high CO_2-over-N_2 selectivities and high capacities to adsorb CO_2 rapidly, Energy & Environmental Science, 5 (2012) 7664-7673.

[58] R. Krishna, Adsorptive separation of CO_2/CH_4/CO gas mixtures at high pressures, Microporous and Mesoporous Materials, 156 (2012) 217-223.

[59] M. Miyamoto, Y. Fujioka, K. Yogo, Pure silica CHA type zeolite for CO_2 separation using pressure swing adsorption at high pressure, Journal of Materials Chemistry, 22 (2012) 20186-20189.

[60] S. Cavenati, C.A. Grande, A.E. Rodrigues, Adsorption equilibrium of methane, carbon dioxide, and nitrogen on zeolite 13X at high pressures, Journal of Chemical & Engineering Data, 49 (2004) 1095-1101.

[61] J. Yang, Q. Zhao, H. Xu, L. Li, J. Dong, J. Li, Adsorption of CO_2, CH_4, and N_2 on gas diameter grade ion-exchange small pore zeolites, Journal of Chemical & Engineering Data, 57 (2012) 3701-3709.

[62] J. Lara-Medina, M. Torres-Rodríguez, M. Gutierrez-Arzaluz, V. Mugica-Alvarez, Separation of CO_2 and N_2 with a lithium-modified silicalite-1 zeolite membrane, International Journal of Greenhouse Gas Control, 10 (2012) 494-500.

[63] M. Palomino, A. Corma, J.L. Jordá, F. Rey, S. Valencia, Zeolite Rho: a highly selective adsorbent for CO_2/CH_4 separation induced by a structural phase modification, Chemical Communications, 48 (2012) 215-217.

[64] A. Phan, C.J. Doonan, F.J. Uribe-Romo, C.B. Knobler, M. O'keeffe, O.M. Yaghi, Synthesis, structure, and carbon dioxide capture properties of zeolitic imidazolate frameworks, Acc. Chem. Res, 43 (2010) 58-67.

[65] G. Yilmaz, S. Keskin, Predicting the performance of zeolite imidazolate framework/polymer mixed matrix membranes for CO_2, CH_4, and H_2 separations using molecular simulations, Industrial & Engineering Chemistry Research, 51 (2012) 14218-14228.

[66] A. Huang, Y. Chen, N. Wang, Z. Hu, J. Jiang, J. Caro, A highly permeable and selective zeolitic imidazolate framework ZIF-95 membrane for H_2/CO_2 separation, Chemical Communications, 48 (2012) 10981-10983.

[67] G.-P. Hao, W.-C. Li, A.-H. Lu, Novel porous solids for carbon dioxide capture, Journal of Materials Chemistry, 21 (2011) 6447-6451.

[68] C. Ji, X. Huang, L. Li, F. Xiao, N. Zhao, W. Wei, Pentaethylenehexamine-loaded hierarchically porous silica for CO_2 adsorption, Materials, 9 (2016) 835.

[69] R. Sanz, G. Calleja, A. Arencibia, E. Sanz-Perez, CO_2 adsorption on branched polyethyleneimine-impregnated mesoporous silica SBA-15, Applied Surface Science, 256 (2010) 5323-5328.

[70] C. Chen, S.-T. Yang, W.-S. Ahn, R. Ryoo, Amine-impregnated silica monolith with a hierarchical pore structure: enhancement of CO_2 capture capacity, Chemical Communications, issue 24 (2009) 3627-3629.

[71] M.A. Alkhabbaz, R. Khunsupat, C.W. Jones, Guanidinylated poly (allylamine) supported on mesoporous silica for CO_2 capture from flue gas, Fuel, 121 (2014) 79-85.

[72] R. Sanz, G. Calleja, A. Arencibia, E. Sanz-Perez, CO_2 adsorption on branched polyethyleneimine-impregnated mesoporous silica SBA-15, Applied Surface Science, 256 (2010) 5323-5328.

[73] Y. Liu, J. Shi, J. Chen, Q. Ye, H. Pan, Z. Shao, Y. Shi, Dynamic performance of CO_2 adsorption with tetraethylenepentamine-loaded KIT-6, Microporous and Mesoporous Materials, 134 (2010) 16-21.

[74] Y. Du, Z. Du, W. Zou, H. Li, J. Mi, C. Zhang, Carbon dioxide adsorbent based on rich amines loaded nano-silica, Journal of Colloid and Interface Science, 409 (2013) 123-128.

[75] Y. Le, D. Guo, B. Cheng, J. Yu, Amine-functionalized monodispersed porous silica microspheres with enhanced CO_2 adsorption performance and good cyclic stability, Journal of Colloid and Interface Science, 408 (2013) 173-180.

[76] X. Xu, C. Song, J.M. Andresen, B.G. Miller, A.W. Scaroni, Novel polyethylenimine-modified mesoporous molecular sieve of MCM-41 type as high-capacity adsorbent for CO_2 capture, Energy & Fuels, 16 (2002) 1463-1469.

[77] J.C. Hicks, J.H. Drese, D.J. Fauth, M.L. Gray, G. Qi, C.W. Jones, Designing adsorbents for CO_2 capture from flue gas-hyperbranched aminosilicas capable of capturing CO_2 reversibly, Journal of the American Chemical Society, 130 (2008) 2902-2903.

[78] X. Guo, L. Ding, K. Kanamori, K. Nakanishi, H. Yang, Functionalization of hierarchically porous silica monoliths with polyethyleneimine (PEI) for CO_2 adsorption, Microporous and Mesoporous Materials, 245 (2017) 51-57.

[79] N.H. Khdary, M.A. Ghanem, M.G. Merajuddine, F.M.B. Manie, Incorporation of Cu, Fe, Ag, and Au nanoparticles in mercapto-silica (MOS) and their CO_2 adsorption capacities, Journal of CO_2 Utilization, 5 (2014) 17-23.

[80] M.R. Mello, D. Phanon, G.Q. Silveira, P.L. Llewellyn, C.M. Ronconi, Amine-modified MCM-41 mesoporous silica for carbon dioxide capture, Microporous and Mesoporous Materials, 143 (2011) 174-179.

[81] M. Plaza, S. García, F. Rubiera, J. Pis, C. Pevida, Post-combustion CO_2 capture with a commercial activated carbon: comparison of different regeneration strategies, Chemical Engineering Journal, 163 (2010) 41-47.

[82] B.-K. Na, K.-K. Koo, H.-M. Eum, H. Lee, H. Song, CO_2 recovery from flue gas by PSA process using activated carbon, Korean J. Chem. Eng., 18 (2001) 220-227.

[83] S. Himeno, T. Komatsu, S. Fujita, High-pressure adsorption equilibria of methane and carbon dioxide on several activated carbons, Journal of Chemical & Engineering Data, 50 (2005) 369-376.

[84] F. Raganati, P. Ammendola, R. Chirone, CO_2 adsorption on fine activated carbon in a sound assisted fluidized bed: Effect of sound intensity and frequency, CO_2 partial pressure and fluidization velocity, Applied Energy, 113 (2014) 1269-1282.

[85] P. Davini, Flue gas treatment by activated carbon obtained from oil-fired fly ash, Carbon, 40 (2002) 1973-1979.

[86] L. Kong, M. Su, Y. Peng, L.a. Hou, J. Liu, H. Li, Z. Diao, K. Shih, Y. Xiong, D. Chen, Producing sawdust derived activated carbon by co-calcinations with limestone for enhanced Acid Orange II adsorption, Journal of Cleaner Production, 168 (2017) 22-29.

[87] J. Baek, H.-M. Lee, J.-S. Roh, H.-S. Lee, H.S. Kang, B.-J. Kim, Studies on preparation and applications of polymeric precursor-based activated hard carbons: I. Activation mechanism and microstructure analyses, Microporous and Mesoporous Materials, 219 (2016) 258-264.

[88] B. Viswanathan, P.I. Neel, T. Varadarajan, Methods of activation and specific applications of carbon materials, National Centre for Catalysis Research, IIT Madras, Chennai, India (2009).

[89] P. González-García, Activated carbon from lignocellulosics precursors: A review of the synthesis methods, characterization techniques and applications, Renewable and Sustainable Energy Reviews, 82 (2018) 1393-1414.

[90] R. Wang, P. Wang, X. Yan, J. Lang, C. Peng, Q. Xue, Promising porous carbon derived from celtuce leaves with outstanding supercapacitance and CO_2 capture performance, ACS Applied Materials & Interfaces, 4 (2012) 5800-5806.

[91] J. Wang, A. Heerwig, M.R. Lohe, M. Oschatz, L. Borchardt, S. Kaskel, Fungi-based porous carbons for CO_2 adsorption and separation, Journal of Materials Chemistry, 22 (2012) 13911-13913.

[92] W. Shen, Y. He, S. Zhang, J. Li, W. Fan, Yeast-based microporous carbon materials for carbon dioxide capture, ChemSusChem, 5 (2012) 1274-1279.

[93] W. Xing, C. Liu, Z. Zhou, L. Zhang, J. Zhou, S. Zhuo, Z. Yan, H. Gao, G. Wang, S.Z. Qiao, Superior CO_2 uptake of N-doped activated carbon through hydrogen-bonding interaction, Energy & Environmental Science, 5 (2012) 7323-7327.

[94] M. Sevilla, P. Valle-Vigón, A.B. Fuertes, N-doped polypyrrole-based porous carbons for CO_2 capture, Advanced Functional Materials, 21 (2011) 2781-2787.

[95] A. González, M. Plaza, F. Rubiera, C. Pevida, Sustainable biomass-based carbon adsorbents for post-combustion CO_2 capture, Chemical Engineering Journal, 230 (2013) 456-465.

[96] M. Sevilla, A.B. Fuertes, Sustainable porous carbons with a superior performance for CO_2 capture, Energy & Environmental Science, 4 (2011) 1765-1771.

[97] G. Singh, I.Y. Kim, K.S. Lakhi, S. Joseph, P. Srivastava, R. Naidu, A. Vinu, Heteroatom functionalized activated porous biocarbons and their excellent performance for CO_2 capture at high pressure, Journal of Materials Chemistry A, 5 (2017) 21196-21204.

[98] Y. Guangzhi, Y. Jinyu, Y. Yuhua, T. Zhihong, Y. DengGuang, Y. Junhe, Preparation and CO_2 adsorption properties of porous carbon from camphor leaves by hydrothermal carbonization and sequential potassium hydroxide activation, RSC Advances, 7 (2017) 4152-4160.

[99] M. Gil, M. Martínez, S. García, F. Rubiera, J. Pis, C. Pevida, Response surface methodology as an efficient tool for optimizing carbon adsorbents for CO_2 capture, Fuel Processing Technology, 106 (2013) 55-61.

[100] D. Li, T. Ma, R. Zhang, Y. Tian, Y. Qiao, Preparation of porous carbons with high low-pressure CO_2 uptake by KOH activation of rice husk char, Fuel, 139 (2015) 68-70.

[101] P. Karandikar, K. Patil, A. Mitra, B. Kakade, A. Chandwadkar, Synthesis and characterization of mesoporous carbon through inexpensive mesoporous silica as template, Microporous and Mesoporous Materials, 98 (2007) 189-199.

[102] J. Lee, J. Kim, T. Hyeon, Recent progress in the synthesis of porous carbon materials, Advanced Materials, 18 (2006) 2073-2094.

[103] Z. Liu, Y. Yang, Z. Du, W. Xing, S. Komarneni, Z. Zhang, X. Gao, Z. Yan, Furfuralcohol co-polymerized urea formaldehyde resin-derived N-doped microporous carbon for CO_2 capture, Nanoscale Research Letters, 10 (2015) 333.

[104] J. Przepiórski, M. Skrodzewicz, A. Morawski, High temperature ammonia treatment of activated carbon for enhancement of CO_2 adsorption, Applied Surface Science, 225 (2004) 235-242.

[105] J. Wang, H. Chen, H. Zhou, X. Liu, W. Qiao, D. Long, L. Ling, Carbon dioxide capture using polyethylenimine-loaded mesoporous carbons, Journal of Environmental Sciences, 25 (2013) 124-132.

[106] C. Chen, J. Kim, W.-S. Ahn, Efficient carbon dioxide capture over a nitrogen-rich carbon having a hierarchical micro-mesopore structure, Fuel, 95 (2012) 360-364.

[107] E. Raymundo-Pinero, D. Cazorla-Amorós, A. Linares-Solano, S. Delpeux, E. Frackowiak, K. Szostak, F. Béguin, High surface area carbon nanotubes prepared by chemical activation, Carbon, 40 (2002) 1614-1617.

[108] L.K. de Souza, N.P. Wickramaratne, A.S. Ello, M.J. Costa, C.E. da Costa, M. Jaroniec, Enhancement of CO_2 adsorption on phenolic resin-based mesoporous carbons by KOH activation, Carbon, 65 (2013) 334-340.

[109] N.P. Wickramaratne, M. Jaroniec, Importance of small micropores in CO_2 capture by phenolic resin-based activated carbon spheres, Journal of Materials Chemistry A, 1 (2013) 112-116.

[110] J.A. Thote, K.S. Iyer, R. Chatti, N.K. Labhsetwar, R.B. Biniwale, S.S. Rayalu, In situ nitrogen enriched carbon for carbon dioxide capture, Carbon, 48 (2010) 396-402.

[111] X. Zhu, Y. Fu, G. Hu, Y. Shen, W. Dai, X. Hu, CO_2 capture with activated carbons prepared by petroleum coke and KOH at low pressure, Water, Air, & Soil Pollution, 224 (2013) 1387.

[112] D. Saha, G. Orkoulas, J. Chen, D.K. Hensley, Adsorptive separation of CO_2 in sulfur-doped nanoporous carbons: Selectivity and breakthrough simulation, Microporous and Mesoporous Materials, 241 (2017) 226-237.

[113] H. Seema, K.C. Kemp, N.H. Le, S.-W. Park, V. Chandra, J.W. Lee, K.S. Kim, Highly selective CO_2 capture by S-doped microporous carbon materials, Carbon, 66 (2014) 320-326.

[114] S. Hu, C. Li, D. Wan, K. Li, C. Yu, W. Kong, Chemical activation of mesoporous carbon with ultrahigh pore volume for highly supported adsorption of CO_2, Journal of Porous Materials, 25 (2018) 1691-1696.

[115] Y.K. Kim, G.M. Kim, J.W. Lee, Highly porous N-doped carbons impregnated with sodium for efficient CO_2 capture, Journal of Materials Chemistry A, 3 (2015) 10919-10927.

[116] B.C. Bai, E.A. Kim, C.W. Lee, Y.-S. Lee, J.S. Im, Effects of surface chemical properties of activated carbon fibers modified by liquid oxidation for CO_2 adsorption, Applied Surface Science, 353 (2015) 158-164.

[117] W. Shen, S. Zhang, Y. He, J. Li, W. Fan, Hierarchical porous polyacrylonitrile-based activated carbon fibers for CO_2 capture, Journal of Materials Chemistry, 21 (2011) 14036-14040.

[118] M. Plaza, A. González, C. Pevida, J. Pis, F. Rubiera, Valorisation of spent coffee grounds as CO_2 adsorbents for postcombustion capture applications, Applied Energy, 99 (2012) 272-279.

[119] A. González, M. Plaza, J. Pis, F. Rubiera, C. Pevida, Post-combustion CO_2 capture adsorbents from spent coffee grounds, Energy Procedia, 37 (2013) 134-141.

[120] J.P. Marco-Lozar, M. Kunowsky, F. Suárez-García, A. Linares-Solano, Sorbent design for CO_2 capture under different flue gas conditions, Carbon, 72 (2014) 125-134.

[121] F.M. Sayler, A.J. Grano, J.-H. Smått, M. Lindén, M.G. Bakker, Nanocasting of hierarchically porous Co_3O_4, Co, NiO, Ni, and Ag, monoliths: Impact of processing conditions on fidelity of replication, Microporous and Mesoporous Materials, 184 (2014) 141-150.

[122] X. Deng, K. Chen, H. Tüysüz, Protocol for the nanocasting method: Preparation of ordered mesoporous metal oxides, Chemistry of Materials, 29 (2016) 40-52.

[123] C. Goel, H. Bhunia, P.K. Bajpai, Resorcinol–formaldehyde based nanostructured carbons for CO_2 adsorption: kinetics, isotherm and thermodynamic studies, RSC Advances, 5 (2015) 93563-93578.

[124] D. Tiwari, H. Bhunia, P.K. Bajpai, Epoxy based oxygen enriched porous carbons for CO_2 capture, Applied Surface Science, 414 (2017) 380-389.

[125] Y. Xia, Y. Zhu, Y. Tang, Preparation of sulfur-doped microporous carbons for the storage of hydrogen and carbon dioxide, Carbon, 50 (2012) 5543-5553.

[126] M. Sevilla, A.B. Fuertes, CO_2 adsorption by activated templated carbons, Journal Of Colloid And Interface Science, 366 (2012) 147-154.

[127] A.-H. Lu, G.-P. Hao, X.-Q. Zhang, Porous carbons for carbon dioxide capture, in: Porous Materials for Carbon Dioxide Capture, Springer, 2014, pp. 15-77.

[128] B. Gaweł, K. Gaweł, G. Oye, Sol-gel synthesis of non-silica monolithic materials, Materials, 3 (2010) 2815-2833.

[129] A. El Kadib, R. Chimenton, A. Sachse, F. Fajula, A. Galarneau, B. Coq, Functionalized inorganic monolithic microreactors for high productivity in fine chemicals catalytic synthesis, Angewandte Chemie, 121 (2009) 5069-5072.

[130] M.E. Davis, Ordered porous materials for emerging applications, Nature, 417 (2002) 813-821.

[131] G.P. Hao, W.C. Li, D. Qian, A.H. Lu, Rapid synthesis of nitrogen-doped porous carbon monolith for CO_2 capture, Advanced Materials, 22 (2010) 853-857.

[132] A.C. Juhl, C.-P. Elverfeldt, F. Hoffmann, M. Fröba, Porous carbon monoliths with pore sizes adjustable between 10 nm and 2 μm prepared by phase separation – New insights in the relation between synthesis composition and resulting structure, Microporous and Mesoporous Materials, 255 (2018) 271-280.

[133] S. Hosseini, E. Marahel, I. Bayesti, A. Abbasi, L.C. Abdullah, T.S. Choong, CO_2 adsorption on modified carbon coated monolith: effect of surface modification by using alkaline solutions, Applied Surface Science, 324 (2015) 569-575.

[134] D. Qian, C. Lei, G.-P. Hao, W.-C. Li, A.-H. Lu, Synthesis of hierarchical porous carbon monoliths with incorporated metal–organic frameworks for enhancing volumetric based CO_2 capture capability, ACS Applied Materials & Interfaces, 4 (2012) 6125-6132.

[135] S. Ding, Q. Dong, J. Hu, W. Xiao, X. Liu, L. Liao, N. Zhang, Enhanced selective adsorption of CO_2 on nitrogen-doped porous carbon monoliths derived from IRMOF-3, Chemical Communications, 52 (2016) 9757-9760.

[136] M. Nandi, K. Okada, A. Dutta, A. Bhaumik, J. Maruyama, D. Derks, H. Uyama, Unprecedented CO_2 uptake over highly porous N-doped activated carbon monoliths prepared by physical activation, Chemical Communications, 48 (2012) 10283-10285.

[137] Y. Jin, S.C. Hawkins, C.P. Huynh, S. Su, Carbon nanotube modified carbon composite monoliths as superior adsorbents for carbon dioxide capture, Energy & Environmental Science, 6 (2013) 2591-2596.

[138] Z. Geng, Q. Xiao, H. Lv, B. Li, H. Wu, Y. Lu, C. Zhang, One-step synthesis of microporous carbon monoliths derived from biomass with high nitrogen doping content for highly selective CO_2 capture, Scientific Reports, 6 (2016) 30049.

[139] R. Thiruvenkatachari, S. Su, X.X. Yu, J.-S. Bae, Application of carbon fibre composites to CO_2 capture from flue gas, International Journal of Greenhouse Gas Control, 13 (2013) 191-200.

[140] R.S. Dassanayake, C. Gunathilake, T. Jackson, M. Jaroniec, N. Abidi, Preparation and adsorption properties of aerocellulose-derived activated carbon monoliths, Cellulose, 23 (2016) 1363-1374.

[141] S.Y. Sawant, R.S. Somani, H.C. Bajaj, S.S. Sharma, A dechlorination pathway for synthesis of horn shaped carbon nanotubes and its adsorption properties for CO_2, CH_4, CO and N_2, Journal of Hazardous Materials, 227 (2012) 317-326.

[142] C. Goel, H. Bhunia, P.K. Bajpai, Synthesis of nitrogen doped mesoporous carbons for carbon dioxide capture, RSC Advances, 5 (2015) 46568-46582.

[143] S. Lagergren, About the theory of so-called adsorption of soluble substances, Kungliga Svenska Vetenskapsakademiens Handlingar, 24 (1898) 1-39.

[144] H. Yuh-Shan, Citation review of Lagergren kinetic rate equation on adsorption reactions, Scientometrics, 59 (2004) 171-177.

[145] Y.S. Ho, G. McKay, Pseudo-second order model for sorption processes, Process Biochemistry, 34 (1999) 451-465.

[146] J.-P. Simonin, On the comparison of pseudo-first order and pseudo-second order rate laws in the modeling of adsorption kinetics, Chemical Engineering Journal, 300 (2016) 254-263.

[147] A. Heydari-Gorji, A. Sayari, CO_2 capture on polyethylenimine-impregnated hydrophobic mesoporous silica: Experimental and kinetic modeling, Chemical Engineering Journal, 173 (2011) 72-79.

[148] Q. Liu, J. Shi, S. Zheng, M. Tao, Y. He, Y. Shi, Kinetics studies of CO_2 adsorption/desorption on amine-functionalized multiwalled carbon nanotubes, Industrial & Engineering Chemistry Research, 53 (2014) 11677-11683.

[149] I. Langmuir, The constitution and fundamental properties of solids and liquids. Part I. Solids, Journal of The American Chemical Society, 38 (1916) 2221-2295.

[150] H.M.F. Freundlich, Over the adsorption in solution, J. Phys. Chem., 57 (1906) 385-471.

[151] M.I. Temkin, V. Pyzhev, Kinetics of ammonia synthesis on promoted iron catalyst, Acta Physicochimica URSS, 12 (1940) 327–356.

[152] R. Veneman, H. Kamphuis, D. Brilman, Post-Combustion CO_2 capture using supported amine sorbents: a process integration study, Energy Proced, 37 (2013) 2100-2108.

[153] S. Sjostrom, H. Krutka, Evaluation of solid sorbents as a retrofit technology for CO_2 capture, Fuel, 89 (2010) 1298-1306.

[154] D. Fauth, M. Gray, H. Pennline, H. Krutka, S. Sjostrom, A. Ault, Investigation of porous silica supported mixed-amine sorbents for post-combustion CO_2 capture, Energy & Fuels, 26 (2012) 2483-2496.

[155] M. Sharma, P. Jain, A. Mishra, A. Mehta, D. Choudhury, S. Hazra, S. Basu, Variation of surface area of silica monoliths by controlling ionic character/chain length of surfactants and polymers, Materials Letters, 194 (2017) 213-216.

[156] H.-L. WANG, X.-H. LIU, Synthesis of N-doped mesoporous titania with high visible-light photocatalytic activity, Journal of Inorganic Materials, 29 (2014).

[157] A.D. Roberts, J.-S.M. Lee, S.Y. Wong, X. Li, H. Zhang, Nitrogen-rich activated carbon monoliths via ice-templating with high CO_2 and H_2 adsorption capacities, Journal of Materials Chemistry A, 5 (2017) 2811-2820.

[158] M. Ignat, E. Popovici, Synthesis of mesoporous carbon materials via nanocasting route–comparative study of glycerol and sucrose as carbon sources, Rev. Roum. Chim, 56 (2011) 947-952.

[159] Y.-K. Hwang, H.-S. Shin, J.-Y. Hong, S. Huh, Preparation of micro-/macroporous carbons and their gas sorption properties, Bulletin of the Korean Chemical Society, 35 (2014) 377-382.

[160] N. Querejeta, M.G. Plaza, F. Rubiera, C. Pevida, Water vapor adsorption on biomass based carbons under post-combustion CO_2 capture conditions: Effect of Post-Treatment, Materials, 9 (2016) 359.

[161] D. Tiwari, C. Goel, H. Bhunia, P.K. Bajpai, Melamine-formaldehyde derived porous carbons for adsorption of CO_2 capture, Journal of Environmental Management, 197 (2017) 415-427.

[162] J. Wang, D. Yang, X. Gao, X. Wang, Q. Li, Q. Liu, Tip and inner walls modification of single-walled carbon nanotubes (3.5 nm diameter) and preparation of polyamide/modified CNT nanocomposite reverse osmosis membrane, Journal of Experimental Nanoscience, 13 (2018) 11-26.

[163] D. Wang, Y. Hu, J. Zhao, L. Zeng, X. Tao, W. Chen, Holey reduced graphene oxide nanosheets for high performance room temperature gas sensing, Journal of Materials Chemistry A, 2 (2014) 17415-17420.

[164] P. Bhagat, K. Patil, D. Bodas, K. Paknikar, Hydrothermal synthesis and characterization of carbon nanospheres: a mechanistic insight, RSC Advances, 5 (2015) 59491-59494.

[165] C. Pevida, T. Drage, C. Snape, Silica-templated melamine–formaldehyde resin derived adsorbents for CO_2 capture, Carbon, 46 (2008) 1464-1474.

[166] C. Goel, H. Bhunia, P.K. Bajpai, Mesoporous carbon adsorbents from melamine–formaldehyde resin using nanocasting technique for CO_2 adsorption, Journal of Environmental Sciences, 32 (2015) 238-248.

[167] M. Plaza, S. García, F. Rubiera, J. Pis, C. Pevida, Evaluation of ammonia modified and conventionally activated biomass based carbons as CO_2 adsorbents in postcombustion conditions, Separation and Purification Technology, 80 (2011) 96-104.

[168] Y. Guo, C. Zhao, X. Chen, C. Li, CO_2 capture and sorbent regeneration performances of some wood ash materials, Applied Energy, 137 (2015) 26-36.

[169] C. Goel, H. Bhunia, P.K. Bajpai, Novel nitrogen enriched porous carbon adsorbents for CO_2 capture: breakthrough adsorption study, Journal of Environmental Chemical Engineering, 4 (2016) 346-356.

[170] M. Balsamo, T. Budinova, A. Erto, A. Lancia, B. Petrova, N. Petrov, B. Tsyntsarski, CO_2 adsorption onto synthetic activated carbon: kinetic, thermodynamic and regeneration studies, Separation and Purification Technology, 116 (2013) 214-221.

[171] M. Olivares-Marín, S. Garcia, C. Pevida, M. Wong, M. Maroto-Valer, The influence of the precursor and synthesis method on the CO_2 capture capacity of carpet waste-based sorbents, Journal of Environmental Management, 92 (2011) 2810-2817.

[172] C. Goel, H. Bhunia, P.K. Bajpai, Development of nitrogen enriched nanostructured carbon adsorbents for CO_2 capture, Journal of Environmental Management, 162 (2015) 20-29.

[173] D. Tiwari, H. Bhunia, P.K. Bajpai, Urea-formaldehyde derived porous carbons for adsorption of CO_2, RSC Advances, 6 (2016) 111842-111855.

[174] D. Tiwari, C. Goel, H. Bhunia, P.K. Bajpai, Dynamic CO_2 capture by carbon adsorbents: Kinetics, isotherm and thermodynamic studies, Separation and Purification Technology, 181 (2017) 107-122.

[175] I.A. Esteves, M.S. Lopes, P.M. Nunes, J.P. Mota, Adsorption of natural gas and biogas components on activated carbon, Separation and Purification Technology, 62 (2008) 281-296.

[176] L. Liu, J. Lu, Y.-x. Zhang, M. Liu, Y.-f. Yu, A.-b. Chen, Synthesis of nitrogen-doped graphitic carbon nanocapsules from a poly (ionic liquid) for CO_2 capture, New Carbon Materials, 32 (2017) 380-384.

[177] V.K. Singh, E.A. Kumar, Measurement and analysis of adsorption isotherms of CO_2 on activated carbon, Applied Thermal Engineering, 97 (2016) 77-86.

[178] D. Tiwari, H. Bhunia, P.K. Bajpai, Synthesis of nitrogen enriched porous carbons from urea formaldehyde resin and their carbon dioxide adsorption capacity, Journal of CO_2 Utilization, 21 (2017) 302-313.

[179] Y.-C. Chiang, Y.-J. Chen, C.-Y. Wu, Effect of relative humidity on adsorption breakthrough of CO_2 on activated carbon fibers, Materials, 10 (2017) 1296.

[180] J. Shi, N. Yan, H. Cui, Y. Liu, Y. Weng, D. Li, X. Ji, Nitrogen doped hierarchically porous carbon derived from glucosamine hydrochloride for CO_2 adsorption, Journal of CO_2 Utilization, 21 (2017) 444-449.

[181] E. Jagst, Surface functional group characterization using Chemical Derivatization X-ray Photoelectron Spectroscopy (CD-XPS), BAM-Dissertationsreihe, Freie Universitat Berlin, 2011.

[182] Y.-Y. Yao, G. Gedda, W.M. Girma, C.-L. Yen, Y.-C. Ling, J.-Y. Chang, Magnetofluorescent carbon dots derived from crab shell for targeted dual-modality bioimaging and drug delivery, ACS Applied Materials & Interfaces, 9 (2017) 13887-13899.

[183] D. Tiwari, H. Bhunia, P.K. Bajpai, Adsorption of CO_2 on KOH activated, N-enriched carbon derived from urea formaldehyde resin: kinetics, isotherm and thermodynamic studies, Applied Surface Science, 439 (2018) 760-771.

[184] Y.A. Alhamed, S.U. Rather, A.H. El-Shazly, S.F. Zaman, M.A. Daous, A.A. Al-Zahrani, Preparation of activated carbon from fly ash and its application for CO_2 capture, Korean Journal of Chemical Engineering, 32 (2015) 723-730.

[185] S. Hosseini, E. Marahel, I. Bayesti, A. Abbasi, L.C. Abdullah, T.S. Choong, CO_2 adsorption on modified carbon coated monolith: effect of surface modification by using alkaline solutions, Applied Surface Science, 324 (2015) 569-575.

[186] A. Boonpoke, S. Chiarakorn, N. Laosiripojana, S. Towprayoon, A. Chidthaisong, Synthesis of activated carbon and MCM-41 from bagasse and rice husk and their carbon dioxide adsorption capacity, Journal of Sustainable Energy & Environment, 2 (2011) 77-81.

[187] C. Zhao, Y. Guo, C. Li, S. Lu, Removal of low concentration CO_2 at ambient temperature using several potassium-based sorbents, Applied Energy, 124 (2014) 241-247.

[188] T. Drage, A. Arenillas, K. Smith, C. Pevida, S. Piippo, C. Snape, Preparation of carbon dioxide adsorbents from the chemical activation of urea–formaldehyde and melamine–formaldehyde resins, Fuel, 86 (2007) 22-31.

[189] M.M. Maroto-Valer, Z. Tang, Y. Zhang, CO_2 capture by activated and impregnated anthracites, Fuel Processing Technology, 86 (2005) 1487-1502.

[190] M.-S. Chiou, H.-Y. Li, Equilibrium and kinetic modeling of adsorption of reactive dye on cross-linked chitosan beads, Journal of Hazardous Materials, 93 (2002) 233-248.

[191] S.-C. Hsu, C. Lu, F. Su, W. Zeng, W. Chen, Thermodynamics and regeneration studies of CO_2 adsorption on multiwalled carbon nanotubes, Chemical Engineering Science, 65 (2010) 1354-1361.

REPRINTS OF PUBLISHED ARTICLES

Journal of the Taiwan Institute of Chemical Engineers 89 (2018) 140–150

Contents lists available at ScienceDirect

Journal of the Taiwan Institute of Chemical Engineers

journal homepage: www.elsevier.com/locate/jtice

Synthesis of porous carbon monolith adsorbents for carbon dioxide capture: Breakthrough adsorption study

Jasminder Singh[a], Haripada Bhunia[b,*], Soumen Basu[a,*]

[a] School of Chemistry and Biochemistry, Thapar Institute of Engineering and Technology, Patiala 147004, Punjab, India
[b] Chemical Engineering Department, Thapar Institute of Engineering and Technology, Patiala 147004, Punjab, India

ARTICLE INFO

Article history:
Received 15 January 2018
Revised 20 April 2018
Accepted 24 April 2018

Keywords:
Carbon monoliths
Bimodal porosity
Carbon dioxide capture
Adsorption
Breakthrough curve
Regeneration

ABSTRACT

Carbon monoliths with bimodal porosity were obtained through nanocasting technique from silica monoliths (hard template) and furfuryl alcohol (precursor). These carbon adsorbents were evaluated as sorbents for CO_2 capture by using a fixed-bed adsorption set up under dynamic conditions. Carbonization at different temperatures (550 to 950 °C) was carried out that resulted in the generation of different carbon adsorbents containing oxygen functional groups. The textural characterization results reveal the effect of nanocasting technique, which is confirmed from the generation of mesopores (0.41), micropores (0.85 $cm^3\ g^{-1}$) and high surface area (1225.1 $m^2\ g^{-1}$) of adsorbent synthesized at 950 °C, as shows highest CO_2 uptake of 1.0 mmol g^{-1} at 30 °C and 12.5% CO_2 concentration. The increase in the adsorption capacity with increasing CO_2 concentration and decrease with the increasing adsorption temperature confirms the physisorption process. Five adsorption–desorption cycles show established materials with excellent regeneration stability as an adsorbent. Furthermore, three kinetic models along with three isotherms were used in the present study to analyze the adsorption data and found that fractional order kinetic model and Temkin isotherm fitted best. Thermodynamic studies suggested the exothermic, spontaneous as well as the feasibile nature of the adsorption process.

1. Introduction

In the Earth's atmosphere, major greenhouse gases, including methane (CH_4), nitrous oxide (N_2O), carbon dioxide (CO_2), and ozone (O_3), is considered responsible for rapid climate change and among these gases CO_2 is the second largest contributor to the global warming after water because of its emission has been identified as a main contributor to the atmosphere. The anthropogenic CO_2 emissions are almost entirely caused by combustion of fossil fuels like coal and natural gas to produce energy [1, 2]. The CO_2 concentration increased from 280 ppm to 406.75 ppm at present year (2018) [3] which is expected to increase up to a level of 570 ppm by 2100 [4] which will rise the global surface temperature and create problem such as climate change, increase in the acidity of oceans and serious health issues for the living-beings [5, 6]. Currently, carbon capture and storage (CCS) technology are the important technology to reduce the concentration of CO_2 and play a significant role to obtain the required reduction in greenhouse gas (GHG) emissions [7]. CCS includes three basic types: post-combustion, pre-combustion and oxy-fuel combustion capture. The most widely adopted technology is the post-combustion for CO_2 capture from emission source due to its flexibility and ease of retrofit to existing combustion technologies [8]. It includes chemical absorption, cryogenic separation, adsorption, membrane separation and biological fixation [9, 10]. Among the various methods, the chemical solvent absorption for CO_2 capture is efficient but it requires a large amount of energy for regeneration due to the large emission of flue gases and low CO_2 concentration. Also, it causes equipment corrosion and need for a large absorber volume [11].

CO_2 capture by adsorption method is considered one of the potential in terms of cost-effective options because of the cost advantage, low energy consumption and ease of applicability over a wide range of temperature and pressure. However, the choice of the adsorbents with high CO_2 selectivity and adsorption capacity, high stability, and easy regenerability make it successful [10, 12]. The CO_2 adsorption on solid adsorbents, including porous carbons [13], amine-modified silicas [14], zeolites [15], and metal-organic framework compounds [16] have received considerable research interest recently. Carbon-based materials are considered to be one of the outstanding materials for CO_2 adsorption due to their large surface area [17], wide availability [18], low cost [19], adjustable porosity [20] and low energy for regeneration [17]. On the other hand,

* Corresponding authors.
E-mail addresses: hbhunia@thapar.edu (H. Bhunia), soumen.basu@thapar.edu (S. Basu).

https://doi.org/10.1016/j.jtice.2018.04.031
1876-1070/

Microporous and Mesoporous Materials 280 (2019) 357–366

Contents lists available at ScienceDirect

Microporous and Mesoporous Materials

journal homepage: www.elsevier.com/locate/micromeso

Dynamic CO_2 adsorption on activated carbon adsorbents synthesized from polyacrylonitrile (PAN): Kinetic and isotherm studies

Jasminder Singh[a], Soumen Basu[a,**], Haripada Bhunia[b,*]

[a] School of Chemistry and Biochemistry, Thapar Institute of Engineering & Technology, (Deemed to be University), Patiala, 147004, Punjab, India
[b] Department of Chemical Engineering, Thapar Institute of Engineering & Technology, (Deemed to be University), Patiala, 147004, Punjab, India

ARTICLE INFO

Keywords:
Porous carbons
Activating agents
CO_2 adsorption
Breakthrough curve
Regenerability
Adsorption kinetics

ABSTRACT

In this research work, PAN-based activated carbon adsorbents have been synthesized by using the simple and cost-effective route of carbonization and chemical activation. The effect of different activating agents like $NaNH_2$, NaOH, K_2CO_3, and KOH on the textural properties of PAN and its adsorption potential for CO_2 under dynamic conditions was investigated. The KOH activated carbon adsorbent exhibited the surface area of 1890 $m^2 g^{-1}$ whereas, $NaNH_2$, NaOH, and K_2CO_3 activated carbons showed the surface area of 833 $m^2 g^{-1}$, 1020 $m^2 g^{-1}$ and 1250 $m^2 g^{-1}$ respectively. The porosity of the adsorbents was affirmed by SEM and HRTEM analysis. Whereas, XPS analysis have been revealed the various types of basic functional groups which contains oxygen and nitrogen on the carbon surface. The adsorbent, PAN-KOH shows the best CO_2 uptake of 1.2 mmol g^{-1} which is about four times the adsorption capacity of the carbonized PAN (0.32 mmol g^{-1}) under 12.5% CO_2 concentration flow. Moreover, the adsorbents showed a stable adsorption capacity over multiple sorption cycles. The best information of the adsorption at all adsorption temperatures was given by fractional order kinetic model whereas, the best fit of Freundlich isotherm model with the adsorption data and high Q_{st} values confirms the adsorbent's surface heterogeneity. Thus, the present study provides a two-step synthesis process to produce nitrogen and oxygen-containing activated carbons from low-cost and commercially available PAN for its use in CO_2 capture practical applications.

1. Introduction

Nowadays, the major critical issue is the increase in global warming constantly [1], which leads to rising the average global temperature and ocean acidification [2]. Whereas, CO_2 emissions into the environment from both natural and human sources contribute greatly to global warming [3,4]. The rising CO_2 concentration in the air is mainly due to the burning of fossil fuels (coal, natural gas, and oil) [5]. The present CO_2 atmospheric concentration is 410.79 ppm [6] which is expected to increase up to 570 ppm by the year 2100 [7] which will be responsible for climatic changes, as well as cause the serious health problems in humans [8,9]. A viable short-term solution to reduce CO_2 emissions and mitigate global warming is CO_2 capture and sequestration (CCS) from large point emission sources like coal and gas-fired power plants, refineries, and cement manufacturing facilities [10,11]. Among the various techniques in CCS, the amine absorption using the solvents (like alkanolamines) known as a conventional technology but it is limited by the higher operation costs for the CO_2 separation unit to separate CO_2 after the absorption process [12].

Adsorptive separation of CO_2 by the carbon-based nanoporous adsorbents is the most suitable technique as compared to other techniques because of its low-cost operation along with good regenerability, high thermal stability, tunable porosity, high surface area, and fast adsorption kinetics [13]. However, the carbon adsorbents for the adsorption process can be prepared from various low-cost materials by adopting different methods like carbonization, sol-gel and nanocasting technique [14]. Goel et al. [15] developed nitrogen enriched adsorbents by using nanocasting technique from melamine and MCM-41 silica and found the adsorption of 0.80 mmol g^{-1} CO_2 at an adsorption temperature of 30 °C. Hao et al. [16] have been carbonized the resorcinol-formaldehyde resin at different temperatures (400–800 °C) with the addition of catalyst (L-lysine) to prepare carbon monoliths and found the CO_2 uptake capacity of 3.1 mmol g^{-1}. Liu et al. [17] synthesized carbon adsorbents from furfural resin by using the carbonization temperature of 600 °C for 4 h under N_2 flow and obtained the maximum adsorption capacity (1.6 mmol g^{-1}) at 25 °C. In literature, it has been found that

* Corresponding author.
** Corresponding author.
E-mail addresses: soumen.basu@thapar.edu (S. Basu), hbhunia@thapar.edu (H. Bhunia).

https://doi.org/10.1016/j.micromeso.2019.02.031
Received 13 November 2018; Received in revised form 21 February 2019; Accepted 22 February 2019
Available online 23 February 2019
1387-1811/

Jasminder Singh

Senior research scholar
School of Chemistry and Biochemistry
Thapar Institute of Engineering and Technology,
Patiala 147004, Punjab-India
Mobile No: +91-8437587536, 9465265103
Email: jasminder.singh91@gmail.com, jsingh1_phd16@thapar.edu

Academic Qualification:

1. **2019: Ph.D. (submitted- June 2019)** in **Chemistry** (Advanced Nanomaterials), School of Chemistry and Biochemistry, Thapar Institute of Engineering and Technology, Punjab- India.
   Thesis Title: "Study on CO_2 capture using nanostructure carbon adsorbents"
2. **2014: B.Ed.** (First division) Punjab University, Chandigarh, India.
3. **2013: M.Sc**. in Chemistry (First division), SLIET Longowal, Punjab, India.
4. **2011: B.Sc.** in Chemistry, Physics, and Maths (First division) Punjab University, Chandigarh, India.
5. **2008: Senior Secondary** (First division), Punjab School Education Board, Punjab, India.

Research/Teaching Experience:

1. **August 2017- June 2019: Teaching Associate** (for postgraduate and undergraduate students) in School of Chemistry and Biochemistry, Thapar Institute of Engineering and Technology, Patiala, Punjab, India.
2. **June 2014- July 2016: Part-time Researcher** in the advanced nanomaterials laboratory at Thapar Institute of Engineering and Technology, Patiala, Punjab, India.

Research Interest: Synthesis of meso-/micro-/macro porous adsorbents, CO_2 capture, heavy metal ion adsorption, photodegradation of organic pollutants and photo-Fenton catalysis.

List of Publications

1. **Jasminder Singh**, Haripada Bhunia, Soumen Basu, Synthesis of sulphur enriched carbon monoliths for dynamic CO_2 capture, *Chemical Engineering Journal*, 374 (2019) 1-9. **(I.F: 8.3)**
2. **Jasminder Singh**, Haripada Bhunia, Soumen Basu, CO_2 adsorption on oxygen enriched porous carbon monoliths: kinetics, isotherm and thermodynamic studies, *Journal of Industrial and Engineering Chemistry,* 60 (2018) 321–332. **(I.F: 4.9)**
3. **Jasminder Singh**, Soumen Basu, Haripada Bhunia, Adsorption of CO_2 on KOH activated carbon adsorbents: Effect of different mass ratios, *Journal of Environmental Management,* 250 (2019) 109457. **(I.F: 4.8)**
4. **Jasminder Singh**, Soumen Basu, Haripada Bhunia, Dynamic CO_2 adsorption on activated carbon adsorbents synthesized from polyacrylonitrile (PAN): kinetic and isotherm studies, *Microporous and Mesoporous Materials* 280 (2019) 357-66. **(I.F: 4.1)**
5. **Jasminder Singh,** Ankita Arora, Soumen Basu, Synthesis of coral like WO_3/g-C_3N_4 nanocomposites for the removal of hazardous dyes under visible light, *Journal of Alloys and Compounds,* 808 (2019) 151734 . **(I.F: 4.1)**
6. **Jasminder Singh**, Soumen Basu, Haripada Bhunia, CO_2 capture by modified porous carbon adsorbents: Effect of various activating agents, *Journal of the Taiwan Institute of Chemical Engineers,* 102 (2019) 438-447. **(I.F: 3.8)**
7. **Jasminder Singh**, Haripada Bhunia, Soumen Basu, Synthesis of porous carbon monolith adsorbents for carbon dioxide capture: breakthrough adsorption study, *Journal of the Taiwan Institute of Chemical Engineers*, 89 (2018) 140-150. **(I.F: 3.8)**
8. **Jasminder Singh**, Manisha Sharma, Soumen Basu, Heavy metal ions adsorption and photodegradation of remazol black xp by iron oxide/silica monoliths: kinetic and equilibrium modelling, *Advanced Powder Technology*, 29 (2018) 2268-2279. **(I.F: 3.2)**
9. **Jasminder Singh**, Surbhi Sharma, Aanchal and Soumen Basu, Synthesis of Fe_2O_3/TiO_2 monoliths for the enhanced degradation of industrial dye and pesticide via photo-Fenton catalysis, *Journal of Photochemistry and Photobiology A: Chemistry*, 376 (2019) 32-42. **(I.F: 3.2)**
10. **Jasminder Singh**, Pooja kumari, Soumen Basu, Degradation of toxic industrial dyes using SnO_2/g-C_3N_4 nanocomposites: role of mass ratio on photocatalytic activity, *Journal of Photochemistry and Photobiology A: Chemistry,* 371 (2019) 136-143. **(I.F: 3.2)**

11. **Jasminder Singh,** Soumen Basu, Haripada Bhunia, Furfuryl alcohol-derived carbon monoliths for CO_2 capture: adsorption isotherm and kinetic study, IOP Conf. Series: Materials Science and Engineering, 625 (2019) 012014.
12. Balpreet Kaur, **Jasminder Singh,** Raj Kumar Gupta, Haripada Bhunia, Porous carbons derived from polyethylene terephthalate (PET) waste for CO_2 capture studies, *Journal of Environmental Management,* 242 (2019) 68-80. **(I.F: 4.8)**
13. Manish Sharma, **Jasminder Singh**, Satyajit Hazra, Soumen Basu, Adsorption of heavy metal ions by mesoporous ZnO and TiO_2@ZnO monoliths: adsorption and kinetic studies, *Microchemical Journal*, 145 (2019) 105-112. **(I.F: 3.2)**
14. Manisha Sharma, **Jasminder Singh**, Soumen Basu, Efficient metal ion adsorption and photodegradation of rhodamine-b by hierarchical porous Fe-Ni@SiO_2 monolith, *Microchemical Journal,* 145, (2019) 708-717. **(I.F: 3.2)**
15. Manisha Sharma, **Jasminder Singh**, Satyajit Hazra, Soumen Basu, Remediation of heavy metal ions using hierarchically porous carbon monolith synthesized via nanocasting method, *Journal of Environmental Chemical Engineering,* 6 (2018) 2829-2836.

Conferences/Workshops Attended:

- 2nd National Conference on Advanced Oxidation Processes at Dr. S.S. Bhatnagar University Institute of Chemical Engineering & Technology and Energy Research Centre, Panjab University, Chandigarh on October 15-16, 2015.
- International Workshop on Carbon Capture & Sequestration at GNDU, Amritsar, Punjab on November 12-16, 2016.
- National Symposium on Applications of Radioisotopes and Radiation Technology in Industry, Healthcare, and Agriculture at Thapar University, Patiala, Punjab on November 28-29, 2016.
- 70th Annual Session of Indian Institute of Chemical Engineers, CHEMCON – 2017 at Dept. of Chemical Engineering, Haldia Institute of Technology, Kolkata, India on December 27 – 30, 2017.